SYNTHETIC AND MECHANISTIC STUDY OF CATALYTIC DINITROGEN REDUCTION

BY

WALTER WARREN WEARE

B.S. in General Science, *magna cum laude*
University of Oregon
June, 2000

Submitted to the Department of Chemistry
in Partial Fulfillment of the Requirements
for the Degree of

DOCTOR OF PHILOSOPHY

at the

MASSACHUSETTS INSTITUTE OF TECHNOLOGY

May, 2006

Signature of Author _____
Department of Chemistry
May 12, 2006

Certified by _____
Richard R. Schrock
Thesis Supervisor

Accepted by _____
Robert W. Field
Chairman, Departmental Committee on Graduate Students

This doctoral thesis has been examined by a committee of the Department of Chemistry as follows:

Professor Richard R. Schrock _____
Thesis Supervisor

Professor Daniel G. Nocera _____
Chairman

Professor Christopher C. Cummins _____

SYNTHETIC AND MECHANISTIC STUDY OF CATALYTIC DINITROGEN REDUCTION

BY

WALTER WARREN WEARE

Submitted to the Department of Chemistry on May 12, 2006
in Partial Fulfillment of the Requirements
for the Degree of Doctor of Philosophy in
Chemistry

Abstract

The dinitrogen reduction capability of a series of new triamidoamine based molybdenum compounds has been studied. The synthesis of a number of different triamidoamine ligands, and their resulting molybdenum compounds, is described. While symmetric variants containing electron-withdrawing hexaisopropyl terphenyl substituents can successfully catalyze dinitrogen reduction to ammonia, only the most bulky unsymmetric "hybrid" compounds can facilitate this reaction.

Further study of these systems reveals a different pathway for catalyst failure than had previously been observed. It was discovered that, at least for the smaller ligands, a base-catalyzed hydrogenase reaction occurs at a rate much faster than that of ammonia formation. The Mo(IV) diazenido ($\mathbf{L}MoN_2H$) compound undergoes net H• loss, forming the Mo(III) dinitrogen ($\mathbf{L}MoN_2$) species with concomitant release of H_2.

Examination of the "parent" system has also revealed previously unknown intricacies of the dinitrogen reduction reaction. By developing a means to measure H_2 formation, we are now able to fully quantify the reducing equivalents added to our system. This supports our belief that only NH_3 and H_2 are formed during catalysis. In addition, control experiments demonstrate that the proton source typically utilized for catalytic study, [2,6-lutidinium][BAr_4'], can be reductively coupled under catalytic conditions. Therefore an acid that avoids this coupling reaction ([2,4,6-collidinium][BAr_4']) is now utilized during most catalytic experiments.

Thesis Supervisor: Richard R. Schrock

Title: Frederick G. Keyes Professor of Chemistry

Table of Contents

List of Figures

List of Equations

List of Tables

List of Abbreviations Used in the Text

Å	angstrom
Anal	elemental analysis
Ar	aryl
BAr_4'	Tetra-bis(trifluoromethyl)phenyl borate $[(3.5\text{-bis}(CF_3)C_6H_3)_4B]^-$
BINAP	2,2'-bis(diphenylphosphino)-1,1'-binaphthyl
br	broad
°C	degrees Celsius
calc'd	calculated
collidine	2,4,6-trimethylpyridine
Cp	cyclopentadienyl (C_5H_5)
Cp^*	pentamethylcyclopentadienyl (Me_5C_5)
CV	cyclic voltammetry
δ	chemical shift downfield from tetramethylsilane, $CFCl_3$, or NH_3
d	doublet
dba	dibenzylideneacetone
dd	doublet of doublets
°	degrees
DMF	N,N-dimethylformamide
EI	electron impact (mass spectrometry)
Et	ethyl (CH_2CH_3)
eV	electron volts
η_x	hapticity of a ligand bound to a metal through x atoms
g	grams
h	hour(s)
H_2	dihydrogen

Hz	hertz
HRMS	high resolution mass spectrometry
^{i}Pr	isopropyl ($CH(CH_3)_2$)
IR	infrared
J_{AB}	coupling constant between atoms A and B
kcal	kilocalories
L	liters, ligand
lutidine	dimethylpyridine
μ	magnetic moment
μB	Bohr magneton
M	molar
m	multiplet
μ-N_2	bridging dinitrogen
Me	methyl (CH_3)
mesityl	trimethylbenzene
mg	milligrams
MHz	megahertz
min	minute(s)
mL	milliliters
mmol	millimoles
mV	millivolts
ν	frequency
n-Bu, Bu	normal butyl ($CH_2CH_2CH_2CH_3$)
Nα	nitrogen directly bound to the metal
Nβ	nitrogen 2 bonds from the metal
NMR	nuclear magnetic resonance
Ph	phenyl (C_6H_5)

ppm	parts per million
q	quartet
RT	room temperature
rac	racemic
s	singlet
sept	septet
T	temperature
t	triplet
^{t}Bu	tertiary butyl ($C(CH_3)_3$)
THF	tetrahydrofuran
TREN	triamidoamine, $N(CH_2CH_2NH_2)_3$
UV	ultraviolet
V	volts
VT	variable temperature
[N_3N]	$[(RNCH_2CH_2)_3N)]^{3-}$

CHAPTER 1

Highlights of Transition Metal Mediated Dinitrogen Reduction

Dinitrogen is an unreactive molecule. Its high bond strength ($D_{N\text{-}N}$ = 225 kcal/mol)[1] and kinetic sluggishness pose a significant challenge for nature (and chemists) when attempting to utilize this abundant source of elemental nitrogen for synthesis.[2] While many natural processes (such as lightning) contribute to the fixation of nitrogen, the major sources of fixed nitrogen are from bacteria (through the nitrogenase enzyme) and man (through the Haber-Bosch process).[3]

Nature has solved the problem of dinitrogen utilization through the use of the nitrogenase enzyme.[4] Nitrogenase is a multiple component enzyme, in which electrons and protons reduce dinitrogen to the more chemically useful ammonia. Energy, in the form of ATP, is also used to drive this reaction to completion.[5] The protein delivers the protons and electrons into the active site, which contains the iron-molybdenum cofactor (FeMoCo, Figure 1.1). Surprisingly, considering the stability of N_2, the rate-limiting step in this process is the delivery of electrons into the nitrogenase protein.[4]

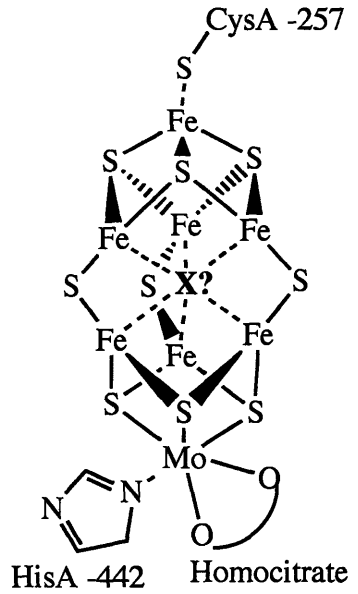

$$N_2 + 8\,H^+ + 8\,e^- + 16\,ATP \longrightarrow 2\,NH_3 + H_2 + 16\,ADP + 16\,P_i$$

Figure 1.1) Structure of FeMoCo and the overall stoichiometry for the reduction of N_2 to NH_3 at nitrogenase.

The crystal structure of nitrogenase was first solved in 1992,[6] with the structure having been refined several times since. Recently an atom (X) in the center of the cofactor was revealed from such work. This was initially suggested to be N,[7] but that assignment has been shown to be erroneous.[8,9] The structure of FeMoCo is so far unique to nitrogenase; no other cofactors have been found which contain the same structural motif. The resting state, which is the only crystallographically characterized state, does not bind N_2. Therefore crystallography provides only structural information of one state (the resting state), which offers only minimal mechanistic insight into the catalytic cycle. The mechanism of N_2 reduction at FeMoCo therefore remains controversial; even the site of dinitrogen binding is not universally accepted. Arguments supporting both iron[10,11] and molybdenum[12,13] as the primary site of N_2 binding remains speculative, at best. Our work, which shows that only one molybdenum atom is necessary for N_2 reduction,[14] is suggestive that molybdenum may be the site for N_2 reduction. However, other workers have demonstrated that iron containing dinitrogen complexes exist,[15,16,17] although these systems lack to ability to catalytically form NH_3. Interestingly, iron-only nitrogenases are also reported in the literature[5] The field remains focused on the mechanism of nitrogenase, and as new spectroscopic tools become available the secrets of nitrogenase will eventually be revealed.

The Haber-Bosch process is the manner by which mankind fixes dinitrogen to ammonia.[18] Other means to fix dinitrogen, such as its reaction with CaC_2 or oxidation utilizing electronic arcs, have failed to economically compete with the Haber-Bosch

$$N_2 + 3\,H_2 \xrightarrow[350°\text{-}555°C]{\text{Fe catalyst}\atop 150\text{-}350\ \text{atm}} 2\,NH_3 \qquad \textbf{(1.1)}$$

process.[19] Requiring high pressures and temperatures (Equation 1.1), the Haber-Bosch process is energy intensive even though the overall reaction is exothermic by ~30

kcal/mol with ~1.4% of the world's total energy is used in this process.[2] Due to the harsh conditions of the reaction, mechanistic information is scarce. However, it is believed that subsurface nitrides and hydrides combine to form ammonia.[20]

The high costs associated with Haber-Bosch conditions led to extensive interest in transition metal dinitrogen complexes due to the possibility of discovering a milder route for dinitrogen reduction. The first such compound to be characterized, (Figure 1.2) possesses both N_2 and NH_3 coordinated to ruthenium.[21] This turned out to be merely an interesting coincidence, and not indicative of the reactivity of the dinitrogen ligand in this system as it proved to be inert to further functionalization. The first transition metal compound that was able to functionalize the bound dinitrogen ligand was the system developed by Chatt and Hidai at molybdenum (tungsten was also used) (Figure 1.2).[22] This compound, when treated with mineral acids, released between one and two equivalents of ammonia per metal depending on conditions. Compounds were also discovered with bridging dinitrogen ligands (both μ-N_2 (Figure 1.2) and η_2-N_2).[23] The chemistry of η_2-N_2 complexes has been the subject of a recent review.[24]

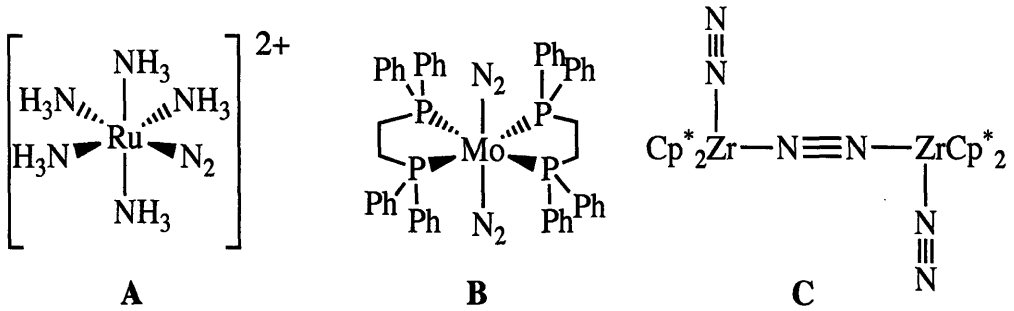

A **B** **C**

Figure 1.2) Some early transition metal dinitrogen complexes. A) $[Ru(NH_3)_5N_2]^{2+}$ as discovered by Allen and Senhoff in 1965.[21] B) $Mo(N_2)_2(dppe)_2$ as discovered by Hidai and Chatt in 1969.[22] C) The bimetallic $Cp^*_2Zr(N_2)\mu$-$N_2(N_2)ZrCp^*_2$ discovered by Bercaw in 1974.[23]

Of the several mechanistic cycles proposed for the formation of NH_3 from N_2 at a single metal center, the most applicable to the research described in this thesis is that put

forward by Chatt.[22] In this cycle, all the reducing equivalents to produce NH_3 are provided directly by the metal (Figure 1.3). While the reaction can continue along this path it precludes the cycle from closing, as the required 6 electron reduction of the final Mo(VI) compound back to the starting Mo(0) complex has not been observed. The catalytic cycle described in our lab circumvents this difficulty by not accessing any oxidation states below Mo(III) (Figure 3.1). Details of the Chatt reduction cycle have been the subject of a series of papers by Tuczek *et. al.*[25]

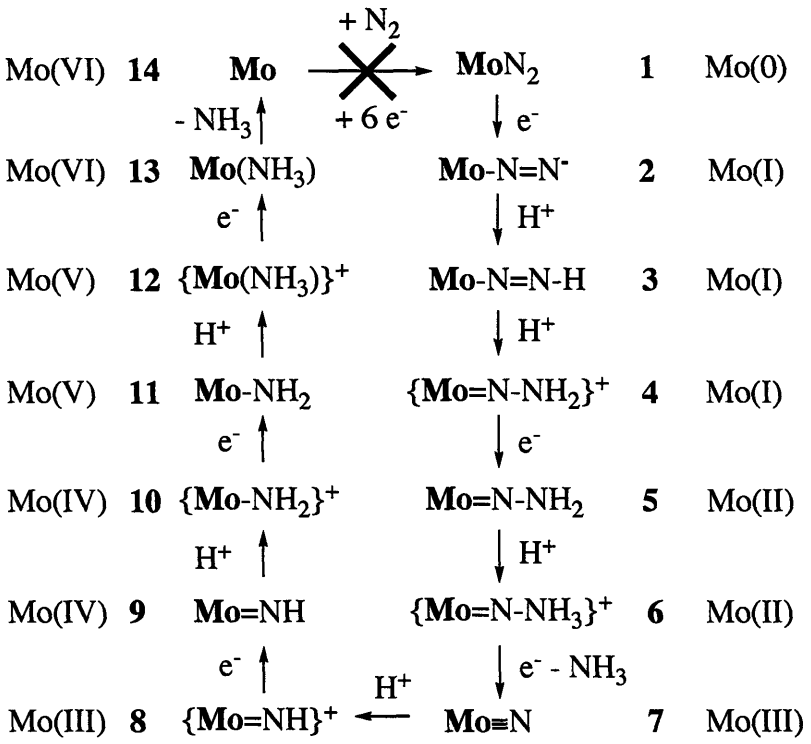

Figure 1.3) The Chatt cycle.

Dinitrogen Formation Through Coupling of M-NH_x Fragments

The primary focus of this thesis is the reduction of N_2 to form NH_3. There is, however, an interesting body of work on reactions that oxidizes NH_3 (or other reduced nitrogen sources such as metal nitrides) to form N_2. The primary motivation for studying these oxidative coupling reactions is that it is the microscopic reverse of the desired ammonia formation reaction. Therefore, understanding what controls the kinetic and

thermodynamic properties of this reaction could, at some point, be utilized for the reductive cleavage of N_2. While our results that show a single metal center is all that is necessary for N_2 reduction to ammonia, this field remains interesting in light of recent systems that utilize two metal centers to cleave the N_2 bond.[35]

The initial report of a nitride coupling reaction was made in 1979 by Taube (Equation 1.2).[26] In this reaction, oxidation of the Os(II) ammonia complex with Ce(IV) results in the formation of an Os(II) μ–N_2 compound. This reaction apparently proceeds through an Os(IV) intermediate, which is suggested to be an osmium nitride. It is interesting to note that the CO ligand is necessary to promote this reaction, as oxidation reactions with compounds possessing SO_2, H_2O, or NO^+ ligands do not result in the formation of an N_2 coupled dimer (presumably due to CO coordination driving the formation of Os(II) species, while the other ligands preferentially support the Os(IV) oxidation state).

$$2\,[Os(NH_3)_5CO]^{2+} \xrightarrow{\text{oxidation}} [(Os(NH_3)_4CO)_2N_2]^{4+} \quad \textbf{(1.2)}$$

Many other osmium compounds have since been found to undergo similar coupling reactions. These include osmiun terpyridine (Tp) and bipyridine (Bp) systems as studied by Meyer.[27] Recently, a system that involved the coupling of osmium nitrides with molybdenum nitrides was studied by Brown[28] (Figure 1.4). These studies demonstrate that osmium coupling most likely proceeds not through direct end-on coupling, but *via* a transition state that involves one electrophilic and one nucleophilic nitride. In Taube's systems, this is provided by different resonance states of the same molecule.[29] In Brown's case, mixing discreet electrophilic ($TpOs(N)Cl_2$) and nucleophilic ($(Et_2NCS_2)_3MoN$) nitrides results in the release of free N_2 (Figure 1.5). The resulting metal fragments go on to react in a cascade, with a multitude of metal products obtained in the final product mixture.

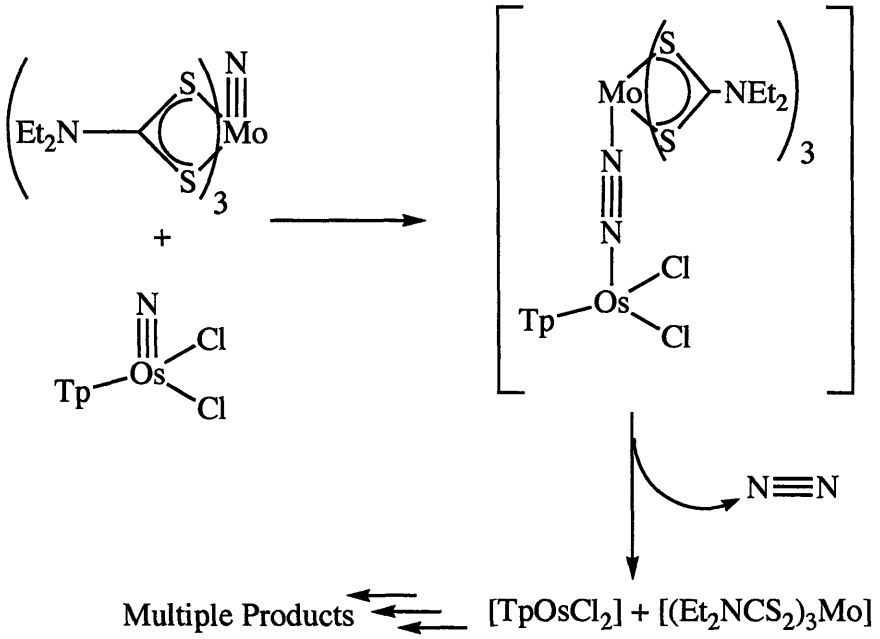

Figure 1.4) Multimetallic nitride coupling system as described by Brown.[28]

Osmium is not the only element that supports this chemistry. Recently, Peters described the synthesis of Fe(IV) nitrides that decompose at room temperature to form Fe(I) μ-N_2 complexes (Figure 1.5).[30] While this result complicates in-depth study of iron(IV) nitrides, it demonstrates that each group 8 element can support nitride coupling chemistry ((salen)RuN can couple to release N_2[31]).

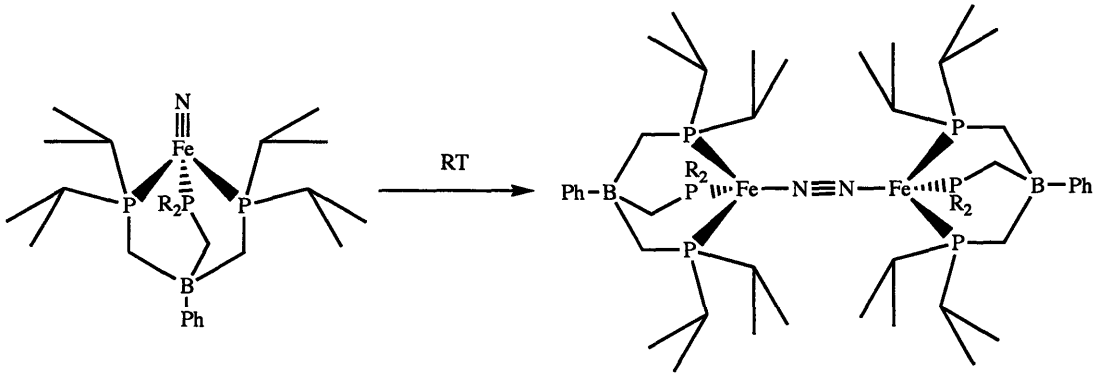

Figure 1.5) Coupling of iron nitride compounds to form μ_2-dinitrogen complexes.

A rather different approach to studying ammonia coupling was taken by Collman in the early 1990's.[1,32,33] Cofacial porphyrins were utilized to restrict the geometry of two Ru-NH_x fragments in between the porphyrin planes. With this geometry in place, he was able to oxidize (and deprotonate) these framents stepwise, isolating the μ_2-hydrazine, μ_2 diazene, and μ_2-N_2 complexes (Figure 1.6). The ultimate goal for these complexes was to drive this reaction in the opposite direction electrochemically, forming NH_3 from N_2. However, this proved to be problematic, as Ru μ_2-N_2 resisted reduction and the Ru-NH_3 units could not be displaced by N_2 under reasonable conditions[34] (the bis-NH_3 and μ_2-hydrazine complexes were most easily synthesized by displacement of N_2 with the appropriate ligand).

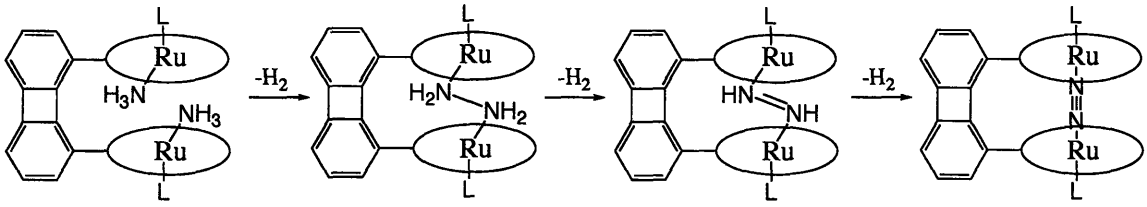

Figure 1.6) Coupling of ammonia to form dinitrogen using a Ru-cofacial porphyrin.[32]

The overriding principle of microscopic reversibility that guides this work demands that nitride formation from N_2 actually be feasible. Taube suggested that Os(III) μ-N_2 complexes may be able to do such a splitting (due to the strength of a Os(VI)-nitride bond),[26] but no evidence for nitride formation from osmium N_2 complexes has appeared since this observation. Apparently, even Os(VI) nitrides are unable to drive this reaction. In 1995, Cummins demonstrated that nitride formation from N_2 could occur, using the high bond strength of Mo(VI) nitrides as the driving force (Figure 1.7).[35] This chemistry was the first demonstration that the work invested studying nitride coupling was potentially useful for understanding N_2 cleavage. Utilization of the resulting nitride atom (which originates from N_2) into other compounds has proven to be

quite a challenge. However, recent work has begun to yield methods by which the nitride can be used to form other interesting compounds.[36]

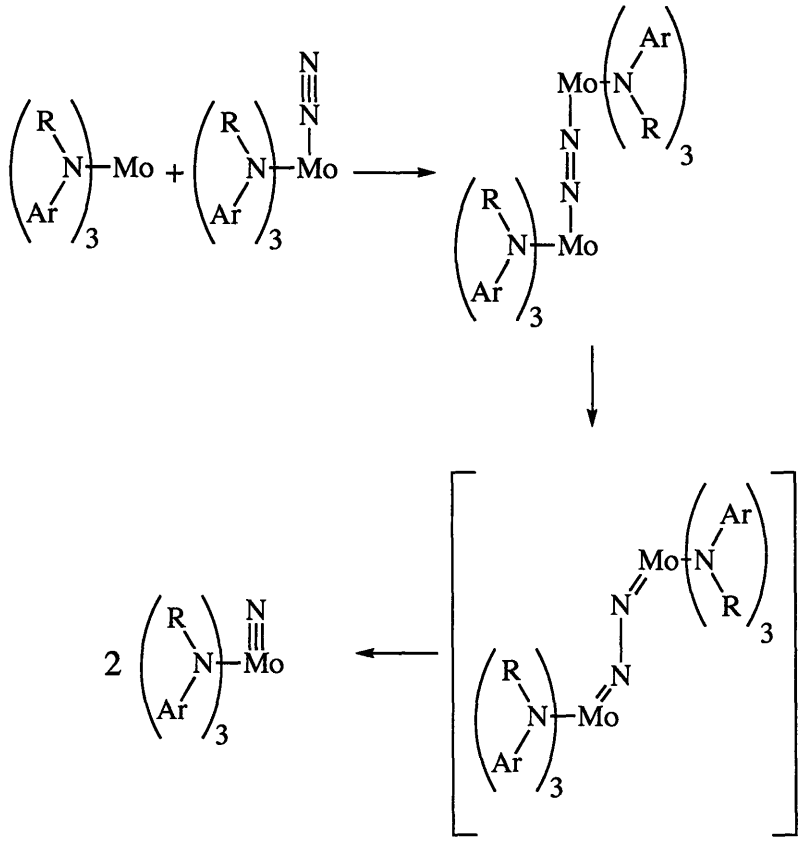

Figure 1.7) Nitride formation from N_2 utilizing Molybdenum triamido complexes.[37]

The Schrock group has long been interested in dinitrogen reduction chemistry. The first dinitrogen complex described by the group was synthesized via the reduction of $Ta(CHCMe_3)(PMe_3)_2Cl_3$ with Na/Hg amalgam.[38] The resulting compound was readily alkylated, resulting in the structurally characterized $[Ta(CHCMe_3(PMe_3)_2(CH_2CMe_2)]_2\mu$-$N_2$ dimer (Figure 1.8). The bridging N_2 in this molecule could be further functionalized with acetone, yielding dimethylketazine quantitatively and a mixture of unidentifiable metal fragments.

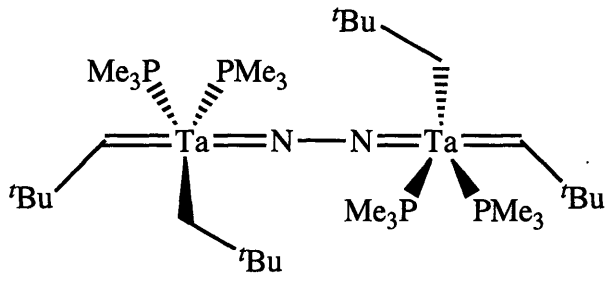

Figure 1.8) Tantalum N_2 dimer which has "diimidolike" character for the bridging N_2.

The study of bridging N_2 ligands continued with the synthesis of tungsten complexes. The reaction of $W(C_2Ph_2)(OR)_4$ with hydrazine results in the loss of two alkoxide groups and the formation of a N_2 bridged $[W(C_2Ph_2(OR)_2]_2(N_2)$ from deprotonation of N_2H_4. This can then be treated with HCl in dimethoxyethane to yield the crystallographically characterized chloro complex (Figure 1.9).[39] This approach again

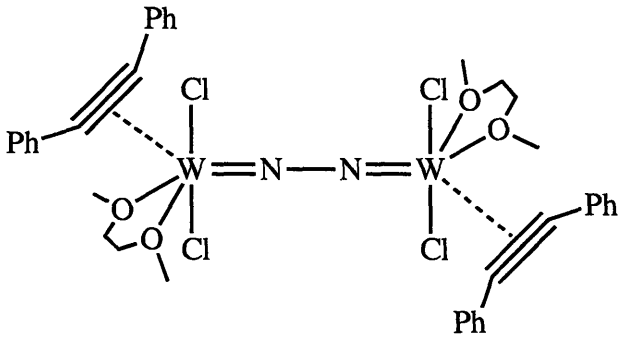

Figure 1.9) A "W(IV)" bridging dinitrogen complex.

shows interest in understanding microscopic reversibility of N_2 reduction, with hydrazine being "oxidized" to form the bridging N_2 unit. This is probably not the case in this particular compound, as the metals most likely remain W(IV).

Bridging dinitrogen containing unambiguous W(VI) species were realized a few years later. Cp^* ligands were utilized for steric protection of the metal center, with the remaining ligands simply being methyl groups. Reaction of $Cp^*WMe_3(NNH_2)$ with $[Cp^*WMe_4][PF_6]$ results in the formation of the symmetric $[Cp^*WMe_3]_2N_2$.[40] This

compound undergoes protonation of the N_2 unit upon treatment with mineral acids, to form NH_3 and N_2H_4.[41] Molybdenum compounds of this type (as well as the W/Mo mixed dimer) also form ammonia and hydrazine when treated with mineral acids. The yields are somewhat increased if an electron source is added, such as Zn/Hg amalgam. However, these species do not turnover, and less than 1 equivalent of NH_3 is produced per briding N_2 unit in nearly all cases.

With the introduction of triamidoamine compounds into our group, the study dinitrogen activation was revitalized. Triamidoamine compounds are ideally set up to react with N_2,[42] and they were found to readily do so. Reaction of $MoCl_3(THF)_3$ and $Li_3(SiMe_3N_3N)$ resulted in the formation of a bridging N_2 complex in poor yield.[43] The use of **L**MoCl as a starting material enabled the study of a wide range of dinitrogen complexes in the trimethylsilyl system.[44] Particularly interesting is the formation of a system containing three dinitrogen TREN complexes surrounding a single iron atom (Figure 1.10).[44] This was formed by reacting a magnesium bridged **L**MoN_2 dimer with $FeCl_2$.

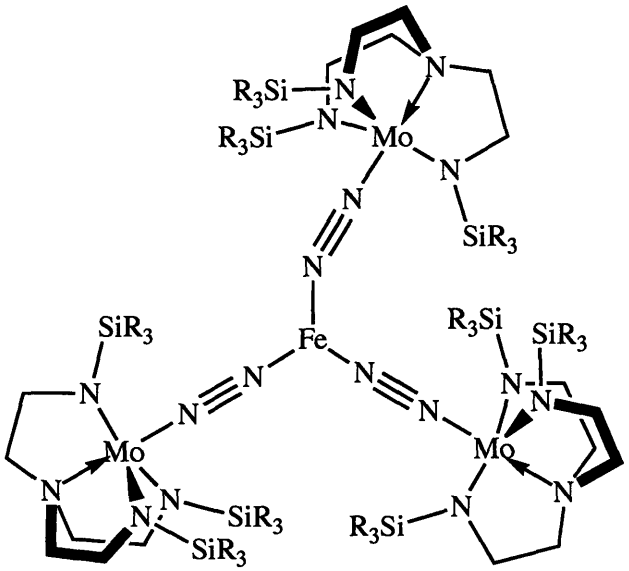

Figure 1.10) The structurally interesting compound $([SiMe_3N_3N]MoN_2)_3Fe$,

As described in the rest of this thesis, the Schrock lab has utilized similar triamidoamine systems to catalytically reduce dinitrogen to ammonia using only protons and electrons.[14] Catalytic sinks, such as the multimetallic compounds exemplified above, were eventually prevented by the incorporation of bulky hexaisopropyl terphenyl groups into the TREN framework.[14] This thesis describes the continuation of this work, both through the synthesis of new variants of the triamidoamine ligand design and the detailed study of catalytic intermediates.

References

1. Collman, J.P.; Hutchison, J.E.; Lopez, M.A.; Gullard, R. *J. Am. Chem. Soc.* **1992**, *114*, 8066.

2. Leigh, G.J. *Science* **1998**, *279*, 506.

3. Galloway, J.N.; Schlesinger, W.H.; Levy II, H.; Michaels, A.; Schnoor, J.L. *Global Biogeochem. Cycles* **1995**, *9*, 235.

4. Burgess, B.K. *Chem. Rev.* **1990**, 1377.

5. Burgess, B.K.; Lowe, D.J. *Chem. Rev.* **1996**, 2983.

6. Georgiadis, M.M.; Komiya, H.; Chakrabarti, P.; Woo, D.; Kornuc, J.J.; Rees, D.C. *Science* **1992**, *257*, 1653.

7. Einsle, O.; Tezcan, F.A.; Andrade, S.L.A.; Schmid, B.; Yoshima, M.; Howard, J.B.; Reed, D.C. *Science*, **2002**, *297*, 1696.

8. Lee, H-I.; Benton, P.M.C.; Laryukhin, M.; Igarashi, R.Y.; Dean, D.R.; Seefeldt, L.C.; Hoffman, B.M. *J. Am. Chem. Soc.* **2003**, *125*, 5604.

9. Yang, T-C.; Maeser, N.K.; Laryukhin, M.; Lee, H-I.; Dean, D.R.; Seefeldt, L.C.; Hoffman, B.M. *J. Am. Chem. Soc.* **2005**, *127*, 12804.

10. Barney, B. M.; Laryukhin, M.; Igarashi, R. Y.; Lee, H.-I.; Dos Santos, P. C.; Yang, T.-C.; Hoffman, B. M.; Dean, D. R.; Seefeldt, L. C. *Biochemistry* **2005**, *44*, 8030.

11. Dos Santos, P. C.; Igarashi, R. Y.; Lee, H.-I.; Hoffman, B. M.; Seefeldt, L. C.; Dean, D. R. *Acc. Chem. Res.* **2005**, *38*. 208.

12. Schimpl, J.; Petrilli, H. M.; Blochl, P. E. *J. Am. Chem. Soc.* **2003**, *125*, 15772.

13. Shilov, A.E. *Pure and Appl. Chem.* **1992**, *64*, 1409.

14. Yandulov, D.V.; Schrock, R.R. *Science* **2003**, *76*, 301.

15. Betley, T. A.; Peters, J. C. *J. Am. Chem. Soc.* **2003**, *125*, 10782.

16. Smith, J. M.; Sadique, A. R.; Cundari, T. R.; Rodgers, K. R.; Lukat-Rodgers, G.; Lachicotte, R. J.; Flaschenriem, C. J.; Vela, J.; Holland, P. L. *J. Am. Chem. Soc.* **2006**, *128*, 756.

17. Gilbertson, J.D.; Szymczak, N.K.; Tyler, D.R. *J. Am Chem. Soc.* **2005**, *127*, 10184.

18. Greenwood, N.N.; Earnshaw, A. *Chemistry of the Elements*; University Press; Cambridge (England), 1984.

19. Hooper, C. W. in *Catalytic Ammonia Synthesis: Fundamentals and Practice*; Jennings, J. R., Ed.; Plenum Press: New York, 1991.

20. Caselli, A.; Solari, E.; Scopelliti, R.; Floriani, C.; Re, N.; Rizzoli, C.; Chiesi-Villa, A. *J. Am. Chem. Soc.* **2000**, *122*, 3652.

21. Allen, A.D.; Senoff, C.V. *Chem. Commun.* **1965**, 621.

22. Chatt, J.; Leigh, G.J. *Chem. Soc. Rev.* **1972**, *1*, 121.

23. Manriquez, J.M.; Bercaw, J.E. *J. Am. Chem. Soc.* **1974**; *96*, 6229.

24. MacLachlan, E.A.; Fryzuk, M.D. *Organometallics*, **2006**, *25*, 1530.

25. a) Lehnert, N.; Tuczek, F. *Inorg. Chem.* **1999**, *38*, 1659-1670. **b)** Lehnert, N.; Tuczek, F. *Inorg. Chem.* **1999**, *38*, 1671-1682. **c)** Horn, K. H.; Lehnert, N.; Tuczek, F. *Inorg. Chem.* **2003**, *42*, 1076-1086. **d)** Horn, K. H.; Böres, N.; Lehnert, N.; Mersmann, K.; Näther, C.; Peters, G.; Tuczek, F. *Inorg. Chem.* **2005** *44*, 3016. **e)** Mersmann, K.; Horn, K. H.; Böres, N.; Lehnert, N.; Studt, F.; Paulat, F.; Peters, G.; Evanovic-

Burmazovic, I.; van Eldik, R.; Tuczek, F. *Inorg. Chem.* **2005**, *44*, 3031.

26. Buhr, J.D.; Taube, H. *Inorg. Chem.* **1979**, *18*, 2208.

27. El-Samanody, E-S.; Demadis, K.D.; Meyer, T.J.; White, P.S. *Inorg. Chem.* **2001**, *40*, 3677.

28. Seymore, S.B.; Brown, S.D. *Inorg. Chem.* **2002**, *41*, 462.

29. Ware, D.C.; Taube, H. *Inorg. Chem.* **1991**, *30*, 4605.

30. Betley, T.A.; Peters, J.C. *J. Am. Chem. Soc.* **2004**, *126*, 6252.

31. Man, W-L.; Tang, T-M.; Wong, T-W.; Lau, T-C.; Peng, S-M.; Wong, W-T. *J. Am Chem. Soc.* **2004**, *126*, 478.

32. Collman, J.P.; Hutchison, J.E.; Lopez, M.A.; Guilard, R.; Reed, R.A. *J. Am. Chem. Soc.* **1991**, *113*, 2794.

33. Collman, J.P.; Hutchison, J.E.; Ennis, M.S.; Lopez, M.A.; Guilard, R. *J. Am. Chem. Soc.* **1992**, *114*, 8074.

34. Hutchison, J.E. *personal communication.*

35. Laplaza, C.E.; Johnson, A.R.; Cummins, C.C. *Science* **1995**, *268*, 861-863.

36. Figueroa, J. S.; Piro, N. A.; Clough, C. R.; Cummins, C. C. *J. Am. Chem. Soc.* **2006**, *128*, 940.

37. Laplaza, C. E.; Johnson, M. J. A.; Peters, J. C.; Odom, A. L.; Kim, E.; Cummins, C. C.; George, G. N.; Pickering, I. J. *J. Am. Chem. Soc.* **1996**, *118*, 8623.

38. Turner, H.W.; Fellmann, J.D.; Rocklage, S.M.; Schrock, R.R.; Churchill, M.R.; Wasserman, H.J. *J. Am. Chem. Soc.* **1980**, *102*, 7809.

39. Churchill, M.R., Li, Y.J., Theopold, K.H., Schrock, R.R. *Inorg. Chem.* **1984**. *23*, 4472.

40. Murray, R.C.; Schrock, R.R. *J. Am. Chem. Soc.* **1985**, *107*, 4557.

41. Schrock, R.R.; Kolodziej, R.M.; Liu, A.H.; Davis, W.M.; Vale, M.G.; *J. Am. Chem. Soc.* **1990**, *112*, 4338.

42. Schrock, R.R. *Acc. Chem. Res.* **1997**, *30*, 9.

43. Shih, K-Y.; Schrock, R.R.; Kempe, R. *J. Am. Chem. Soc.* **1994**, *116*, 8804.

44. O'Donoghue, M.B.; Zanetti, N.C.; Davis, W.M.; Schrock, R.R. *J. Am. Chem. Soc.* **1997**, *119*, 2753.

CHAPTER 2

Synthesis of Triamidoamine Based Ligands for the Study of Catalytic Dinitrogen Reduction

Portions of the material covered in this chapter have appeared in print:

Ritleng, V.; Yandulov, D. V.; Weare, W. W.; Schrock, R. R.; Hock, A. S.; Davis, W. M. *J. Am. Chem. Soc.* **2004**, *126*, 6150-6163.

Introduction

Since their introduction into early transition metal chemistry in 1992,[1] triamidoamine based ligands have proven successful as supporting ligands for a broad range of organometallic and inorganic reactivity.[2,3,4,5,6,7] The ligand provides an open and stable binding pocket while enforcing geometric constraints on the metal. Binding interactions with the incoming apical ligand therefore occur in a specified manner, with 1 σ and 2 π interactions available for metal/ligand reactivity.[2] The most commonly seen compounds have 5-coordinate metal centers, although 6-coordinate compounds are also known.[2,8]

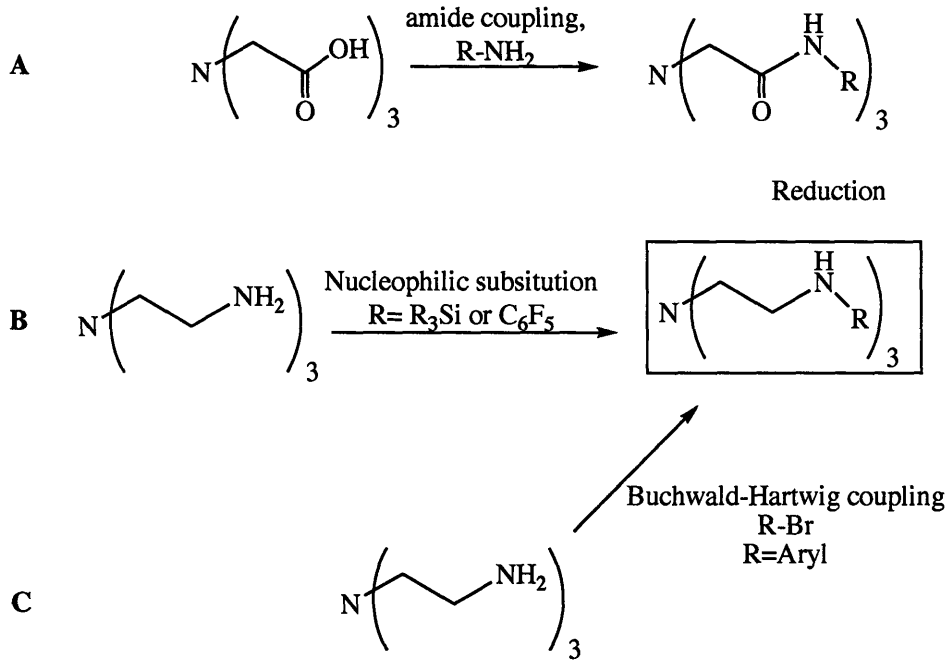

Figure 2.1) Synthesis of substituted TREN ligands. **A)** Amid coupling route. **B)** Nucleophilic substitution. **C)** Palladium catalyzed aryl-Br, alkyl-NH_2 coupling.

The first TREN ligands were synthesized *via* nucleophilic substitution of trialkylsilylchlorides directly with tris(2-ethylamino)amine.[1] While these silyl substituted TREN compounds allowed for extensive study of this ligand environment, the N-Si

linkage proved to be too reactive for many of the systems (such as dinitrogen reduction) under study. To allay this, aryl substituents that possess a C-N bond were used. The first ligands of this type were again synthesized *via* nucleophilic substitution, this time using C_6F_6 with tris(2-ethylamino)amine (Figure 2.1).[9]

Unfortunately, the ligands available *via* nucleophilic substitution were limited to highly electron deficient aryl groups. To overcome this limitation, TREN ligands were synthesized through a two-step synthesis beginning with the formation of a tris-amide from nitrilotriacetic acid, followed by reduction to the desired ligand (Figure 2.1).[10] While this expanded the available ligands, it also had its limitations. These chiefly were that the necessary aniline was often not commercially available and that the harsh reduction conditions ($LiAlH_4$) synthetically eliminated many functional groups from consideration.

In 1995, Buchwald[11] and Hartwig[12] began to popularize palladium catalysis to form N-C bonds. This route, which directly couples aryl halides to amines, has become the exclusive means for synthesizing aryl-substituted TREN ligands (Figure 2.1). It is amenable to a wide variety of functional groups, is high yielding, and has minimal side products.[13] This was particularly useful in the synthesis of the HexaIsoPropylTerphenyl TREN parent ligands **[HIPTN$_3$N]**H_3 that resulted in the discovery of the first *well-characterized* dinitrogen reduction catalytic cycle under ambient conditions that only uses protons and electrons.[14]

This chapter outlines the synthesis of a number of new ligands for the continued study of catalytic dinitrogen reduction. They are all based upon the triamidoamine motif, with variations that effect the steric and electronic environment around the metal and binding pocket.

Results and Discussion

Symmetric Ligands

With a catalytic system in hand, we elected to explore the reactivity of similar compounds to further understand the factors that control catalytic dinitrogen reduction. Initially, I focused on the synthesis of terphenyl variants that were electronically different from the parent system, but maintained the steric environment afforded by HIPT (Dr. Vincent Ritleng synthesized two steric variants – hexa-*t*-butyl terphenyl [**HTBTN$_3$N**]H$_3$ and hexamethylterphenyl [**HMTN$_3$N**]H$_3$).[15] The goal was to synthesize both electron withdrawing and electron donating ligands through substitution at the *para* position of the terphenyl ring. This was to be accomplished through quenching the intermediate Grignard (present after the terphenyl forming double benzyne reaction) with a variety of electrophiles. However, only a few reactions of this type are reported, and those focused

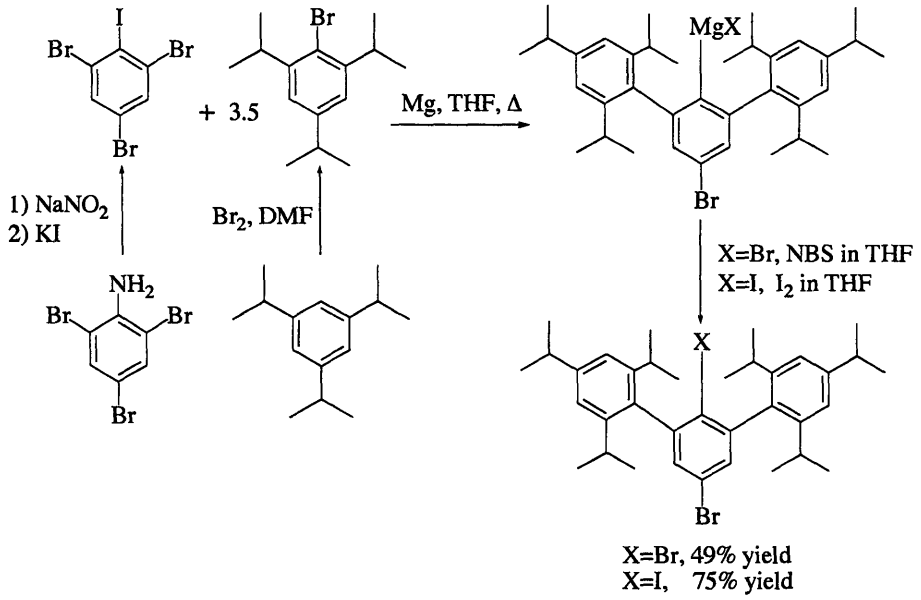

Figure 2.2) Synthesis of electron withdrawing hexaisopropylterphenyl bromides.

on placing electrophilic groups into the internal pocket of one or more linked 2,6-terphenyl ring systems to alter substrate binding interactions within the resulting pocket.[16] These systems focused on unsubstituted terphenyls, so the steric encumbrance present in

our hexaisopropyl systems was not addressed. As mentioned later, this proves to be a limiting factor in this chemistry.

Electron withdrawing hexaisopropylterphenyl bromides were synthesized with the appropriate choice of quenching reagent (Figure 2.2). For the *para*-bromo system, *N*-bromosuccinimide resulted in a good yield for ***p*BrHIPTBr** (Br_2 resulted in the formation of a significant amount of the undesired **HIPTBr**, which is difficult to separate from the *para*-substituted species). Use of I_2 as the quenching agent resulted in ***p*IHIPTBr**, also in good yield. Use of chlorinating agents such as CCl_4 or C_2Cl_6 resulted in a 1:1 mixture of ***p*ClHIPTBr** and **HIPTBr**, so *para*-chloro terphenyls were not investigated further.

Attempts to synthesize relatively electron donating terphenyls using the same route met with universal failure (only **HIPTBr** was isolated from these attempts). Reagents such as dimethylsulfate, tetramethyloxonium reagents, carbon dioxide, various dialkyl peroxides, methyl iodide, Me_3SiCl and methyl triflate were used. Oxygen was not attempted.

The only electron donating terphenyl bromide that I have been able to synthesize is hexamethoxyterphenyl bromide. The usual type of intermediate to make this compound, 1-bromo-2,4,6-trimethoxybenzene, could only be selectively synthesized via difficult and/or expensive routes. It was found, however, that 1-iodo-2,4,6-trimethoxybenzene could be synthesized in refluxing water with treatment of 0.5

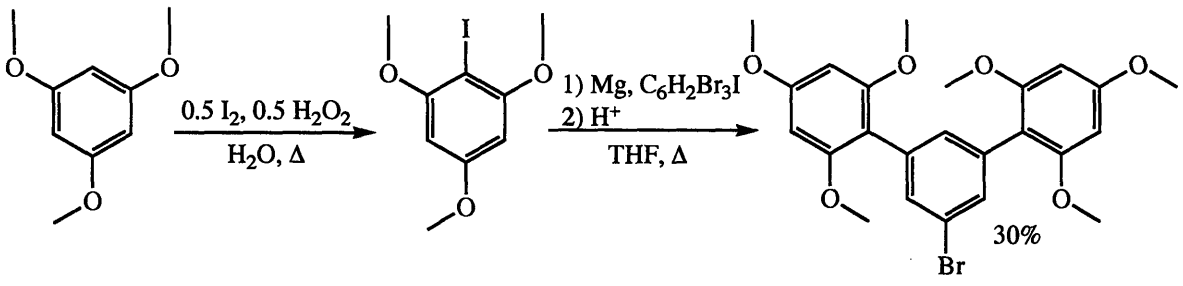

Figure 2.3) Synthesis of **HMOTBr**

equivalents of I_2 and 0.5 equivalents of hydrogen peroxide[17] (Note: over-halogenation is quite facile in this reaction, so care needs to be taken when measuring out reagents). This compound successfully forms hexamethoxyterphenyl bromide (**HMOTBr**) (Figure 2.3). Unfortunately, it is not reactive under standard Buchwald-Hartwig coupling procedures using both X-Phos or *rac*-BINAP in toluene. Whether this is due to low solubility or catalyst deactivation has not been thoroughly explored. However, new discoveries in C-N coupling may eventually allow **HMOTBr** to be placed into triamidoamine systems.[18]

With these new electron withdrawing terphenyls, synthesis of both **[*p*BrHIPTN$_3$N]H$_3$** and **[*p*IHIPTN$_3$N]H$_3$** could proceed. As mentioned in the introduction, our primary method for synthesizing triamidoamine based ligands is the palladium catalyzed route popularized by Buchwald and Hartwig (Figure 2.4). While the yield of **[pBrHIPTN$_3$N]H$_3$** was acceptable, **[pIHIPTN$_3$N]H$_3$** was formed in only meager yields. Therefore, we decided to focus entirely upon **[pBrHIPTN$_3$N]H$_3$** for all of our subsequent work using these symmetric ligands to study catalytic dinitrogen reduction (see chapters 3 and 4).

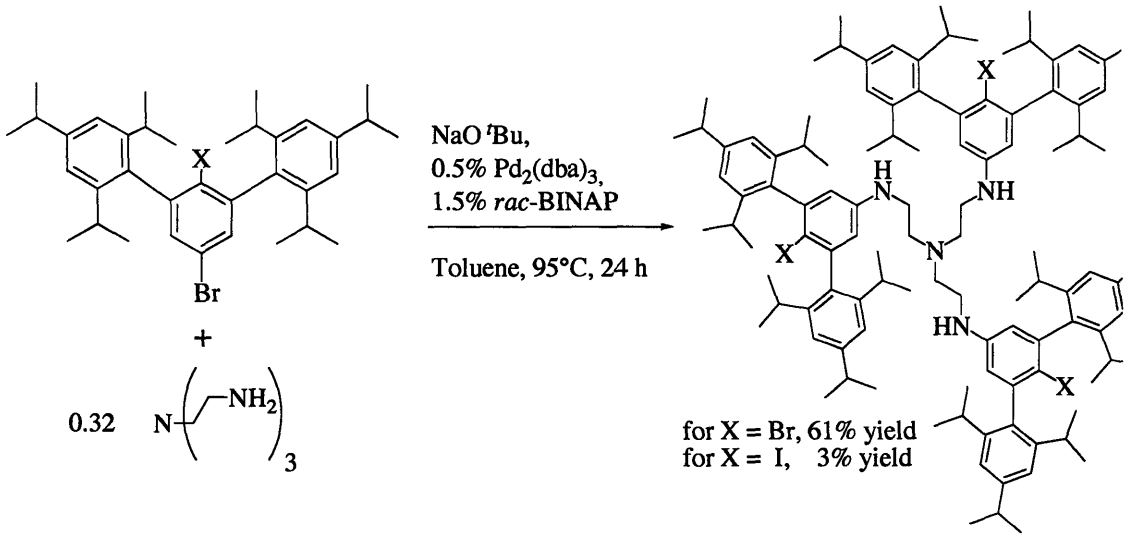

Figure 2.4) Synthesis of the electron withdrawing triamidoamine ligands **[*p*BrHIPTN$_3$N]H$_3$** and **[*p*IHIPTN$_3$N]H$_3$**

A Propyl Triamidoamine HIPT Ligand

Another ligand type synthesized utilizes a propyl backbone, while retaining the triamidoamine motif. Trimethylsilyl substituted propyl ligands were previously synthesized by our group for the study of titanium reaction chemistry, and no major differences in reactivity were observed.[5] **[HIPTpropylN$_3$N]H$_3$** was readily synthesized through the coupling of **HIPTBr** and tris(3-aminopropyl)amine under similar conditions employed to synthesize TREN compounds (Figure 2.5). I have only preliminarily worked with this compound (see chapter 3): studies using this ligand are being led by Ms. Jia Min Chin.

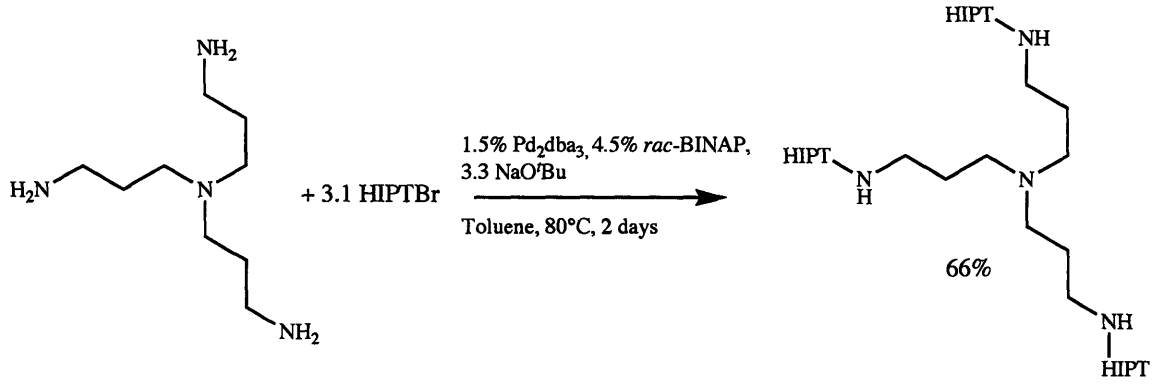

Figure 2.5) Synthesis of **[HIPTN$_3$propylN]H$_3$**

Unsymmetric TREN Ligands

While the symmetric variants synthesized by Dr. Ritleng showed that catalytic success is highly sensitive to the steric bulk of the ligand environment,[15] the absence of electron donating arms and the overall difficulty in synthesizing different terphenyl groups led us to consider other means to introduce variation into the triamidoamine system. To accomplish this desired variation, we decided to synthesize unsymmetric "hybrid" ligands that contain two arms substituted with HIPT (to maintain the steric bulk necessary to prevent dimer formation) leaving the third arm available for substitution by a variety of aryl groups. While such a compound had been reported previously,[15] rational

synthesis of "hybrid" triamidoamine ligands had not been undertaken except in the case where the backbone itself was varied (2 arms ethyl, 1 arm propyl).[19]

In order to prepare this ligand library, we needed a partially substituted triamidoamine to serve as the platform for later modification. Fortunately, simple stoichiometric variation of the **HIPTBr**:tris(2-aminoethyl)amine ratio during the N-C coupling reaction allowed for the isolation of the doubly arylated "2 arm" compound in good yield (Figure 2.6). Due to the primary amine of this "2 arm" compound, it is necessary to treat the silica gel used for column purification with Et_3N prior to use. We were also able to isolate the parent symmetric ligand as a minor product for use in other studies.

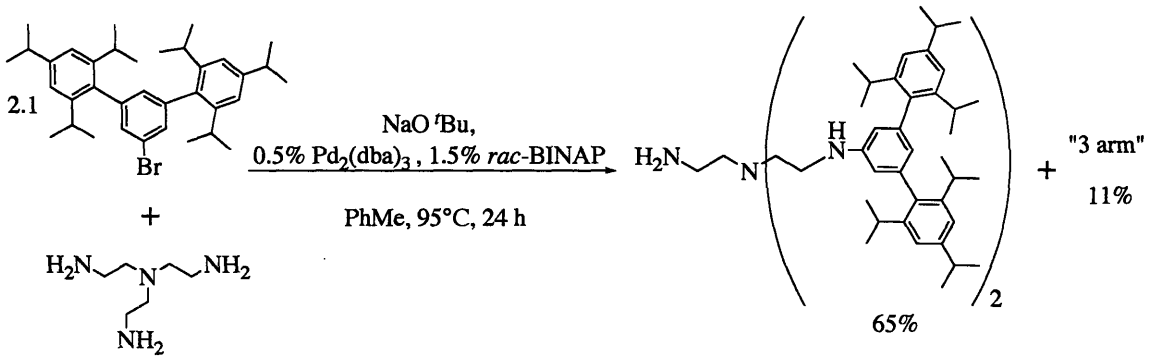

Figure 2.6) Synthesis of unsymmetric "2 arm" HIPT substituted TREN.

Our initial direction with these unsymmetric ligands was to incorporate pyridine-based third arms into the TREN framework, with the hope that this would ease proton entry into the dinitrogen reduction intermediates. This would facilitate formation of cationic intermediates, lowering the reduction potentials necessary to complete the cycle.[20] We targeted the 3,5-dimethyl and 3,5-diphenyl substituted pyridine compounds for our initial synthesis. Unfortunately, neither 1-bromo-3,5-lutidine or 1-bromo-3,5-diphenylpyridine was commercially available. Therefore, we synthesized these compounds. While the complete synthesis of 1-bromo-3,5-lutidine has been reported in the literature,[21] it is fragmented and is therefore repeated in this thesis (Figure 2.7). The

synthesis reported here of 1-bromo-3,5-diphenylpyridine is also reported in its entirety. The critical step for the synthesis of 1-bromo-3,5-diphenylpyridine involves the Stille coupling of tri-*n*-butyl-phenylstannane with 3,5-dibromo-1-nitro-pyridine[22] (Figure 2.7) (this route was chosen because direct nitration of 2,6-diphenylpyridine was not selective in my hands). Coupling of these newly synthesized aryl-bromides with the "2-arm" intermediate afforded the desired unsymmetric ligands ([**LutHIPT$_2$N$_3$N**]H$_3$ and [**PhLutHIPT$_2$N$_3$N**]H$_3$ for the lutidine and diphenylpyridine containing ligands respectively) containing a basic site for easier proton transfer into the catalytic cycle.

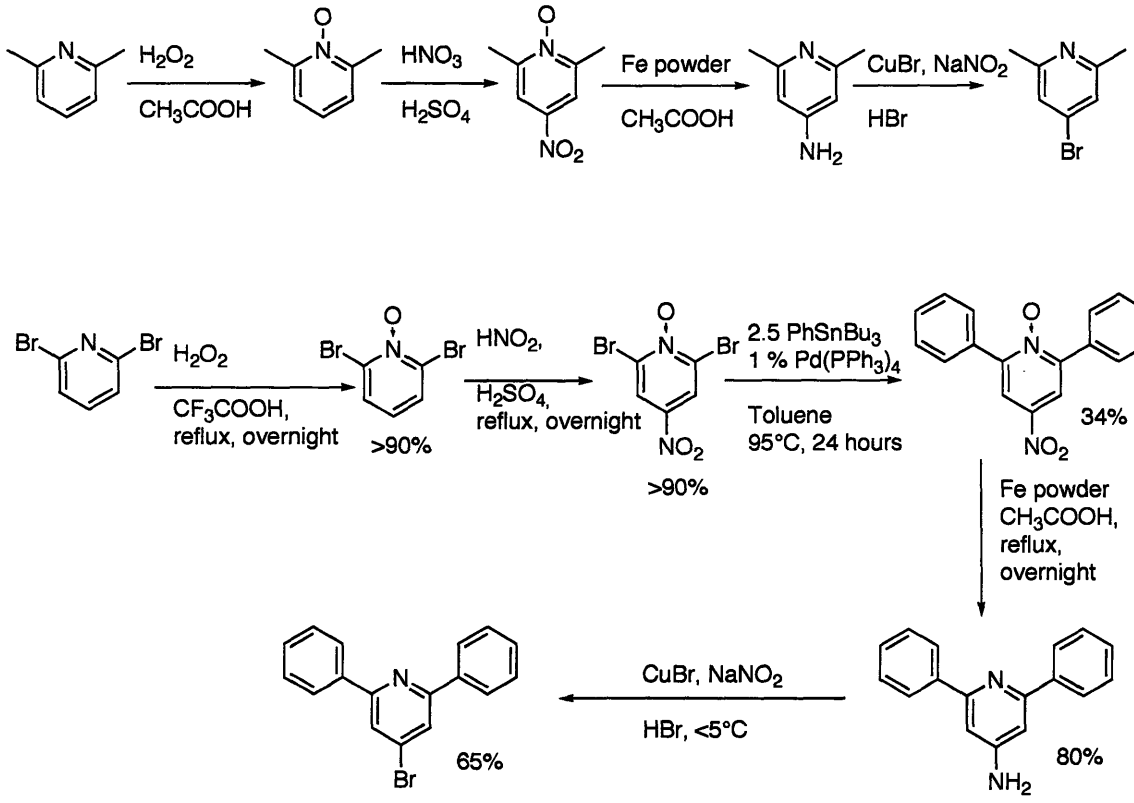

Figure 2.7) Synthesis of 1-bromo-3,5-dimethylpyridine and 1-bromo-3,5-diphenylpyridine.

With these pyridine-based ligands in hand, we turned our attention to simpler aryl groups to append onto the unsymmetric TREN arm. We initially encountered some synthetic difficulties in attaching 3,5 substituted aryl groups due to problems with over-arylation.[10] To bypass this difficulty, we turned our attention to 2,4,6-substituted aryl

groups, in particular 2,4,6-mesityl and 2,4,6-triisopropylphenyl arms. At this point in time, we believed that the exchange of ammonia for dinitrogen in the catalytic pathway involved dissociation of the ammonia, and we felt that these ligands might speed this reaction due to direct steric pressure into the binding pocket through their *ortho* substituents. It is interesting to note that symmetric mesityl substituted TREN ligands do not support molybdenum compounds due to steric hindrance.[10] 2,4,6-Mesitylbromide is commercially available, and 1-bromo-2,4,6-triisopropylbenzene was available for use from our synthesis of **HIPTBr**. 2,4,6-Mesitylbromide was cleanly coupled onto the third arm using *rac*-BINAP to make **[MesHIPT$_2$N$_3$N]**H$_3$, while 1-bromo-2,4,6-triisopropylbenzene required the use of X-Phos to couple, although the yield of **[TripHIPT$_2$N$_3$N]**H$_3$ remained low (Figure 2.8). These ligands allowed us to observe the effects of steric pressure on the dinitrogen binding pocket as described in chapters 3 and 4.

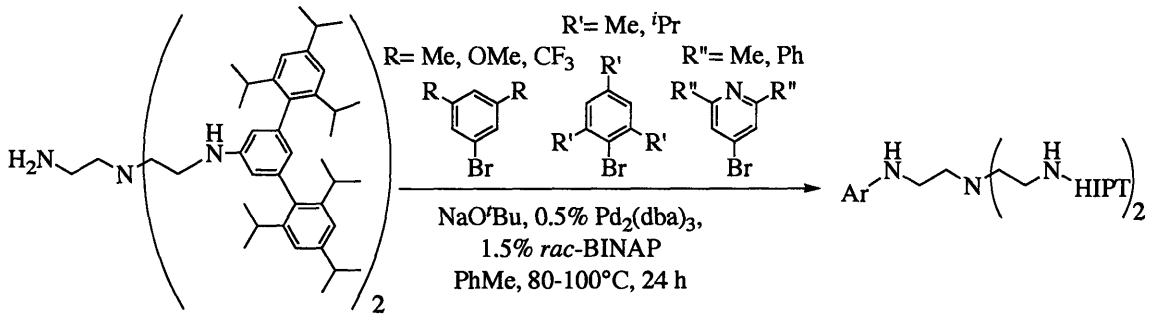

Figure 2.8) Synthesis of unsymmetric "hybrid" ligands

Through temperature optimization of the Buchwald-Hartwig coupling, we were eventually able to synthesize a series of ligands that contain 3,5-substituted aryl groups on the third arm. The 3,5-substituted aryls chosen provide a gradient of electronic induction, from the relatively electron withdrawing 3,5-bis(CF$_3$)phenyl to the relatively electron donating 3,5-dimethoxyphenyl. 3,5-Dimethylphenyl was used as an

intermediate to the two (σ_p = 0.54 (CF_3), -0.17 (CH_3), -0.27 (OMe)). The corresponding aryl bromides are all commercially available, and the ligands **[3,5-bis(CF_3)$_2$HIPT$_2$N$_3$N]H$_3$**, **[3,5-dimethoxyHIPT$_2$N$_3$N]H$_3$**, and **[3,5-dimethylHIPT$_2$N$_3$N]H$_3$** were isolated and fully characterized. A ^{1}H NMR of **[3,5-bis(CF_3)HIPT$_2$N$_3$N]H$_3$** is shown below and is representative of the spectral features observed in these unsymmetric hybrid ligands. Most noticeable is the presence of two peaks attributable to the N-*H* protons, as well as two sets of peaks for each C*H*$_2$ in the ethyl backbone of TREN. These spectral features clearly demonstrate the unsymmetric nature of these ligands.

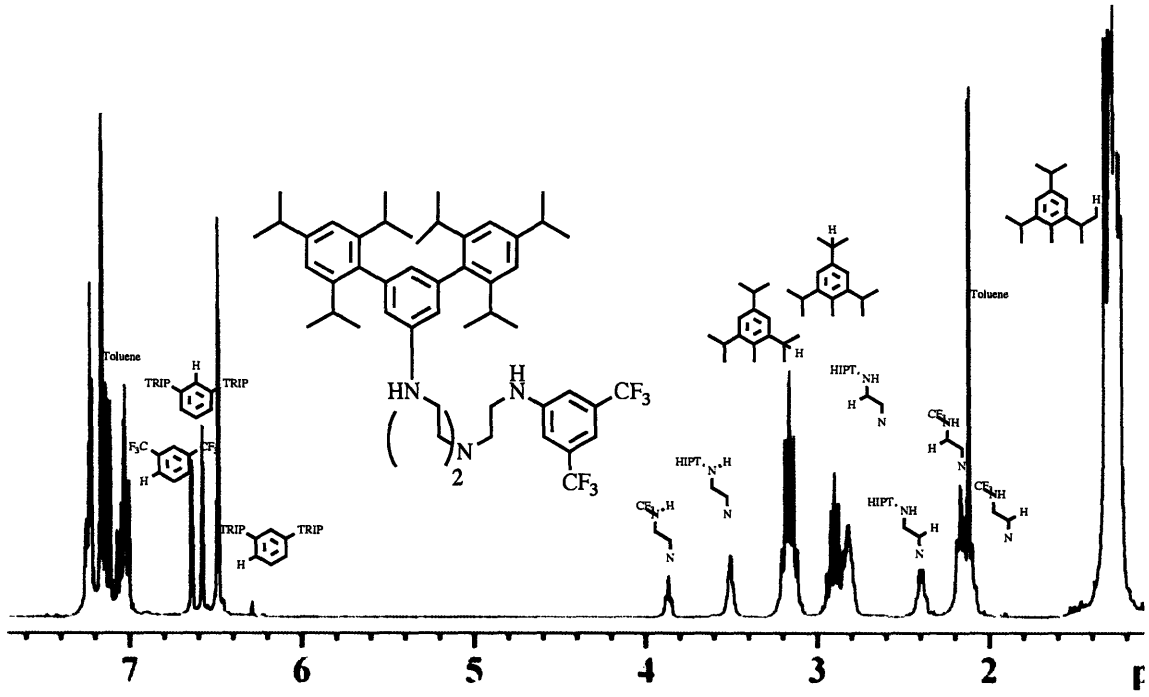

Figure 2.9) ^{1}H NMR of **[3,5-bis(CF_3)HIPT$_2$N$_3$N]H$_3$**.

Conclusions

The synthesis of these ligands has afforded us the ability to probe the dinitrogen reduction cycle in directions not possible when only one ligand is available. The ligands

described in this chapter are not meant to be the end-all of variation in this system, but have proven to be a good starting point for such studies. Exploitation of this hybrid ligand system has just begun, and we are now focusing on ligands that contain variable terphenyl groups on the third arm to less drastically alter the steric and electronic environment in the dinitrogen reduction pocket than those presented in this thesis. As catalytic N-C coupling technology improves, the spectrum of compounds available for incorporation into TREN will continue to expand. As we learn more about what controls catalytic dinitrogen reduction, synthesis of new ligands will continue to attempt to provide the ideal conditions for this important reaction.

Experimental Section

General. Air and moisture sensitive compounds were manipulated utilizing standard Schlenk and dry-box techniques under an atmosphere of dinitrogen. All glassware used was oven and/or flame dried immediately prior to use. Pentane, diethyl ether, toluene, and benzene were purged with dinitrogen and passed through activated alumina columns. Benzene was additionally passed through a Q5 column.[23] THF and benzene-d_6 were dried over sodium/benzophenone ketyl and vacuum transferred prior to use. All other solvents mentioned were freeze-pump-thaw degassed 3 times prior to use. All dried and deoxygenated solvents were stored in a dinitrogen-filled glove box over molecular sieves or in teflon sealed glass solvent bombs. 1,3,5 triisopropylbenzene (Aldrich), 2,4,6 tribromoaniline (Lancaster), *N*-bromo-succinimide (Aldrich), NaO^{t}Bu (Aldrich), $Pd_2(dba)_3$ (Strem), *rac*-BINAP (Strem), and tris(2-aminoethyl)amine (Aldrich) were used as received, unless indicated otherwise. HexaIsoPropyTerphenyl bromide (**HIPTBr**),[2425] 2,4,6-trimethoxy-1-iodobenzene,[17] tributylphenylstannane were prepared according to published procedures or with slight modifications. ^{1}H and ^{13}C NMR spectra were recorded on a Varian Mercury 300. NMR spectra are referenced to internal residual solvent peaks (^{1}H and ^{13}C NMR) or to external C_6H_5F (δ = -113.15 ppm in ^{19}F NMR).

2',5'-Dibromo-2,4,6,2'',4'',6''-hexaisopropyl-1,1':3'1''-terphenyl (*p*BrHIPTBr)[15] A procedure similar to that for **HIPTBr** was used up until the quenching of the final Grignard reagent. Briefly, 2,4,6-triisopropylbromobenzene (10.6 g, 37 mmol) in 100mL of THF was added to Mg turnings (2 g, 82 mmol) and refluxed for 1 h. Then, 2,4,6-tribromoiodobenzene (5 g, 11 mmol) in 100 mL of THF was added and the solution refluxed for an additional 2 h. The entire solution was cooled using and ice bath, and added to an ice-cooled slurry of *N*-bromosuccidinimide (NBS) (12.1 g, 68 mmol) in 200 mL THF and allowed to stir for 1 h. (**Note**: it is important to keep both solutions cool and add all reagents slowly to prevent the formation of HBr). A saturated aqueous solution of sodium nitrite was then added, stirred for 2 hours, followed by extraction with ether. The combined organic phases were washed with water and the volatiles removed *in vacuo*. The resulting orange-colored solid was washed with methanol to yield an off-white solid that was recrystallized from ether yielding 3.47 g (49%) of a white powder. ^{1}H NMR ($CDCl_3$, 20°C) δ 7.37 (s, 2H, 4'6'-*H*), 7.08 (s 4H, 3,5,3'',5'' –*H*), 2.98 (septet, J_{HH}= 6.9 Hz, 2H, 4,4'' -C*H*Me$_2$), 2.56 (septet, J_{HH}= 6.9 Hz, 4H, 2,6,2'',6''-C*H*Me$_2$), 1.33 (d, J_{HH}= 6.9 Hz, 12H, 4,4''-CH(C*H*$_3$)$_2$), 1.19 (d, J_{HH}= 6.9 Hz, 12H, 2,6,2'',6'' -CH(C*H*$_3$)$_2$), 1.17 (d, J_{HH}= 6.9 Hz, 12H, 2,6,2'',6'' -CH(C*H*$_3$)$_2$). ^{13}C NMR ($CDCl_3$, 20°C) δ 148.85, 145.82, 144.32, 135.29, 132.33, 127.69, 120.95, 120.61, 34.56, 31.26, 24.96, 24.36, 23.87. MS (ESI) 639.2216 ([M+H]$^+$, calc'd. 639.2196).

2' Iodo-, 5' Bromo-2,4,6,2'',4'',6''-hexaisopropyl-1,1':3'1''-terphenyl (*p*IHIPTBr) The procedure used to synthesize **HIPTBr** was followed up until the quenching of the resulting Grignard. 2,4,6-triisopropylbromobenzene (10.6 g, 37 mmol) in 100mL of THF was added to Mg turnings (2 g, 82 mmol) and refluxed for 1 h. Then, 2,4,6-tribromoiodobenzene (5 g, 11 mmol) in 100 mL of THF was added and the solution refluxed for an additional 2 h. The final Grignard solution was added slowly to an iced mixture of 12 g (46 mmol) of I_2 in 50 mL THF and allowed to stir for 10 hours. A saturated aqueous solution of sodium nitrite was then added, and stirred for 2 hours,

followed by extraction with ether. The combined organic phases were then washed with water and reduced *in vacuo*. The resulting solid was washed with methanol, and recrystallized from ether to yield 3.62 g (75%) of an off-white powder. Attempts to use this terphenyl to make a symmetric ligand have been low yielding and not pursued. ^{1}H NMR ($CDCl_3$, 20°C) δ 7.34 (s, 2H, 4'6'-*H*), 7.06 (s 4H, 3,5,3",5" –*H*), 2.97 (septet, J_{HH}= 6.9 Hz, 2H, 4,4" -C*H*Me_2), 2.51 (septet, J_{HH}= 6.9 Hz, 4H, 2,6,2",6"-C*H*Me_2), 1.33 (d, J_{HH}= 6.9 Hz, 12H, 4,4"-CH(CH_3)$_2$), 1.24 (d, J_{HH}= 6.9 Hz, 12H, 2,6,2",6" -CH(CH_3)$_2$), 1.15 (d, J_{HH}= 6.9 Hz, 12H, 2,6,2",6" -CH(CH_3)$_2$) ^{13}C NMR ($CDCl_3$, 20°C) δ 148.98, 148.69, 145.51, 139.08, 130.83, 121.86, 121.00, 109.80, 34.52, 31.25, 25.23, 24.40, 23.72.

5' Bromo-2,4,6,2'',4'',6''-hexamethoxy-1,1':3'1''-terphenyl (HMOTBr) This was synthesized in a similar manner to other terphenyls of this type. Briefly, 40 g (0.136 mol) of trimethoxyiodobenzene dissolved in 200 mL of THF was added slowly to 50 mL of refluxing THF containing 6.7 g (0.275 mol) of pre-activated magnesium turnings. This was refluxed for 3 hours, at which time the solution was grey and turbid. To this mixture 20 g (0.045 mol) of tribromoiodobenzene dissolved in 200 mL THF was slowly added . The resulting mixture was allowed to reflux overnight, at which time the dark brown solution was transferred *via* cannula to ice cooled HCl/water (150 mL conc. HCl in 400 mL water). This was extracted with ether (2 x 200 mL) followed by extraction with dichloromethane (3 x 200 mL). (note: liquid/liquid extraction over 3 days using dichloromethane yielded ~ 50 mg of additional product) The combined organic layers were washed with sodium hydroxide/water (3 x 100 mL), sodium sulfite/water (3 x 100 mL), and water (3 x 200 mL), and dried with magnesium sulfate. After filtration and removal of the volatiles *in vacuo*, the product was precipitated from the resulting oil with methanol and the solid collected. The solid was triturated with ether and filtered to yield 6.2 g (30%) of a fine tan powder. Attempts to utilize this terphenyl in a Buchwald-Hartwig coupling have so far been unsuccessful. ^{1}H NMR ($CDCl_3$, 20°C) δ 7.43 (t, J_{HH}= 2 Hz, 2H, 2'6'-*H*), 7.29 (d, J_{HH}= 2 Hz, 1H, 4'-*H*), 6.23 (s, 4H, 3,5,3",5"-*H*), 3.87 (s, 6H,

4,4" OCH_3), 3.75 (s, 12H, 2,6,2",6" OCH_3). ^{13}C NMR ($CDCl_3$, 20°C) δ 160.82, 158.54, 134.96, 133.38, 132.31, 120.68, 111.58, 90.99, 56.03, 55.53. MS (ESI) 511.0703 ([M+Na]$^+$, calc'd. 511.0727).

Tris(2-(5'-bromo-2,4,6,2'',4'',6''-hexaisopropyl-1,1':3'1''-terphenyl-5'amino)ethyl)amine ([*p*BrHIPTN$_3$N]H$_3$)[15] The procedure followed was nearly identical to the procedure published for H$_3$[**HIPTN$_3$N**]. Briefly, a solution of ***p*BrHIPTBr** (6.92 g, 11 mmol), NaO^{t}Bu (1.378 g, 14 mmol) and tris(2-aminoethyl)amine (0.54 g, 3.5 mmol) in 100 mL toluene was prepared in the glove box. A catalyst mixture of $Pd_2(dba)_3$ (0.082 g, 0.09 mmol) and *rac*-BINAP (0.166 g, 0.26 mmol) in 100 mL toluene, which had been preformed to the appropriate orange color, was filtered through Celite and added to the ***p*BrHIPTBr** solution. The flask was sealed and and stirred at 90°C for 48 hours, during which time solid NaBr was observed to form. The solids were removed through filtration over Celite, and partially purified by passage through a pad of SiO_2. Volatiles were removed under vacuum, and the resulting solid purified through chromatography on SiO_2 (pentane/toluene). The resulting off-white foamy solid was extensively dried at 65°C under vacuum to yield 3.96 g (2.1 mmol, 61% yield). ^{1}H NMR (C_6D_6, 20°C) δ 7.26 (s, 12H, 3,5,3",5" -*H*), 6.44 (s, 6H, 4',6' -*H*), 3.52 (t, J_{HH}=5.0 Hz, 3H, N*H*), 3.05 (septet, J_{HH}=6.9Hz, 2H, 4,4" -C*H*Me$_2$), 2.90 (septet, J_{HH}=6.9Hz, 4H, 2,6,2",6"-C*H*Me$_2$), 2.70 (br m, 6H, NHCH_2CH$_2$), 2.16 (approx. t, J_{HH}=5.2 Hz, 6H, NHCH$_2$CH_2), 1.47 (d, J_{HH}=6.9, 12H, 4,4"-CH(CH_3)$_2$), 1.29 (m, 72H, 2,6,2'6'-CH(CH_3)$_2$. ^{13}C NMR (C_6D_6, 20°C) δ 149.2, 147.0, 146.6, 144.0, 138.0, 121.5, 116.3, 114.7, 53.0, 41.7, 35.4, 31.9, 25.8, 25.0, 24.7. MS (ESI) 1822.0231([M+H]$^+$, calc'd. 1822.0188). Anal Calc'd for $C_{114}H_{159}Br_3N_4$: C, 75.02; H, 8.78; Br, 13.13; N 3.07. Found: C, 75.11; H, 8.87; Br, 12.98; N, 3.02

2,6-Dimethyl-pyridine 1-oxide This compound was synthesized via the method of Ochiai.[26] Briefly, 2,6 lutidine (100g, .91 mol) was placed in 600 mL of glacial acetic acid. This solution was heated to 75°C, at which time 100 mL of 35% hydrogen peroxide

was slowly added. This solution was heated for 2 hours, upon which time an additional 70 mL of hydrogen peroxide was slowly added. The solution was left at 75 °C overnight. Volatiles were then removed *in vacuo* until approximately 400 mL of solution remained, at which point 100 mL of water was added. This solution was then further reduced *in vacuo* to 200 mL, basified with sodium carbonate, and extracted with chloroform. The chloroform was removed *in vacuo* resulting in a clear liquid that was used without further purification.

2,6-dimethyl-4-nitro-pyridine 1-oxide This compound was synthesized via the method of Evans and Brown.[27] Briefly, the crude 2,6-dimethyl-4-nitro-pyridine 1-oxide was dissolved in 250 mL sulfuric acid. Then, 130 mL of nitric acid was slowly added and allowed to reflux overnight. The solution was then cooled to room temperature and poured over ice, with the resulting solid collected, washed with water, and extracted into chloroform. The organic extracts were then washed with saturated sodium hydroxide and water, dried over magnesium sulfate, and the volatiles removed *in vacuo* to yield 130 g of a light yellow filamentous powder (85% yield from 2,6 lutidine). ^{1}H NMR ($CDCl_3$, 20°C) δ 8.03 (s, 2H, 3,5-*H*), 2.60 (s, 6H, 2,6-CH_3)

2,6-dimethyl-1-oxy-pyridin-4-ylamine This compound was synthesized via the method of Evans and Brown.[28] Briefly, 2,6-dimethyl-4-nitro-pyridine 1-oxide (19.26 g, 0.11 mol) and iron powder (26.5 g, 0.47 mol) were added to 250 mL of glacial acetic acid and allowed to heat at 100°C overnight. This solution was then basified with 250 g of sodium hydroxide in 1.5 L water. The product was extracted with ~ 1.8 L ether and dried over magnesium sulfate. The solvent was removed *in vacuo* to yield 3.21 g of white powder (20%, Evans's yield is 12%). The minimal solubility of this compound in ether significantly lowers the yield. ^{1}H NMR (d_6-acetone, 20°C) δ 6.25 (s, 2H, 3,5-*H*), 5.22 (br s, 2H, NH_2) 2.21 (s, 6H, 2,6-CH_3)

4-bromo-2,6-dimethyl-pyridine This compound was synthesized via a method similar to that of Talik *et. al.*[29] Briefly, 2,6-Dimethyl-1-oxy-pyridin-4-ylamine (1.18 g,

8.9 mmol) was added to copper bromide (5g, 34.9 mmol) in 30 mL 48% hydrobromic acid. This was then cooled in an ice bath to < 5°C. To this dark purple solution, 5.4 g of sodium nitrite (78 mmol) in 50 mL water was added very slowly, ensuring that the temperature stayed under 5°C. When addition was complete, the solution was allowed to stir overnight. The resulting solution was basified with 24 g of potassium hydroxide in 100 mL water, followed by extraction with ether. The combined organic fractions were dried with magnesium sulfate, filtered, and the volatiles removed *in vacuo*. The crude compound was then "distilled" under vacuum (Note: the compound solidifies at ~ 20°C, resulting in the compound freezing in the condenser; the condenser was warmed to collect the product) yielding 1.05 g of a clear liquid (59%). ^{1}H NMR ($CDCl_3$, 20°C) δ 6.84 (s, 2H, 3,5-*H*), 2.30 (s, 6H, 2,6-CH_3)

2,6-dibromo-pyridine 1-oxide This compound was synthesized via the method of Neumann and Vögtle.[21] Briefly, 100 g of 2,6 dibromopyridine was dissolved in 500 mL of trifluoroacetic acid. This was heated to 90°C, at which time 150 mL of 35 % hydrogen peroxide was slowly added. This was heated for 1.5 hours, upon which time an additional 100 mL of 35 % hydrogen peroxide was added. This was then left at 90 °C overnight. The resulting solution was reduced *in vacuo* to 150 mL, at which time 100 mL of water was added and a white solid formed. The mixture was basified with sodium carbonate and extracted with chloroform. The combined organic extracts were dried over magnesium sulfate and reduced *in vacuo* to a liquid/solid mixture, which was triturated with methanol to form a white powder and used in its entirety in the next step.

2,6-dibromo-4-nitro-pyridine-1-oxide This compound was synthesized via the method of Neumann and Vögtle.[21] Briefly, 2,6-dibromo-pyridine 1-oxide was dissolved in 500 mL of sulfuric acid. To this, 200 mL of nitric acid was added and the solution heated to 95°C overnight. This solution was cooled to RT, and poured over ice. The resulting solid separated by filtration and washed with water, resulting in the crude product. This was recrystallized from methanol to yield 114 g of a yellow powder. The

product contained approximately 3:2 ratio of the N-oxo and pyridine compound by ^{1}H NMR. Since both compounds are reasonable substrates for the next coupling, no further purification was done. ^{1}H NMR (C_6D_6, 20°C) δ 7.35 (s, 3,5-*H,* 2H relative), 7.18 (s, 3,5-*H*, 3H relative)

4-nitro-2,6-diphenyl-pyridine-1-oxide This compound was synthesized via a method similar to that which Fallahpour used to make terpyridyl ligands.[22] Briefly, tributyl-phenyl-stannane (38.1 g, 103.7 mmol), 2,6-dibromo-4-nitro-pyridine-1-oxide (13.9 g, 47.2 mmol), and $Pd(PPh_3)_4$ (0.82 g, 0.71 mmol) were added to 200 mL of toluene and heated to 110°C for one day. The solution was filtered through Celite and dried *in vacuo* to a solid/liquid mix. This was triturated with methanol and filtered to yield 4.6 g of a light yellow powder. (34%) ^{1}H NMR (C_6D_6, 20°C) δ 7.95 (m, 4H, 2,6,2",6"-*H*), 7.91 (s, 2H, 3',5'-*H*), 7.24 (m, 6H, 3,4,5,3",4",5"-*H*).

2,6-diphenyl-pyridin-4-ylamine This compound was synthesized via a method similar to that of Evans and Brown.[27] Briefly 4-nitro-2,6-diphenyl-pyridine-1-oxide (4.6 g, 15.7 mmol) and iron powder (4.6 g, 82 mmol) were placed in 120 mL of acetic acid and heated to 95°C overnight. The resulting solution was basified with 120 g of sodium hydroxide in 300 mL of water and extracted with a total of 900 mL ether. The combined organic extractions were washed with water, dried over magnesium sulfate, and removed *in vacuo* to yield 3.75 g of a yellow powder. (97%) ^{1}H NMR (d_6-acetone, 20°C) δ 9.05 (m, 4H, 2,6,2",6"-*H*), 8.34 (m, 6H, 3,4,5,3",4",5"-*H*), 8.06 (s, 2H, 3',5'-*H*). NH_2 not seen. ^{13}C NMR (d_6-acetone, 20°C) δ 158.13, 157.43, 141.62, 120.73, 129.65, 127.91, 105.56.

4-bromo-2,6-diphenyl-pyridene This compound was synthesized via a method similar to that of Talik *et. al.*[29] Briefly, 2,6-diphenyl-pyridin-4-ylamine (3.75 g, 15.4 mmol) and copper bromide (11.5 g, 80.3 mmol) were added to 150 mL of 48% hydrobromic acid and cooled to < 5°C in an ice bath. Sodium nitrite (22.5 g, 326 mmol) in 100 mL water was slowly added, ensuring that the temperature did not rise above 5°C. After addition the mixture was allowed to stir overnight, at which time it was basified

with 150 g of sodium hydroxide in 300 mL water. The product was extracted with ether, which was dried over magnesium sulfate, filtered, and dried *in vacuo*, yielding a bright orange oil. This was triturated with methanol to yield 1.55 g of a bright orange powder, (34%) which is sparingly soluble in most solvents. ^{1}H NMR (C_6D_6, 20°C) δ 7.95 (dd, 4H, , 2,6,2",6"-*H*), 7.42 (s, 2H, 3',5'-*H*) 7.22 (m, 6H, 3,4,5,3",4",5"-*H*). MS (ESI) 309.0146 ([M+H]$^+$, calc'd. 309.0148)

[HIPT$_2$N$_3$N]H$_4$ - "2 armed" TREN (1) This procedure is similar to previous symmetric ligand syntheses, but utilizes 2.1 equivalents of HIPTBr instead of 3.1 equivalents. $Pd_2(dba)_3$ (0.91 g, 0.9 mmol) and *rac*-BINAP (1.85 g, 2.9 mmol) were stirred with mild heating to orange in 100 mL toluene to pre-form the active catalyst, which was then filtered through Celite into a 500 mL toluene solution containing **HIPTBr** (78.21 g, 139 mmol), tris(2-aminoethyl)amine (10.09 g, 67 mmol), and NaO^{t}Bu (20.4g, 212 mmol). This solution was then heated at ~100°C for 2 days, at which time the resulting organic layer was combined with 500 mL water, extracted with ether, and the combined organic layers dried over magnesium sulfate. This was then filtered and the solvent removed *in vacuo*. A silica gel column was then performed, with byproducts eluting in toluene (including 11 g (10%) of the symmetric ligand) and the product eluting in a 1:1 mixture of toluene/THF (Note: it is important to pretreat the silica gel with triethylamine to obtain acceptable separation of products.) Upon removal of solvent from the column fractions *in vacuo*, 47.3 g of a pale yellow solid is isolated (64%). Total isolated yield of products, relative to tris(2-aminoethyl)amine, is 74%. ^{1}H NMR (C_6D_6, 20°C) δ 7.22 (s, 8H, 3,5,3",5" –*H*), 6.50 (s, 6H, 2',4',6'-*H*), 4.92 (t, J_{HH}= 4.9 Hz, 2H, N*H*), 3.17 (septet, J_{HH}= 6.9 Hz, 8H, 2,6,2",6"-C*H*Me$_2$), 2.94 (overlapped septet, J_{HH}= 6.6 Hz, 4H, 4,4" -C*H*Me$_2$), 2.85 (overlapped multiplet, 4H, $NH_2CH_2CH_2$ and $NH_2CH_2CH_2$), 2.74 (br q, J_{HH}= 5.2 Hz, 4H, $NHCH_2CH_2$), 2.03 (br t, J_{HH}= 5.2 Hz, 4H, $NHCH_2CH_2$), 1.32 (d, J_{HH}= 7.1 Hz, 24H, 4,4" -CH(C*H*$_3$)$_2$), 1.26 (br d, J_{HH}= 6.9 Hz, 48H, 2,6,2",6" -CH(C*H*$_3$)$_2$). 0.44 (br s, 2H, N*H*$_2$) ^{13}C NMR (C_6D_6, 20°C) δ 148.77, 148.40, 147.19,

142.48, 138.69, 121.38, 121.03, 112.84, 55.91, 52.97, 41.64, 40.19, 31.18, 25.36, 25.05, 24.91. MS (ESI) 1107.9119 ([M+H]$^+$, calc'd. 1107.9116)

[LutHIPT$_2$N$_3$N]H$_3$ $Pd_2(dba)_3$ (0.054g, 0.058mmol) and *rac*-BINAP (0.11g, 0.18 mmol) were stirred under mild heating in 25 mL toluene to pre-form the activated, bright orange catalyst. This was then filtered through Celite into a 300 mL toluene solution containing **1** (4.41 g, 3.98 mmol), 4-bromo-2,6-dimethyl-pyridine (0.80 g, 4.30 mmol), and NaO^{t}Bu (0.76 g, 7.91 mmol). This solution was then heated at 95°C for 2 days, at which time it was filtered through Celite and concentrated *in vacuo* to dryness. The resulting solid was dissolved in pentane and loaded on a silica column which had been pretreated with triethylamine. Side products were eluted in toluene, and the product was eluted in 1:1 toluene:THF, yielding 3.66 g of a foamy, tan solid (76%). ^{1}H NMR (C_6D_6, 20°C) δ 7.22 (s, 8H, 3,5,3",5" –*H*), 6.53 (br t, J_{HH}= 1.4 Hz, 2H, 4'-*H*), 6.48 (d, J_{HH}= 1.3 Hz, 4H, 2',6'-*H*), 6.02 (s, 2H, Lut-3,5-*H*), 3.93 (t, J_{HH}= 4.9 Hz, 1H, Lut-N*H*), 3.71 (t, J_{HH}= 4.8 Hz, 2H, HIPT-N*H*), 3.16 (septet, J_{HH}= 6.9 Hz, 8H, 2,6,2",6"-C*H*Me$_2$), 2.92 (septet, J_{HH}= 6.9 Hz, 4H, 4,4" -C*H*Me$_2$), 2.80 (br q, J_{HH}= 5.4 Hz, 4H, HIPT-NHCH_2CH$_2$), 2.63 (br q, J_{HH}= 5.9 Hz, 2H, Lut-NHCH_2CH$_2$), 2.39 (s, 6H, Lut-CH_3), 2.16 (br t, J_{HH}= 5.7 Hz, 4H, HIPT-NHCH$_2$CH_2), 2.11 (br t, J_{HH}= 6.8 Hz, 2H, Lut-NHCH$_2$CH_2), 1.32 (d, J_{HH}= 6.9 Hz, 24H, 4,4" -CH(CH_3)$_2$), 1.28 (d, J_{HH}= 6.9 Hz, 24H, 2,6,2",6" -CH(CH_3)$_2$). 1.25 (d, J_{HH}= 6.9 Hz, 24H, 2,6,2",6" -CH(CH_3)$_2$). ^{13}C NMR (C_6D_6, 20°C) δ 158.72, 154.58, 148.55, 148.4, 147.15, 142.68, 138.44, 121.96, 121.09, 112.84, 104.75, 52.78, 52.15, 41.48, 40.51, 35.26, 31.21, 30.94, 25.30, 25.10, 24.93, 24.87. . MS (ESI) 1212.9662 ([M+H]$^+$, calc'd. 1212.9695)

[PhLutHIPT$_2$N$_3$N]H$_3$ $Pd_2(dba)_3$ (0.045g, 0.049mmol) and *rac*-BINAP (0.094g, 0.15 mmol) were stirred under mild heating in 25 mL toluene until orange to preform the active catalyst. This was then filtered through Celite into a 300 mL toluene solution containing **1** (3.75 g, 3.39 mmol), 4-bromo-2,6-diphenyl-pyridine (see supporting information for the synthesis of this compound) (1.55 g, 5.02 mmol), and NaO^{t}Bu (0.64

g, 6.66 mmol). This solution was then heated at 95°C for 2 days, at which time it was filtered through Celite and concentrated *in vacuo* to dryness. The resulting solid was dissolved in pentane and run through a silica column, with 1:10 THF:toluene used to elute 2.07 g of the product as a light yellow foamy solid (46%). ^{1}H NMR (C_6D_6, 20°C) δ 8.32 (m, 4H, PhLut-2,6,2",6"-*H*), 7.33 (m, 6H, PhLut-3,4,5,3",4",5"-*H*), 7.22 (s, 8H, 3,5,3",5" –*H*), 6.75 (s, 2H, PhLut-3',5'-*H*), 6.57 (br t, J_{HH}= 1.3 Hz, 2H, 4'-*H*), 6.51 (d, J_{HH}= 1.4 Hz, 4H, 2',6'-*H*), 3.98 (t, J_{HH}= 5.2 Hz, 1H, PhLut-N*H*), 3.60 (br s, 2H, HIPT-N*H*), 3.17 (septet, J_{HH}= 6.9 Hz, 8H, 2,6,2",6"-C*H*Me$_2$), 2.89 (m, 8H, 4,4" -C*H*Me$_2$ and HIPTNHC*H*$_2$CH$_2$ overlapping), 2.75 (br q, J_{HH}= 5.8 Hz, 2H, PhLutNHC*H*$_2$CH$_2$, 2.24 (m, 6H, HIPTNHCH$_2$C*H*$_2$ and PhLutNHC*H*$_2$CH$_2$ overlapping), 1.31 (d, J_{HH}= 6.9 Hz, 24H, 4,4" -CH(C*H*$_3$)$_2$), 1.29 (d, J_{HH}= 6.9 Hz, 12H, 2,6,2",6" -CH(C*H*$_3$)$_2$). 1.28 (br d, J_{HH}= 6.9 Hz, 36H, 2,6,2",6" -CH(C*H*$_3$)$_2$). ^{13}C NMR (C_6D_6, 20°C) δ 158.41, 155.34, 148.61, 148.28, 147.16, 142.75, 141.27, 138.38, 129.14, 127.88, 122.10, 121.12, 112.82, 103.64, 52.87, 41.42, 35.24, 31.22, 25.31, 25.03, 24.83. MS (ESI) 1337.0025 ([M+H]$^+$, calc'd. 1337.0008)

[3,5-Bis(CF$_3$)HIPT$_2$N$_3$N]H$_3$ This compound was made similarly to other unsymmetrical TREN ligand systems. Briefly, 0.050 g (55 mmol) of $Pd_2(dba)_3$ and 0.101 g (162 mmol) of *rac*-BINAP were preformed in toluene with mild heating until orange. This was filtered through Celite into 100 mL of toluene containing 4 g (3.6 mmol) of **1**, 1.05 g (3.6 mmol) of 1-bromo-3,5-(bis)trifluoromethylbenzene, and 0.69 g (7.2 mmol) of NaO^{t}Bu. This was then heated at 105°C for 2 days, at which time the mixture was filtered, the volatiles removed *in vacuo*, and then dissolved into pentane. The pentane insoluble material was removed *via* filtration, and the resulting solution purified using silica gel column chromatography. Toluene elution purified 0.91 g (20%) of the final product as a light yellow solid. ^{1}H NMR (C_6D_6, 20°C) δ 7.25 (s, 1H, CF$_3$ arm 4-*H*), 7.22 (s, 8H, HIPT 3,5,3",5"-*H*), 6.64 (s, 2H, CF$_3$ arm 2,6-*H*), 6.57 (s, 2H, HIPT 4'-*H*), 6.48 (s, 4H, HIPT-2',6'-*H*), 3.88 (t, J_{HH}= 5.2 Hz, 1H, CF$_3$ arm N*H*), 3.51 (br s, 2H, HIPT-N*H*),

3.15 (septet, 8H, J_{HH}= 6.9 Hz, 8H, 2,6,2",6"-C*H*Me$_2$), 2.90 (septet, J_{HH}= 6.9 Hz, 4H, 4,4" -C*H*Me$_2$), 2.82 (br t, J_{HH}= 5.8 Hz, 4H, HIPT-NC*H*$_2$CH$_2$), 2.40 (br q, J_{HH}= 5.2 Hz, 2H, CF_3 arm-NC*H*$_2$CH$_2$), 2.17 (br t, J_{HH}= 5.8 Hz, 4H, HIPT-NHCH$_2$C*H*$_2$), 2.10 (br t, J_{HH}= 5.8 Hz, 2H, CF_3 arm-NCH$_2$C*H*$_2$) 1.32 (d, J_{HH}= 6.9 Hz, 24H, 4,4"-CH(C*H*$_3$)$_2$), 1.28 (d, J_{HH}= 6.9 Hz, 24H, 2,6,2",6" -CH(C*H*$_3$)$_2$), 1.25 (d, J_{HH}= 6.9 Hz, 24H, 2,6,2",6" -CH(C*H*$_3$)$_2$). ^{13}C NMR (C_6D_6, 20°C) δ 149.41, 148.66, 148.25, 147.13, 142.79, 138.31, 133.33, 132.91, 122.28, 121.12, 122.89, 112.30, 110.36, 52.95, 52.21, 41.55, 40.91, 35.25, 31.21, 25.28, 24.99, 24.83. ^{19}F NMR (C_6D_6, 20°C) δ -62.74. HRMS (ESI) 1319.9156 ([M+H]$^+$, calc'd. 1319.9177).

[3,5-DimethylHIPT$_2$N$_3$N]H$_3$ This was synthesized similarly to other compounds of this type. Briefly, 0.037 g (4 mmol) of $Pd_2(dba)_3$ and 0.075 g (12 mmol) of *rac*-BINAP were stirred with mild heating to form the orange precatalyst. This was then filtered through Celite into a toluene mixture containing 3 g (2.8 mmol) of **1**, 0.5 g (2,7 mmol) of 1-bromo-3,5-dimethylbenzene, and 0.52 g (5.4 mmol) of NaO^{t}Bu. This was then heated at 85°C overnight, with the temperature then being raised to 95°C for one day. The mixture was then filtered through Celite and the solvent removed *in vacuo*. The solid was taken up in pentane, filtered again through Celite, and the product isolated from a silica gel column. The compound was eluted with a 9:1 toluene:THF mixture to yield 0.78 g (24%) of a light yellow solid. ^{1}H NMR (C_6D_6, 20°C) δ 7.22 (s, 8H, HIPT 3,5,3",5"-*H*), 6.52 (br t, J_{HH}= 1.1 Hz, 2H, HIPT 4'-*H*), 6.46 (d, J_{HH}= 1.1 Hz, 4H, HIPT-2',6'-*H*), 6.37 (s, 1H, dimethyl-4-*H*), 6.26 (s, 2H, dimethyl-2,6-*H*), 3.94 (br s, 2H, HIPT-N*H*), 3.75 (br s, 1H, dimethyl-N*H*), 3.16 (septet, J_{HH}= 6.9 Hz, 8H, HIPT-2,6,2",6" -C*H*Me$_2$), 2.95 (septet J_{HH}= 6.9 Hz, 4H, HIPT-4,4" -C*H*Me$_2$), 2.79 (m, 8H, contains HIPT-NC*H*$_2$CH$_2$ and dimethyl-NC*H*$_2$CH$_2$), 2.17 (m, 8H, contains HIPT-NCH$_2$C*H*$_2$ and dimethyl-NCH$_2$C*H*$_2$), 2.08 (s, 6H, dimethyl-C*H*$_3$), 1.46 (d, J_{HH}= 6.9 Hz, 24H, 4,4"-CH(C*H*$_3$)$_2$), 1.38 (d, J_{HH}=6.9 Hz, 24H, 2,6,2",6" -CH(C*H*$_3$)$_2$), 1.27 (d,J_{HH}=6.9 Hz, 24H, 2,6,2",6" -CH(C*H*$_3$)$_2$). ^{13}C NMR (C_6D_6, 20°C) δ 148.79, 148.49, 148.44, 147.17, 142.58,

139.28, 138.58, 121.66, 121.03, 120.74, 112.71, 111.71, 52.59, 52.29, 41.73, 41.41, 35.27, 31.19, 30.84, 25.32, 25.06, 24.89, 21.93. HRMS (ESI) 1211.9734 ($[M+H]^+$, calc'd. 1211.9742)

[3,5-DimethoxyHIPT$_2$N$_3$N]H$_3$ This compound was synthesized similarly to the other unsymmetric ligands of its type. Briefly, 0.037 g (0.04 mmol) of $Pd_2(dba)_3$ and 0.075 g (0.12 mmol) of *rac*-BINAP were preformed with mild heating in toluene. This was filtered through Celite into a solution containing 3g (2.7 mmol) of **1**, 0.56 g (2.5 mmol) of 3,5-dimethoxy bromobenzene, and 0.52 g (5.4 mmol) of NaO^{t}Bu in 75 mL of toluene. This was then sealed and heated at 90°C for 2 days. The resulting brown solution was filtered and the solvent removed *in vacuo*. A column was done to purify the compound, with pentane and toluene as the eluents. This yields 2.2 g (65%) of the ligand as a light yellow powder. ^{1}H NMR (C_6D_6, 20°C) δ 6.46 (s, 4H, 3,5,3",5" HIPT-*H*), 6.42 (s, 4H, 3,5,3",5" HIPT-*H*), 6.40 (d, J_{HH}= 2 Hz, 2H, dimethoxy 2,6-*H*), 6.13 (t, J_{HH}= 2 Hz, 1H, dimethoxy 4-*H*), 5.94 (t, J_{HH}= 1.9 Hz, 2H HIPT 4'-*H*), 5.88 (d, J_{HH}= 1.9 Hz, 4H HIPT 2'6'-*H*), 3.94 (br s, 1H, dimethoxy N-*H*), 3.77 (br s, 2H, HIPT N-*H*), 3.27 (s, 6H, dimethoxy-OC*H*$_3$), 3.11 (septet, J_{HH}= 6.8 Hz, 8H HIPT-2,6,2",6" -C*H*Me$_2$), 2.85 (septet, J_{HH}= 6.8 Hz, 4H HIPT-4,4" -C*H*Me$_2$), 2.75 (m, 10H, contains HIPT-NC*H*$_2$CH$_2$ and dimethoxy-NC*H*$_2$CH$_2$ and dimethoxy NCH$_2$C*H*$_2$), 2.14 (br t, 4H, HIPT-NCH$_2$C*H*$_2$), 1.26 (d, J_{HH}= 6.8 Hz, 24H HIPT-4,4" –CH(C*H*$_3$)$_2$), 1.22 (d, J_{HH}= 6.8 Hz, 24H HIPT-2,6,2",6" –CH(C*H*$_3$)$_2$), 1.19 (d, J_{HH}= 6.8 Hz, 24H HIPT-2,6,2",6" –CH(C*H*$_3$)$_2$). ^{13}C NMR (C_6D_6, 20°C) δ 162.9, 162.5, 150.8, 148.4, 147.2, 142.6, 138.6, 138.2, 129.7, 126.0, 121.0, 112.8, 92.9, 54.9, 52.8, 41.5, 35.3, 31.2, 25.3, 25.0, 24.9. MS (ESI) 1243.9694($[M+H]^+$, calc'd. 1243.9641).

[MesHIPT$_2$N$_3$N]H$_3$ This was synthesized similarly to other unsymmetric TREN ligands. Briefly, 0.037 g (40 mmol) of $Pd_2(dba)_3$ and 0.075 g (12 mmol) of *rac*-BINAP were reacted in toluene with mild heating to pre-form the orange active catalyst. This was then filtered through Celite into toluene mixture containing 3 g (2.7 mmol) of **1**, 0.59

g (29.8 mmol) of 1-bromo-2,4,6-trimethylbenzene, and 0.52 g (5.4 mmol) of NaO^{t}Bu. This was then sealed and heated at 110°C for 2 days, upon which time the reaction was worked up in a manner similar to previous ligands. Column chromatography yields the product in the 8:1 toluene:THF elution as 2 g (60%) of a pale yellow solid. ^{1}H NMR (C_6D_6, 20°C) δ 7.22 (s, 8H, HIPT 3,5,3",5"-*H*), 6.77 (s, 2H, Mes-3,5-*H*), 6.54 (s, 2H, HIPT 4'-*H*), 6.48 (s, 4H, HIPT-2',6'-*H*), 3.79 (br s, 2H, HIPT-N*H*), 3.18 (septet, J_{HH}= 6.9 Hz, 8H, 2,6,2",6"-C*H*Me$_2$), 2.88 (m, 8H, containing 4,4" -C*H*Me$_2$ and HIPT-NC*H*$_2$CH$_2$), 2.78 (br t, J_{HH}= 5.8 Hz, 2H, Mes-NCH$_2$C*H*$_2$), 2.2 (m, 15H, containing Mes-C*H*$_3$, Mes-NCH$_2$C*H*$_2$, and HIPT-NCH$_2$C*H*$_2$), 1.32 (d, J_{HH}= 6.9 Hz, 24H, 4,4"-CH(C*H*$_3$)$_2$), 1.28 (d, J_{HH}= 6.9 Hz, 24H, 2,6,2",6" -CH(C*H*$_3$)$_2$), 1.26 (d, J_{HH}= 6.9 Hz, 24H, 2,6,2",6" -CH(C*H*$_3$)$_2$). ^{13}C NMR (C_6D_6, 20°C) δ 162.80, 148.48, 147318, 144.65, 142.59, 138.54, 131.03, 130.23, 129.14, 121.83, 121.07, 112.77, 55.29, 53.30, 46.83, 41.56, 35.26, 31.19, 25.32, 25.12, 24.86, 21.06, 19.22. HRMS (ESI) 1225.9906 ([M+H]$^+$, calc'd. 1225.9899)

[TripHIPT$_2$N$_3$N]H$_3$ This was synthesized in a manner similar to other unsymmetric ligands of this type. Briefly, 0.037 g (40 mmol) of $Pd_2(dba)_3$ and 0.077 g (162 mmol) of X-Phos were heated mildly in toluene to pre-form the active orange catalyst species. This was then filtered into a toluene mixture containing 3 g (2.7 mmol) of **1**, 0.92 g (3.2 mmol) of 1-bromo,2,4,6-triisopropylbenzene, and 0.39 g (40.5 mmol) of NaO^{t}Bu. This was then heated at 120°C for 2 days, upon which time the solvent was removed *in vacuo*, the resulting solid taken up into pentane and filtered in preparation for silica gel column chromatography. Elution with a 8:1 toluene:THF mixture yields a mixture of starting "2 arm" and the desired product from which the solvent was removed *in vacuo*. The resulting solid was taken up in toluene and passed through a silica plug, yielding 0.35 g (10%) of the desired product as a light yellow solid. ^{1}H NMR (C_6D_6, 20°C) δ 7.21 (s, 8H, HIPT 3,5,3",5"-*H*), 7.06 (s, 2H, Trip-3,5-*H*), 6.54 (br t, J_{HH}= 1.1 Hz, 2H, HIPT 4'-*H*), 6.51 (d, J_{HH}= 1.1 Hz, 4H, HIPT-2',6'-*H*), 3.88 (br s, 2H, HIPT-N*H*), 3.38 (septet, J_{HH}=6.9 Hz, 2H, Trip-2,6-C*H*Me$_2$), 3.17 (septet, J_{HH}= 6.9 Hz, 8H, HIPT-

2,6,2",6" -C*H*Me$_2$), 2.89 (m, 12H, containing HIPT-NC*H*$_2$CH$_2$, Trip-NC*H*$_2$CH$_2$, HIPT-4,4"-CH(C*H*$_3$)$_2$, and Trip-4-CH(C*H*$_3$)$_2$), 2.44 (br t, J_{HH}= 5.5 Hz, 2H, Trip-NCH$_2$C*H*$_2$), 2.33 (br t, J_{HH}= 5.5 Hz, 4H, HIPT-NCH$_2$C*H*$_2$), 1.32 (d, J_{HH}= 6.9 Hz, 24H, 4,4"-CH(C*H*$_3$)$_2$), 1.25 (m, 60H, 2,6,2",6" -CH(C*H*$_3$)$_2$). ^{13}C NMR (C_6D_6, 20°C) δ 148.58, 148.47, 147.17, 144.52, 142.77, 142.10, 138.51, 121.98, 121.91, 121.05, 113.00, 55.60, 53.70, 50.16, 42.13, 35.26, 31.17, 30.84, 28.56, 25.35, 25.01, 24.92, 24.96, 24.87. HRMS (ESI) 1310.0833 ([M+H]$^+$, calc'd. 1310.0838)

[N(propylNHIPT)$_3$]H$_3$] This compound was synthesized similarly to other TREN based ligands. Briefly, **HIPTBr** (5 g, 8.9 mmol) was added to *N,N*-bis(3-aminopropyl)propane-1,3-diamine (0.54 g, 2.7 mmol) and NaO^{t}Bu (0.9 g, 9.3 mmol). A solution of Pd_2dba_3 (0.065 g, 0.07 mmol) and *rac*-BINAP (0.130 g, .21 mmol), that had been pre-reacted until bright orange in ~ 10 mL toluene, was filtered through a Celite plug into the mixture. The total reaction mixture was then taken up to ~85 mL and the reaction vessel sealed. This was then heated at 80°C for 2 days. The solution was filtered through Celite and the solvent removed *in vacuo*. A column was performed, with a 10:1 toluene:THF mixture used to elute the product. Total yield was 3.1 g (66%) of a pale tan foamy solid. ^{1}H NMR (C_6D_6, 20°C) δ 7.23 (s, 8H, 3,5,3",5" –*H*), 6.55 (t, 3H, J_{HH}=1.4 Hz, 4'-*H*), 6.36 (d, 6H, J_{HH}=1.4 Hz, 2',6'-*H*), 3.94 (t, 3H, J_{HH}=5 Hz, N*H*), 3.21 (septet, 12H, J_{HH}=6.9 Hz, 2,6,2",6"-C*H*Me$_2$), 2.87 (m, 12H, contains 4,4"-C*H*Me$_2$ and N(CH$_2$CH$_2$C*H*$_2$NH$_2$)$_3$), 2.09 (t, 6H, J_{HH}=6.9 Hz, N(C*H*$_2$CH$_2$CH$_2$NH$_2$)$_3$), 1.30 (m, 114H, contains 2,4,6,2",4",6" CH(C*H*$_3$)$_2$ and N(CH$_2$C*H*$_2$CH$_2$NH$_2$)$_3$). ^{13}C NMR (C_6D_6, 20°C) δ 148.75, 148.52, 147.20, 142.49, 138.65, 121.44, 121.09, 112.62, 52.83, 43.21, 35.25, 31.20, 25.32, 25.09, 24.83. MS (ESI) 1630.3302([M+H]$^+$, calc'd. 1630.3342).

References

1. Cummins, C.C.; Schrock, R.R.; Davis, W.M. *Organometallics* **1992**, *11*, 1452.

2. Schrock, R. R. *Acc. Chem. Res.* **1997**, *30*, 9.

3. Greco, G. E.; O'Donoghue, M. B.; Seidel, S. W.; Davis, W. M.; Schrock, R. R. *Organometallics* **2000**, *19*, 1132.

4. Reid, S. W.; Neumer, B.; Schrock, R. R.; Davis, W. M. *Organometallics* **1998**, *17*, 4077.

5. Schrock, R. R.; Cummins, C. C.; Wilhelm, T.; Lin, S.; Reid, S. M.; Kol, M.; Davis, W. M. *Organometallics* **1996**, *15*, 1470.

6. Schrock, R.R. *Acc. Chem. Res.* **2005**, *38*, 955.

7. Cummins, C.C.; Schrock, R.R. *Inorg. Chem.* **1994**, *33*, 395.

8. Schrock, R.R.; Shih, K-Y.; Dobbs, D.A.; Davis, W.M. *J. Am. Chem. Soc.* **1995**, *117*, 6609.

9. Kol, M.; Schrock, R.R.; Kempe, R.; Davis, W.M. *J. Am. Chem Soc.* **1994**, *116*, 4382.

10. Greco, G.E. Ph.D. thesis, Massachusetts Institute of Technology, Cambridge, MA, 2000.

11. Guram, A.; Rennels, R.; Buchwald, S. *Angew. Chem. Int. Ed.* **1995**, *34*, 1348.

12. Louie, J.; Hartwig, J. *Tet. Lett.* **1995**, 3609.

13. A) Hartwig, J. *Acc. Chem. Res.* **1998**, *31*, 852. B) Wolfe, J. P.; Wagaw, S.; Marcoux, J.-F.; Buchwald, S. L. *Acc. Chem. Res.***1998**, *31*, 805.

14. Yandulov, D.V.; Schrock, R.R. *Science* **2003**, *76*, 301.

15. Ritleng, V.; Yandulov, D. V.; Weare, W. W.; Schrock, R. R.; Hock, A. S.; Davis, W. M. *J. Am. Chem. Soc.* **2004**, *126*, 6150.

16. Vinod, T.K.; Hart, H. *J. Org. Chem.* **1991**, *56*, 5630.

17. Jereb, M.; Zupan, M.; Stauber, S. *Chem. Comm.* **2004**, 2614.

18. Marion, N.; Navarro, O.; Mei, J.; Stevens, E.D.; Scott, N.M.; Nolan, S.P *J. Am. Chem. Soc.* **2006**, *128*, 4101.

19. Mosch-Zanetti, N. C.; Kopke, S.; Herbst-Irmer, R.; Hewitt, M. *Inorg. Chem.*, **2002**; *41*, 3513.

20. Yandulov, D.V.; Schrock, R.R. *Inorg. Chem.* **2005**, *44*, 1103.

21. Neumann, U.; Vogtle, F. *Chem. Ber.* **1989**, *122*, 589.

22. A) Fallahpour, R.-A.; Neuburger, M. *New J. Chem.* **1999**, 53. B) Fallahpour, R.-A.; Neuburger, M. *Eur. J. Org. Chem.* **2001**, 1853.

23. Pangborn, A.B.; Giardello, M.A.; Grubbs, R.H.; Rosen, R.K.; Timmers, F.J. *Organometallics* **1996**, *15*, 1518.

24. Yandulov, D.V.; Schrock, R.R. *J. Am Chem. Soc.* **2002**, *124*, 6252.

25. Yandulov, D.V.; Schrock, R.R.; Rheingold, A.L.; Ceccarelli, C.; Davis, W.M. *Inorg. Chem.* **2003**, *42*, 796.

26. Ochiai, E. *J. Org. Chem.* **1953**, *18*, 534.

27. Evans, R. F.; Brown, H. C. *J. Org. Chem.* **1962**, *27*, 1329.

28. Evans, R. F.; Brown, H. C. *J. Org. Chem.* **1962**, *27*, 1665.

29. Talik, T.; Talik, Z.; Ban-Oganowska, H. *Synthesis* **1974**, 293.

CHAPTER 3

Synthesis and Characterization of Dinitrogen Reduction Intermediates Using Molybdenum Triamidoamine Compounds

Portions of the material covered in this chapter have appeared in print:

Ritleng, V.; Yandulov, D. V.; Weare, W. W.; Schrock, R. R.; Hock, A. S.; Davis, W. M. *J. Am. Chem. Soc.* **2003**, *126*, 6150-6163.

Introduction

Our group recently has demonstrated that molybdenum compounds supported by triamidoamine ligands act as dinitrogen reduction catalysts at room temperature and ambient pressure.[1] These studies explored the reduction cycle, whose reagents are only protons and electrons, in great detail and crystallographically characterized 8 of the possible 13 intermediates[2,3,4] (Figure 3.1). With stable intermediates, we were able to isolate and study individual steps in the reaction cycle. Ligand modification, as reported in chapter 2, should allow us to study these steps in even more detail and show us more about what is important for catalytic success.

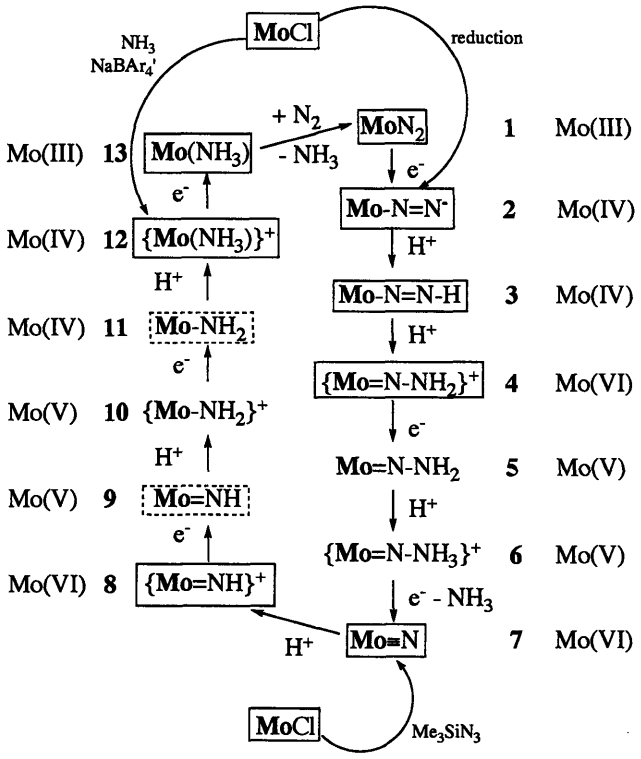

Figure 3.1) Mechanistic cycle for dinitrogen reduction with the entry points directly available from LMoCl. Compounds in solid boxes have been crystallographically characterized. Compounds in dashed boxes have been observed *in situ*. All other compounds are proposed intermediates that have yet to be unambiguously observed.

As described in chapter 2, we have synthesized a variety of ligands in our attempts to broaden our understanding of catalytic dinitrogen reduction at a single molybdenum center. This chapter describes the synthesis and characterization of a number of dinitrogen reduction intermediates (and their precursors) utilizing these ligands. The new ligands do not, in general, drastically alter the reactivity of these complexes from the parent HIPT system,[5] although all of the described unsymmetric compounds are more soluble than their symmetric counterparts.

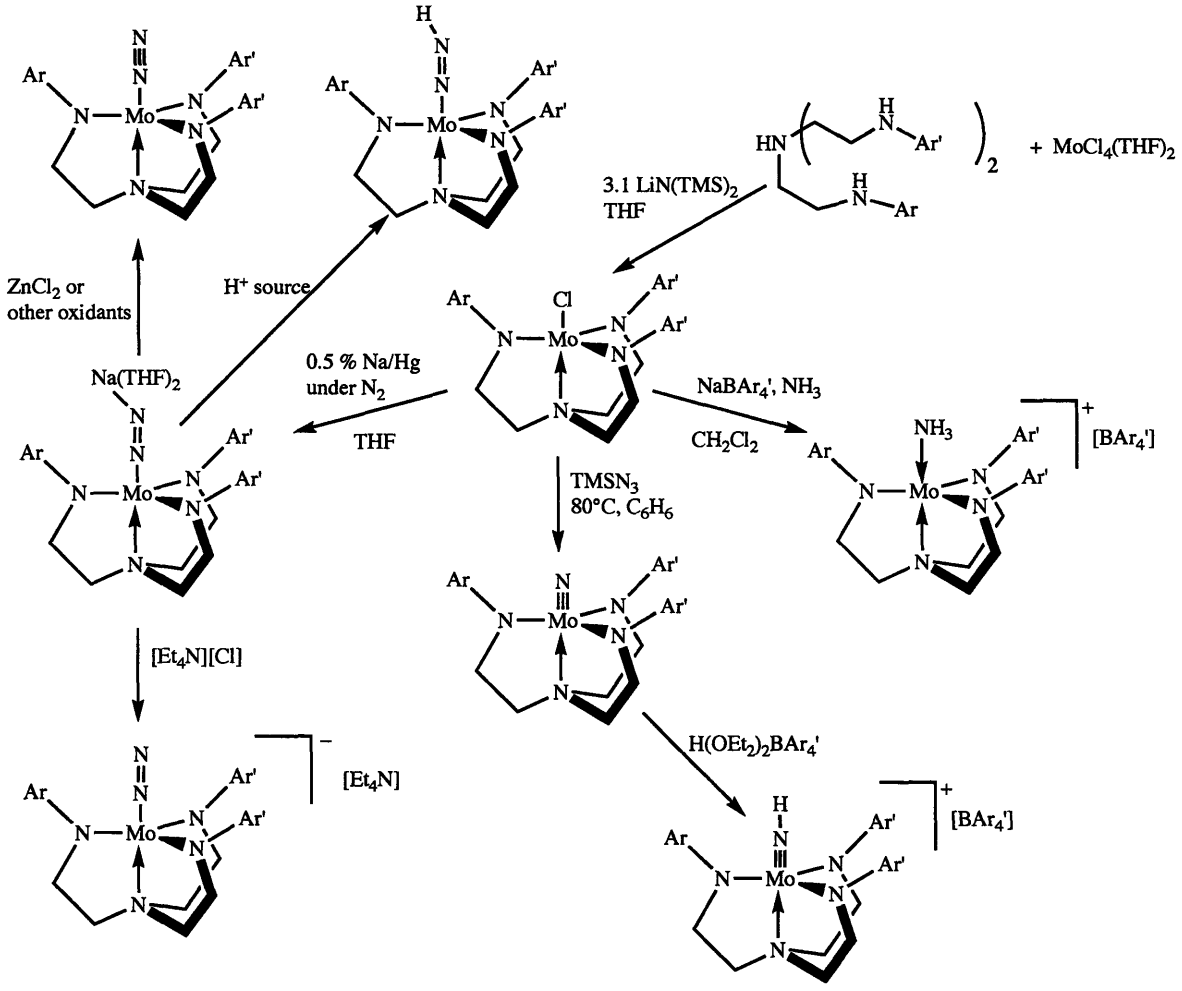

Figure 3.2) Synthesis of metal compounds as described in this chapter

Results and Discussion

Symmetric Compounds

The standard synthetic entry point for molybdenum based TREN compounds is the Mo(IV) chloride complex **L**MoCl.[6,7] Due to the established instability of the lithium salts of [**HIPTN$_3$N**],[8] [***p*BrHIPTN$_3$N**]MoCl was synthesized by *in situ* deprotonation (with LiN(SiMe$_3$)$_2$) of the ill-defined adduct between [***p*BrHIPTN$_3$N**]H$_3$ and MoCl$_4$(THF)$_2$ (Figure 3.2). This reaction produces the desired compound as a bright orange solid in good yield.

For this particular ligand, the simplest entry into the dinitrogen reduction cycle is the synthesis of the relatively stable Mo(VI) nitride. [***p*BrHIPTN$_3$N**]MoN was synthesized from the reaction of [***p*BrHIPTN$_3$N**]MoCl with Me$_3$SiN$_3$ at elevated temperatures. The desired diamagnetic compound was isolated in good yield as a canary yellow solid. With the assistance of Dr. Peter Tsang, variable temperature ^{1}H NMR spectra (Figure 3.3) were taken of [***p*BrHIPTN$_3$N**]MoN to probe the broadened feature attributed to the ortho C-H protons located at ~7.8 ppm. This broadening is also observable in the parent system, but this compound had not been previously studied by VT NMR. All features of these spectra behave as expected, with the aryl C-*H* peaks broadening into the baseline at 0 °C and reappearing at -8.9 ppm when frozen out at -60 °C. Other features also behave as expected. In particular, the shift and broadening of the resonances attributed to the methylene backbone C-*H* groups (at room temperature these peaks are located at 3.6 and 2 ppm) is exactly what one would expect with their assignments as they broaden at a lower temperature than the aryl rings, yet shift extensively as the aryl rings freeze out These broaden into the baseline at -30 °C, and remain broadened even at -60 °C. All the observed resonances behave in a manner consistent with our previous assignments. Therefore, this experiment confirms both the identity of **L**MoN and the assignment of individual resonances for **L**MoN.

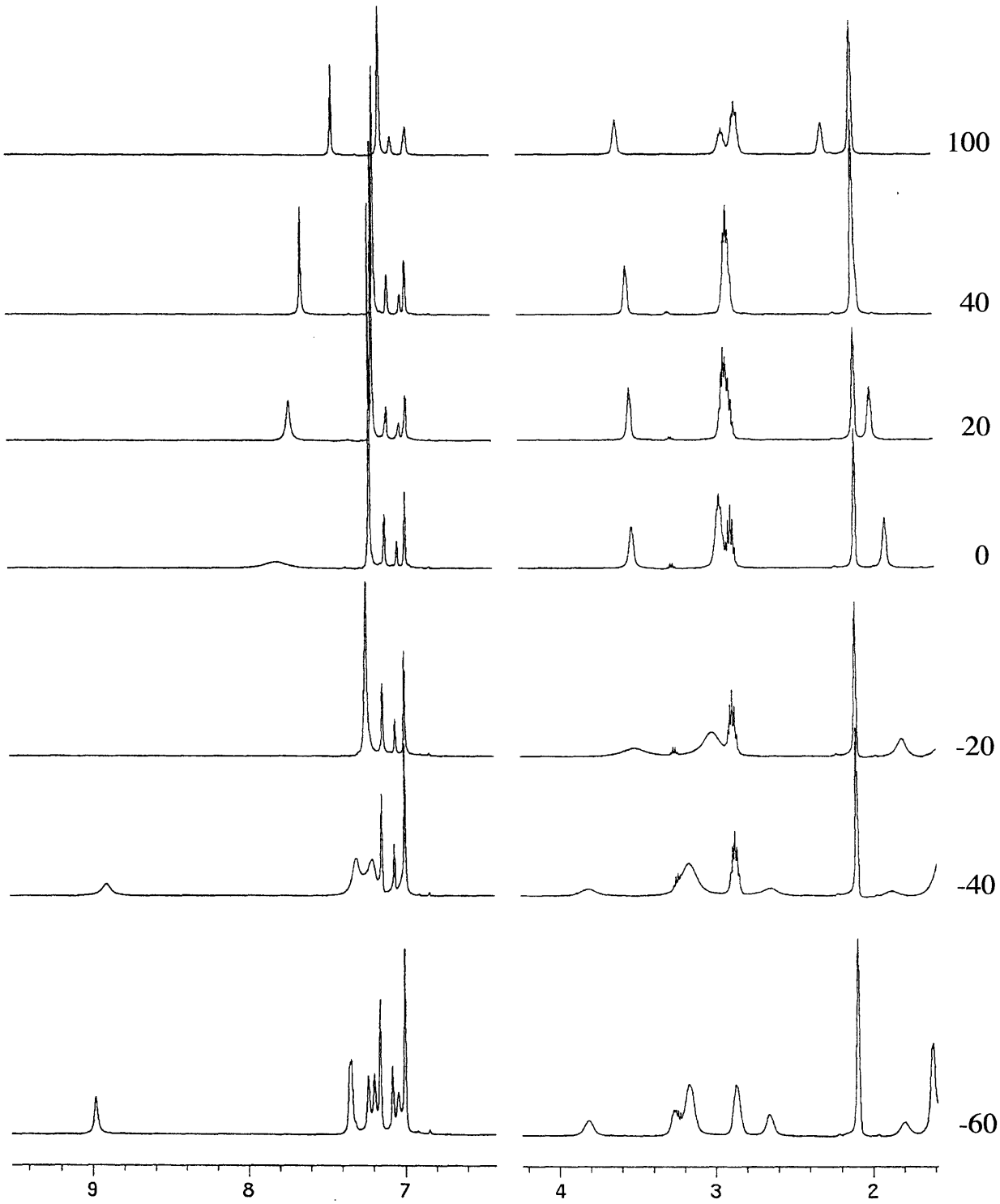

Figure 3.3) Variable temperature ^{1}H NMR of [***p*BrHIPTN$_3$N**]MoN

An x-ray crystallographic study was also performed on [***p*BrHIPTN$_3$N**]MoN[5] (Figure 3.4). The crystal, grown from pentane, retained the bright yellow color of the powder sample. The crystal was solved in $Pna2_1$ with two independent molecules in the unit cell. Analysis of the metric parameters (Table 3.1) show that this compound is quite similar to [**HIPTN$_3$N**]MoN. This was not unexpected as the ligand perturbation from [**HIPTN$_3$N**] to [***p*BrHIPTN$_3$N**] (the addition of a bromine in the *para* position) is not significant close to the metal. The similarity between all the compounds discussed in this thesis with previously described structures shows that the triamidoamine motif is robust to structural change even if the ligand is altered on the periphery.

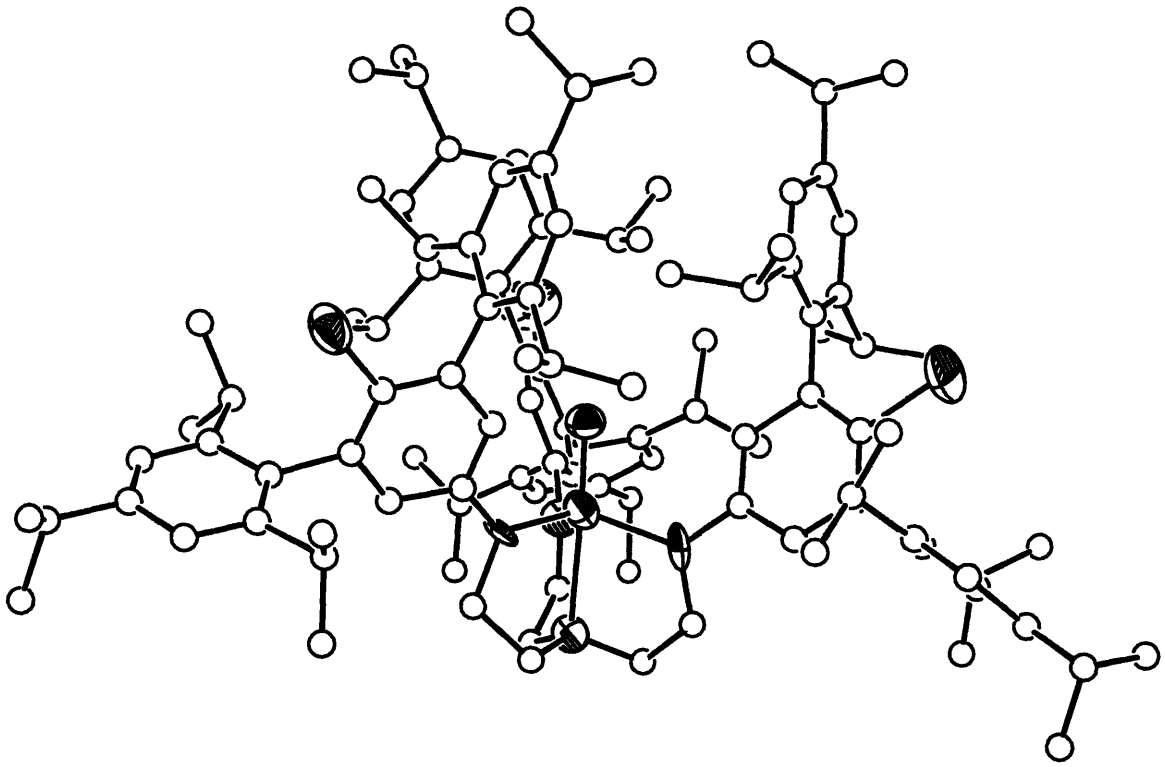

Figure 3.4) X-ray determined crystal structure of [***p*BrHIPTN$_3$N**]MoN. Hydrogen atoms are omitted for clarity. While all atoms were anisotropically refined, carbon atoms are depicted as spheres for clarity's sake.

Table 3.1) Selected Bond Lengths and Angles of [*p*BrHIPTN$_3$N]MoN vs. [HIPTN$_3$N]MoN

Bond	[*p*BrHIPTN$_3$N]MoN [5]	[HIPTN$_3$N]MoN [2]
Mo-N5 (nitride)	1.679(9) Å	1.656(8) Å
Mo-N2 (amide)	2.018(10) Å	2.011(8) Å
Mo-N4 (amine)	2.324(9) Å	2.399(8) Å
N2-Mo-N5	101.1(5)°	101.6(3)°
N4-Mo-N5	178.1(4)°	179.0(3)°
N1-Mo-N2	114.2(4)°	114.5(3)°

Protonation of of [*p*BrHIPTN$_3$N]MoN with H(OEt$_2$)$_2$BAr$_4$' results in the formation of [[*p*BrHIPTN$_3$N]MoNH][BAr$_4$'].[5] The presence of this compound was confirmed by ^{1}H NMR and IR spectroscopy; $\nu_{N\text{-}H}$ was clearly observed at 3336 cm^{-1}. Attempts to estimate the pK$_a$ of this compound by partial protonation with [2,6-lutidinium][BAr$_4$'] or [Et$_3$NH][BAr$_4$'] provide ambiguous results due to the partial solubility of the protonated intermediates (this holds true for all of the compounds synthesized in this chapter).

Reduction of [*p*BrHIPTN$_3$N]MoCl with Mg powder resulted in a mixture of [*p*BrHIPTN$_3$N]MoN$_2$Mg(THF)$_x$ and [*p*BrHIPTN$_3$N]MoN$_2$.[5] This mixture was characterized by both ^{1}H NMR and IR spectroscopy, with IR clearly showing the presence of both species at $\nu_{N\text{-}N}$ = 1992 cm^{-1} for [*p*BrHIPTN$_3$N]MoN$_2$ and a broad peak centered at 1788 cm^{-1} for [*p*BrHIPTN$_3$N]MoN$_2$Mg(THF)$_x$Cl.

The reaction of [HIPTpropylN$_3$N]H$_3$ with MoCl$_4$(THF)$_2$ and LiN(SiMe$_3$)$_2$ resulted in the formation of the desired [HIPTpropylN$_3$N]MoCl in moderate yield. The compound is isolated as a tan solid, but when dissolved the solution is the same bright orange as other triamidoamine molybdenum chloride compounds. An x-ray crystal structure analysis was performed on [HIPTpropylN$_3$N]MoCl (Figure 3.5). with the

compound solved in $P2_12_12_1$ and having one independent molecule in the unit cell. No obvious intermolecular contacts can be observed in the crystal to explain the chromatic shift upon dissolution. The aspect of this crystal structure that stands out is that the metal sits nearly co-planar with the amides, unlike the ethyl based triamidoamine compounds where the molybdenum sits slightly above this plane. The bond distances, however, remain similar despite this alteration in geometry (Table 3.2). The other primary difference is that the amide-aryl bonds are somewhat more tilted away from the N(4)-Mo-Cl axis than that of **[HTBTN$_3$N]**MoCl, resulting in a shallower ligand binding pocket.

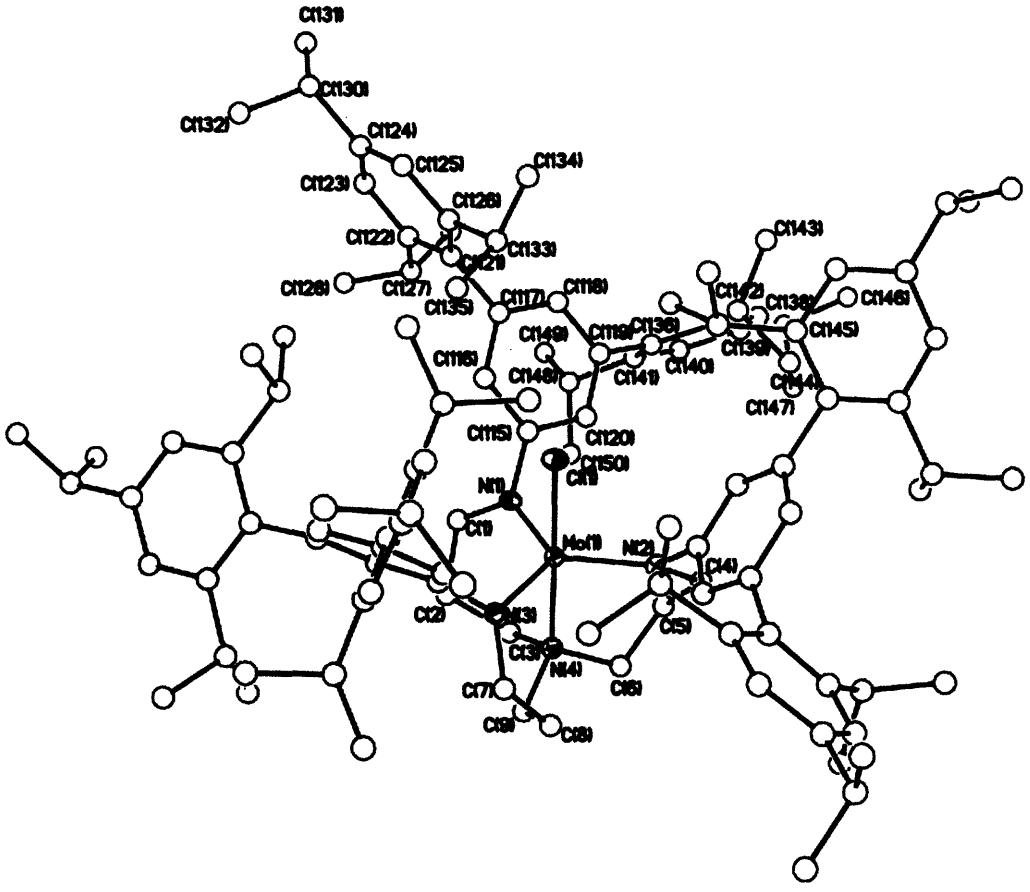

Figure 3.5) X-ray determined crystal structure of **[HIPTpropylN$_3$N]**MoCl. Hydrogen atoms are omitted for clarity. While all atoms were refined anisotropically, carbon atoms are depicted as spheres for clarity.

Table 3.2) Selected Bond Lengths and Angles of [HIPTpropylN$_2$N]MoCl vs. [HTBTN$_3$N]MoCl

Bond	[HIPTpropylN$_3$N]MoCl	[HTBTN$_3$N]MoCl [5]
Mo-Cl	2.3843(5) Å	2.33 Å
Mo-N1 (amide)	1.9688(17) Å	1.99 Å
Mo-N4 (amine)	2.3230(18) Å	2.34 Å
N4-Mo-N1	89.03(7)°	99°
N4-Mo-Cl	178.99(5)°	179°

Reactivity of **[HIPTpropylN$_3$N]**MoCl appears to be much different from that of **[HIPTN$_3$N]**MoCl, particularly when attempting to synthesize **[HIPTpropylN$_3$N]**MoN. Reaction with Me_3SiN_3 at elevated temperatures in a variety of solvents resulted in no reaction, with **[HIPTpropylN$_2$N]**MoCl being isolated cleanly from the reaction mixture. How much the structural differences of **[HIPTpropylN$_2$N]**MoCl can be used to explain this reactivity difference remains an area of speculation. Jia Min Chin is currently studying this and other related compounds in more detail.

Unsymmetric Compounds

The "hybrid" (see Figure 2.8) ligands were reacted with $MoCl_4(THF)_2$ and $LiN(SiMe_3)_2$ to produce paramagnetic **L**MoCl. These bright orange compounds were characterized by ^{1}H NMR and elemental analysis. The paramagnetically shifted ^{1}H NMR resonances are similar to previously identified species of this type, with separate resonances attributed to the unsymmetric arms. In a few cases three resonances are observed, one due to the variant arm and the other two assigned to the inner and outer protons of the remaining arms (see Figure 3.9 for an example of this type of splitting).

An x-ray crystal structure was performed on **[3,5-bis(CF$_3$)HIPT$_2$N$_3$N]**MoCl (Figure 3.6). As seen in Table 3.3, the presence of the smaller third arm does not significantly change the metric parameters around the metal relative to

[HTBTN$_3$N]MoCl. The primary difference with the smaller aryl arm is that it does not sterically shield the binding pocket as efficiently at HIPT, significantly opening one face of the Cl binding pocket. This diminishes the protection available for the dinitrogen reduction site relative to symmetric ligands, providing our first hint as to why these compounds are not catalytically active for N_2 reduction.

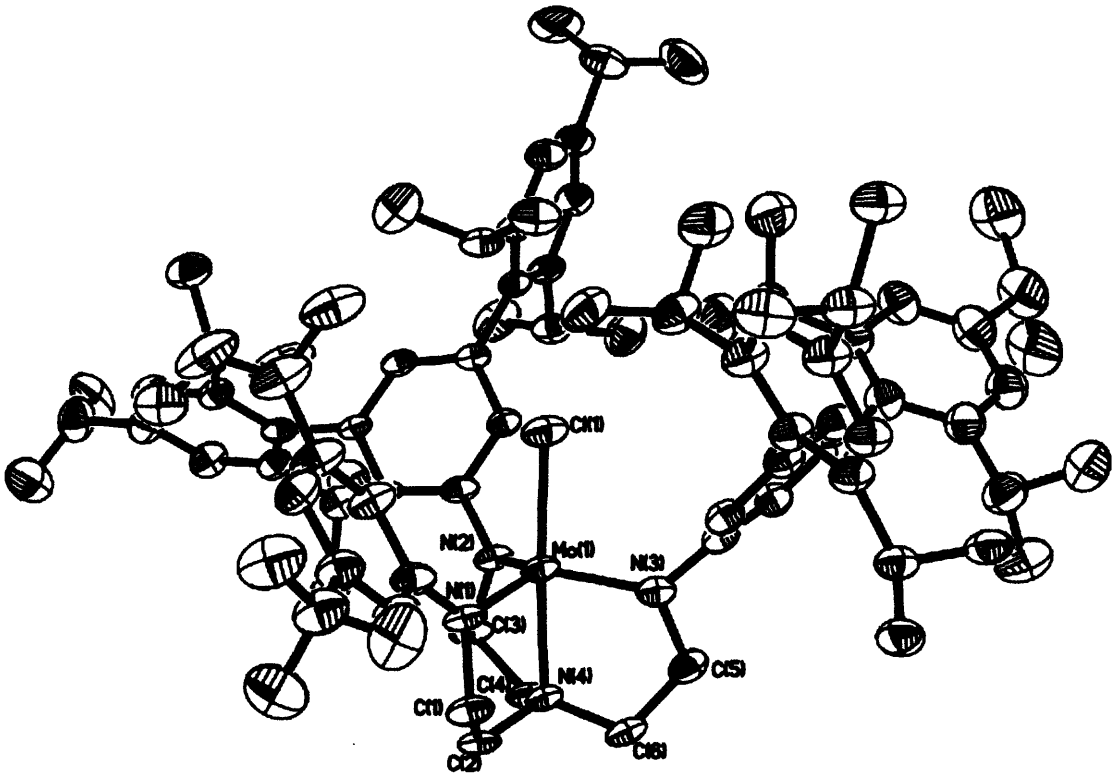

Figure 3.6) X-ray determined crystal structure of **[3,5-bis(CF$_3$)HIPT$_2$N$_3$N]**MoCl. Hydrogen atoms are omitted for clarity.

Table 3.3) Selected Bond Lengths and Angles of [3-5bis(CF_3)HIPT$_2$N$_3$N]MoCl vs. [HTBTN$_3$N]MoCl

Bond	[3,5-bis(CF_3)HIPT$_2$N$_3$N]MoCl	[HTBTN$_3$N]MoCl [5]
Mo-Cl	2.331(2) Å	2.33 Å
Mo-N1 (amide)	1.978(7) Å	1.99 Å
Mo-N4 (amine)	2.199(6) Å	2.34 Å
N4-Mo-N1	100.20(18)°	99°
N4-Mo-Cl	176.10(17)°	179°

As with the symmetric compounds, successful synthesis of LMoCl allows us to enter the dinitrogen reduction pathway at a number of places (Figure 3.1). We synthesized the bright yellow LMoN nitride compounds by the reaction of LMoCl with Me_3SiN_3 in benzene at elevated temperatures. Due to their diamagnetic nature and similarity to symmetric molybdenum nitrides, we were able to assign all the spectral features present in ^{1}H NMR. The nitrides are relatively stable and crystalline, especially when compared to the other dinitrogen reduction intermediates, therefore we typically utilize them as the precatalyst for catalytic investigations.

Reduction of LMoCl with sodium sand or 0.5% sodium/mercury amalgam yields [$LMoN_2$][$Na(THF)_2$]. An x-ray crystal structure was performed on **[3,5-dimethylHIPT$_2$N$_3$N]**$MoN_2Na(THF)_2$ (Figure 3.7). This was solved in R_3, with one independent molecule in the unit cell. Again, as in **[3,5-bis(CF_3)HIPT$_2$N$_3$N]**MoCl, the presence of a hybrid arm does not significantly alter the metric parameters around molybdenum (Table 3.4). The most glaring difference is the off-axis coordination of the sodium atom due to the open space provided by the smaller 3,5-dimethylphenyl group. This tilts the Mo-N=N angle to 174°, different from the 180° seen in the symmetric series. This tilt, and the "open" nature of the binding pocket, may be important in explaining the reactivity of other diazenido intermediates such as LMoNNH.

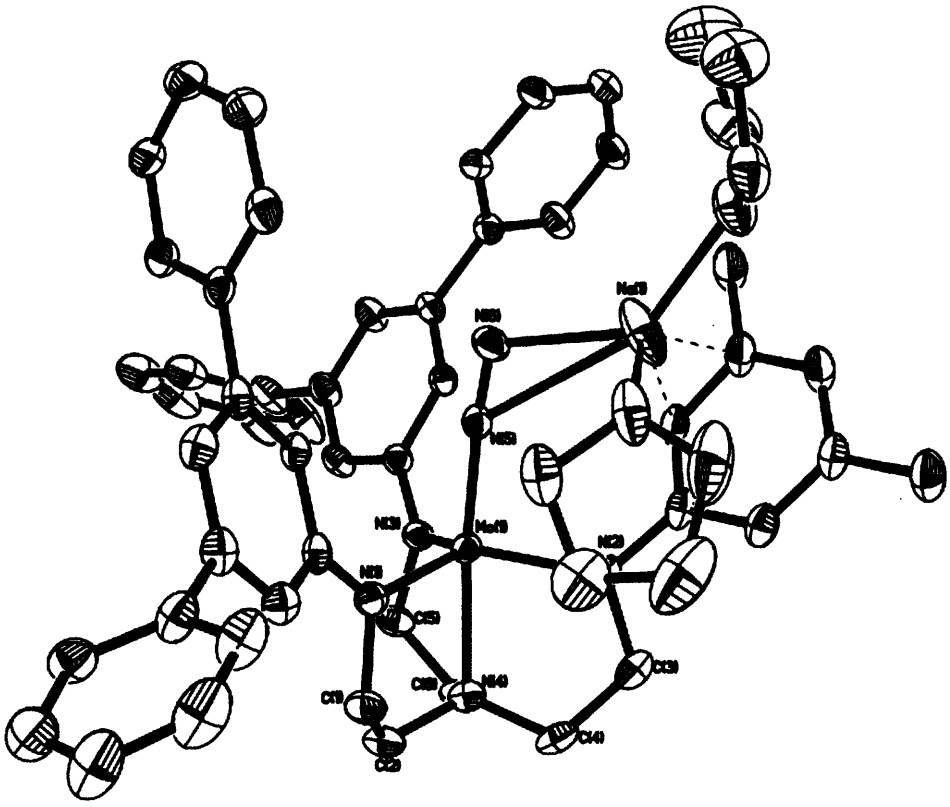

Figure 3.7) Thermal ellipsoid representation of the x-ray structure for [**3,5-dimethylHIPT$_2$N$_3$N**]MoN$_2$Na(THF)$_2$. Hydrogen atoms and isopropyl groups are omitted for clarity.

Table 3.4) Selected Bond Lengths and Angles of [3,5-dimethylHIPT$_2$N$_3$N]MoN$_2$Na(THF)$_2$ vs. [HIPTN$_3$N]MoN$_2$Mg(THF)$_3$

Bond	[3,5-DimethylHIPT$_2$N$_3$N]MoN$_2$Na(THF)$_2$	[HIPTN$_3$N]MoN$_2$Mg(THF)$_3$[3]
N5-N6 (N$_2$)	1.171(6) Å	1.15 Å
Mo-N5 (N$_2$)	1.882(4) Å	1.86 Å
Mo-N4 (amine)	2.209(4) Å	2.24 Å
Mo-N3 (amide)	2.022(4) Å	2.02 Å
N4-Mo-N5	174.09(17)°	178°
N4-Mo-N1	81.25(16)°	80°
Mo-N5-N6	174.2(4)°	178°
N5-N6-Na	110.7(4)°	

Protonation of **[3,5-bis(CF$_3$)HIPT$_2$N$_3$N]**MoN$_2$Na(THF)$_2$ with H(OEt$_2$)BAr$_4$ in C$_6$D$_6$ allowed for the observation of **[3,5-bis(CF$_3$)HIPT$_2$N$_3$N]**MoN$_2$H by ^{1}H NMR. This compound has a resonance attributable to MoNN*H* at 8.6 ppm, with $J_{N\alpha-H}$ = 54 Hz and $J_{N\beta-H}$ = 8 Hz in the $^{15}N_2$ labeled compound. These relatively low values of J_{N-H} are indicative of a weak N-H bond in this compound. Unlike the parent **[HIPTN$_3$N]**MoN$_2$H, this compound was not able to be isolated due to its instability at room temperature. **[3,5-bis(CF$_3$)HIPT$_2$N$_3$N]**MoN$_2$H decomposes cleanly, with a $t_{1/2}$ of ~ 17 ± 2 h, to yield **[3,5-bis(CF$_3$)HIPT$_2$N$_3$N]**MoN$_2$ in a first order reaction with respect to metal (see chapter 4 for a more detailed discussion of this decomposition and what it means for catalysis). As mentioned, $^{15}N_2$ labeled **[3,5-bis(CF$_3$)HIPT$_2$N$_3$N]**Mo^{15}N$_2$H was also observed, with the surprising discovery that the $^{14}N_2$ substituted compound grew in over time, with $t_{1/2}$ = 4.5 h (Figure 3.8). The mechanism of N_2 exchange in this compound has yet to be elucidated, but our preliminary hypothesis is this exchange proceeds through a 6 coordinate intermediate where both NNH and N_2 ligands are bound to the metal. This would allow for H• exchange between the two bound N_2 groups. In light of this result,

we examined the stability of **[HIPTN$_3$N]**Mo^{15}N$_2$H and found that it also undergoes this

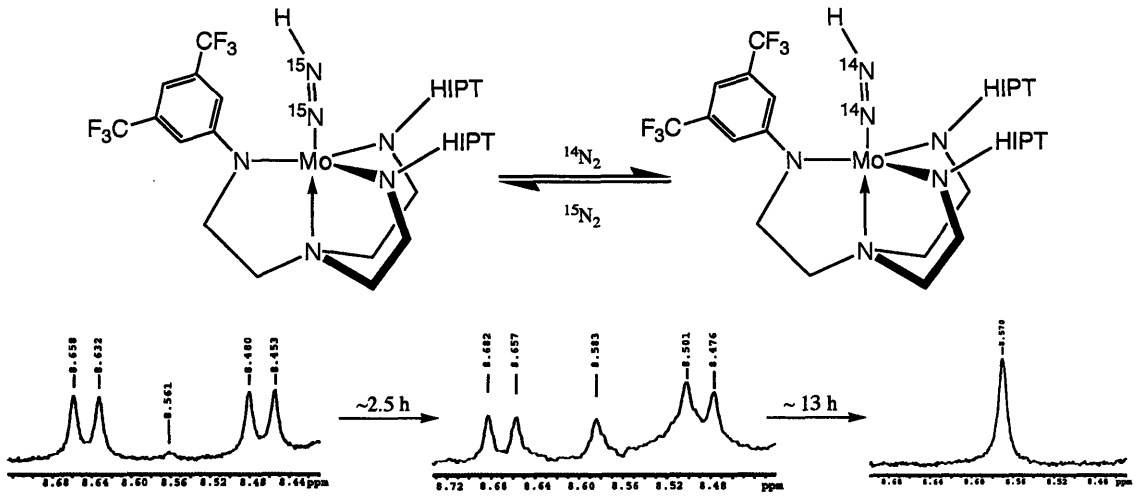

Figure 3.8) Exchange of $^{14}N_2$ for $^{15}N_2$ in **[3,5-bis(CF$_3$HIPT$_2$N$_3$N]**MoN$_2$H.

exchange, but with a $t_{1/2}$ that is at least 50 times longer. We do not know yet whether the rate of this exchange is a universal indicator for catalytic success, although it appears that it is not a reason for the failure of unsymmetric ligands to catalyze the reduction of dinitrogen (see chapter 4 for more details).

[LMoN$_2$][Na(THF)$_2$] can be oxidized with mild oxidants such as $ZnCl_2$ to yield the spectroscopically characterized neutral **L**MoN$_2$ compounds.[3] Due to their high solubility, we were unable to obtain pure samples for elemental analysis (all samples contained 5-10% of free ligand), but IR and NMR spectra clearly show the presence of this compound when compared to previously characterized **L**MoN$_2$ complexes. By ^{1}H NMR we were able to observe multiple peaks attributed to the backbone protons, similar to **L**MoCl (Figure 3.9). IR analysis shows a strong absorption for $\nu_{N\text{-}N}$ at ~1990 cm^{-1}, as previously observed for symmetric MoN$_2$ compounds. Results of these IR spectra are shown in Table 3.5.

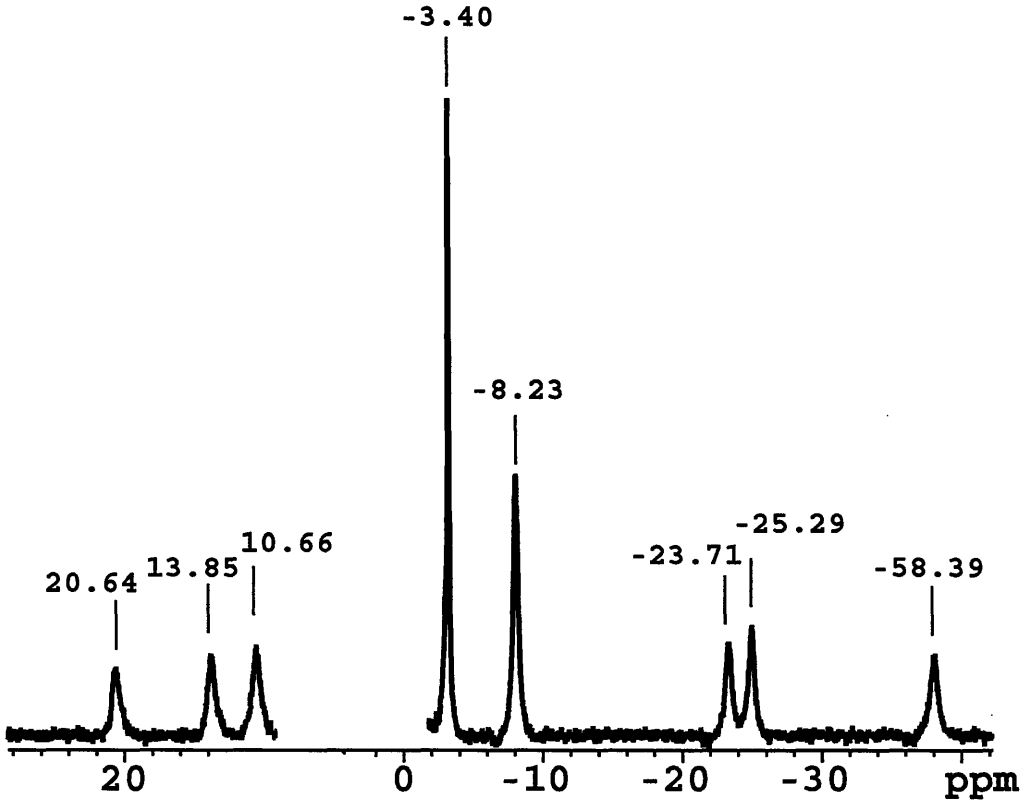

Figure 3.9) ^{1}H NMR of **[3,5-bis(CF_3)HIPT$_2$N$_3$N]**MoN_2. Diamagnetic region is removed for clarity.

Table 3.5) IR Analysis of $LMoN_2$

Compound	$\nu_{N\text{-}N}$ (cm^{-1})
[HIPTN_3N]MoN_2	1990 [2]
[*p*BrHIPTN_3N]MoN_2	1992 [5]
[HTBTN_3N]MoN_2	1990 [5]
[LutHIPT$_2N_3$N]MoN_2	1991
[LutHIPT$_2N_3$N]MoN_2	1988
[3,5-Bis(CF_3)HIPT$_2N_3$N]MoN_2	1992
[3,5-DimethylHIPT$_2N_3$N]MoN_2	1987
[3,5-DimethoxyHIPT$_2N_3$N]MoN_2	1984
[MesitylHIPT$_2N_3$N]MoN_2	1986
[2,4,6-TriisopropylHIPT$_2N_3$N]MoN_2	2007

Examination of the IR data shows that the location of $\nu_{N\text{-}N}$ is sensitive to the relative electron donating nature of the third arm in the hybrid ligands. This is presumably due to alteration of the molybdenum backbonding interaction with the dinitrogen antibonding orbital. The 3,5-substituted compounds best demonstrate this trend, with the $\nu_{N\text{-}N}$ vibration lowering in energy from the most electron withdrawing ligand (**[3,5-bis(CF_3)HIPT$_2N_3$N]**MoN_2 at 1992 cm^{-1}) to the least electron withdrawing ligand (**[3,5-dimethoxyHIPT$_2N_3$N]**MoN_2 at 1984 cm^{-1}). Attempts were made to correlate these values to the Hammet parameters of the ligands, but other factors (such as steric interactions) made the results of such an analysis not predictive. The primary example for this effect is **[2,4,6-TriisopropylHIPT$_2N_3$N]**MoN_2, where $\nu_{N\text{-}N}$ is found at 2007 cm^{-1}. We propose that this unusually high value is due to steric crowding at the metal, destabilizing the Mo-N_2 bond. While the $\nu_{N\text{-}N}$ stretch can demonstrate the relative backbonding abilities of these compounds, it has been shown to NOT be predictive tool for catalytic success[9] (see chapter 4 for more details).

Conclusions

This chapter demonstrates that important dinitrogen reduction intermediates can be synthesized utilizing all of the triamidoamine ligands described in chapter 2. Although our synthetic exploration of these compounds is still somewhat limited, our interests are not ultimately in the synthesis of "new" compounds with these ligands. Instead, we synthesized these compounds in order to access important aspects of catalytic dinitrogen reduction. In particular, we wanted pre-catalysts (**L**MoN) for catalytic study, or compounds to directly probe the important steps in catalysis (**L**MoNH_3 → **L**MoN_2 or **L**MoN_2H). Such studies are described in the following chapter.

Experimental Section

General. Air- and moisture- sensitive compounds were manipulated utilizing standard Schlenk and dry-box techniques under an atmosphere of dinitrogen. All glassware used was oven and/or flame dried immediately prior to use. Pentane, diethyl ether, toluene, and benzene were purged with dinitrogen and passed through activated alumina columns. Benzene was additionally passed through a Q5 column.[10] THF and benzene-d_6 were additionally dried with sodium/benzophenone ketyl and vacuum transferred prior to use. All other solvents mentioned were freeze-pump-thaw degassed 3 times prior to use. All dried and deoxygenated solvents were stored in a dinitrogen-filled glove box over molecular sieves or in Teflon® sealed glass solvent bombs. NaO^{t}Bu (Aldrich), Me_3SiN_3 (Lancaster), 50% terminal 15N NaN_3 (Cambridge Isotopes) $(Me_3Si)_2NLi$ (sublimed, Aldrich), and $MoCl_5$ (Strem), were used as received, unless indicated otherwise. $MoCl_4(THF)_2$,[11] and $H(OEt_2)_2BAr_4$' were prepared according to published procedures or with slight modifications. See chapter 2 for synthesis of the ligands utilized in this chapter. All Mo complexes were stored under dinitrogen at –35°C. ^1H and ^{13}C NMR spectra were recorded on a Varian Mercury 300. NMR spectra are referenced to internal residual solvent peaks (^1H and ^{13}C NMR) or to external C_6H_5F (δ = -113.15 ppm, ^{19}F NMR).

[*p*BrHIPTN$_3$N]MoCl[5] The procedure followed was nearly identical to the procedure published by our lab previously. Briefly, **[*p*BrHIPTN$_3$N]**H$_3$ (2.5 g, 0.14 mmol) and MoCl$_4$(THF)2 (0.524 g, 0.14 mmol) were dissolved in THF (200mL). This was stirred for one hour, at which time (Me$_3$Si)$_2$NLi (0.711 g, 0.42 mmol) was slowly added. This solution was stirred for 2 hours and the solvent evaporated *in vacuo*. The solid residue was extracted with pentane (2 x 10 mL) followed by benzene (3 x 20 mL) and all washed through Celite. The filtrate was then reduced *in vacuo* to dryness. Crystallization from pentane yielded 1.5 g (55 %) of a reddish orange solid in multiple crops. ^{1}H NMR (C$_6$D$_6$, 20°C) δ 13.5 (br s), 7.34 (s), 3.11 (br s), 2.995 (br m), 1.6 (s), 1.388 (d), -18 (br s), -84 (br s). Anal Calc'd for C$_{114}$H$_{156}$Br$_3$ClMoN$_4$: C, 70.09; H, 8.05; N, 2.87; Br, 12.27; Cl, 1.81. Found: C, 69.85; H, 7.79; N, 2.99; Br, 12.70; Cl, 1.87.

[HIPTpropylN$_3$N]MoCl This compound was synthesized similarly to other compounds of its type. Briefly, **[HIPTpropylN$_3$N]**H$_3$(1.23 g, 0.75 mmol) was dissolved in 40 mL of THF. To this was added MoCl$_4$(THF)2 (0.30 g, 0.78 mmol). The reaction was stirred for one hour, and the solution darkened to a deep red. LiN(SiMe$_3$)$_2$ (0.39 g, 2.3 mmol) was then added, and the solution allowed to stir for an additional 2 hours. The solvent was then removed *in vacuo* and the resulting solid taken up into pentane and benzene and filtered through Celite. This solution then was taken to dryness *in vacuo* and the resulting solid triturated in ~15 mL of cold pentane. The product was isolated as a tan solid (0.74 g, 56% yield) that results in a dark orange solution when dissolved. ^{1}H NMR (C$_6$D$_6$, 20°C) δ 21 (br s), 10.2 (br s), 7.33 (br s), 7.22 (br s), 3.16 (br s), 2.95 (br s), 1.34 (m), -54 (br s). This product contains residual lithium salts, which is why initial attempt to analyze have failed (returned low on all elements).

[LutHIPT$_2$N$_3$N]MoCl The procedure followed was nearly identical to published procedures. Briefly, **[LutHIPT$_2$N$_3$N]**H$_3$ (0.6 g, 0.50 mmol) and MoCl$_4$(THF)$_2$ (0.19 g, 0.50 mmol) were dissolved in THF (40 mL). This was stirred for one hour, at which time (Me$_3$Si)$_2$NLi (0.258 g, 0.1.54 mmol) was slowly added. The solution was stirred for 2

hours and the solvent removed *in vacuo* with mild heating. The solid residue was extracted with pentane (2 x 10 mL) followed by benzene (3 x 20 mL) and all washed through Celite. This filtrate was then evaporated *in vacuo* to dryness. Crystallization from pentane yields 0.42 g of an orange solid in multiple crops (63%). ^{1}H NMR (C_6D_6, 20°C) δ 11.8 (br s), 7.3 (m), 3.1 (br s), 3.0 (m), 2.7 (br s), 1.6 (br s), 1.4 (br s), -16.7 (br s), -23.8 (br s), -65.0 (br s), -69.4 (br s). Anal Calc'd for $C_{85}H_{118}ClMoN_5$: C, 76.11; H, 8.87; N, 5.22. Found: C, 76.01; H, 9.06, N, 5.16.

[PhLutHIPT$_2$N$_3$N]MoCl The procedure followed was nearly identical to the procedure published by our lab previously. Briefly, **[PhLutHIPT$_2$N$_3$N]**H$_3$ (1 g, 0.75 mmol) and $MoCl_4(THF)_2$ (0.286 g, 0.75 mmol) were dissolved in THF (75mL). This was stirred for one hour, at which time $(Me_3Si)_2NLi$ (0.388 g, 2.3 mmol) was slowly added. This solution was stirred for 2 hours and the solvent removed *in vacuo*. The solid residue was extracted with pentane (2 x 10 mL) followed by benzene (3 x 20 mL) and all washed through Celite. The filtrate was then reduced *in vacuo* to dryness. Crystallization from pentane yields 0.9 g of an orangish brown solid in multiple crops (82%). ^{1}H NMR (C_6D_6, 20°C) δ 14.4 (br s), 8.3 (br s), 7.50 (br m), 7.2 (s), 3.1 (br s), 2.9 (br s), 2.5 (br s), 1.3 (br s), -21.5 (br s), -62.2 (br s), -81.1 (br s), -86.7 (br s). Anal Calc'd for $C_{95}H_{122}ClMoN_5$: C, 77.86; H, 8.39; N, 4.78. Found: C, 77.73; H, 8.46; N, 4.83.

[3,5-Bis(CF$_3$)HIPT$_2$N$_3$N]MoCl This was synthesized similarly to other compounds of this type. Briefly, 0.75 g (0.57 mmol) of **[3,5-Bis(CF$_3$)HIPT$_2$N$_3$N]**H$_3$ was added to 50 mL THF. To this, 0.24 g (0.62 mmol) of $MoCl_4(THF)_2$ was then slowly added and allowed to stir for one hour, during which time the solution darkened to a deep red. To this red solution 0.30 g (1.8 mmol) of $(Me_3Si)_2NLi$ was added and the reaction stirred for two hours. The solvent was removed *in vacuo*, the resulting solid dissolved in pentane, and filtered through Celite. Recrystallization from pentane yields 0.45 g (55%) of a deep orange powder. ^{1}H NMR (C_6D_6, 20°C) δ 11.1 (br s), 7.27 (s), 7.19 (s), 3.18 (br s), 2.95 (m), 1.62 (br s), 1.49 (br s), 1.34 (br s), -10.3 (br s), -13.8 (br s), -29.7 (br s), -69.5 (br s),

-82.7 (br s), -86.9 (br s). 19F NMR (C6D6, 20°C) d -57.9. Anal Calc'd for $C_{86}H_{113}ClF_6MoN_4$: C, 71.32; H, 7.86; N, 3.87. Found: C, 71.25; H, 7.76; N, 3.94.

[3,5-DimethylHIPT$_2$N$_3$N]MoCl This was synthesized *via* a method similar to other compounds of this type. Briefly, 0.76 g (0.63 mmol) of **[3,5-DimethylHIPT$_2$N$_3$N]**H$_3$ was added to 0.26 g (0.68 mmol) of $MoCl_4(THF)_2$ in 50 mL THF. This was allowed to stir for one hour, at which time 0.33 g (1.9 mmol) of $(Me_3Si)_2NLi$ was added. After two hours the solvent was removed *in vacuo* and the resulting solid dissolved in pentane and filtered through Celite. Recrystallization from pentane yields 0.47 g (56%) of a deep orange solid. ^{1}H NMR (C_6D_6, 20°C) δ 9.68 (br s), 7.26 (s), 7.24 (s), 3.18 (br s), 2.97 (m), 2.05 (s), 1.54 (br s), 1.44 (s), 1.36 (br s), -11.25 (br s), -13.80 (br s), -23.5 (br s), -66.5 (br s), -77.5 (br s), -84.0 (br s). Anal Calc'd for $C_{86}H_{119}ClMoN_4$: C, 77.07; H, 8.95; N, 4.18. Found: C, 76.87; H, 9.06; N, 4.11.

[3,5-DimethoxyHIPT$_2$N$_3$N]MoCl This was synthesized similarly to other compounds of its type. Briefly, 0.41 g (0.3 mmol) of **[3,5-DimethoxyHIPT$_2$N$_3$N]**H$_3$ was added to 0.13 g (0.3 mmol) of $MoCl_4(THF)_2$ in 30 mL of THF. Upon addition of the molybdenum, the solution immediately darkened to a deep red. This was allowed to stir for one hour, at which time 0.17 g (1 mmol) of $(Me_3Si)_2NLi$ was added, with the solution slowly turning orange-red. The solvent was removed *in vacuo* and the solid taken up into pentane and filtered through Celite. The compound was recrystallized from pentane yielding 0.32 g (70%) of the compound as a deep orange powder. ^{1}H NMR (C_6D_6, 20°C) δ 11.6 (br s), 10 (br s), 7.27 (s), 3.96 (s), 3.18 (s), 2.95 (s), 2.63 (s), 1.34 (s), -14.5 (br s), -20.4 (br s), -69.6 (br s), -79.6 (br s). Anal Calc'd for $C_{86}H_{119}ClMoN_4O_2$: C, 75.27; H, 8.74; N, 4.08. Found: C, 75.06; H, 8.65; N, 4.08.

[MesHIPT$_2$N$_3$N]MoCl This was synthesized similarly to other [**RN$_3$N**]MoCl species. Briefly, 1.0g (0.81 mmol) **[MesHIPT$_2$N$_3$N]**H$_3$ was added to 70 mL of THF. Then, 0.32 g (1.0 mmol) of $MoCl_4(THF)_2$ was slowly added and allowed to stir for 2 hours, at which time 0.42 g (2.6 mmol) of $(Me_3Si)_2NLi$ was added. After 1 hour stirring, the solvent was

evaporated *in vacuo* and the resulting solid dissolved into pentane and filtered through Celite. Recrystalization from pentane yields 0.74 g (67%) of a deep orange crystalline solid. ^{1}H NMR (C_6D_6, 20°C) δ 17.73 (br s), 7.28 (s), 7.22 (s), 6.42 (br s), 3.83 (s), 3.5 (br s), 3.17 (br s), 2.97 (m), 1.52 (br s), 1.41 (br s), -20 (br s), -23.5 (br s), -74.68 (br s), -97.50 (br s). Anal Calc'd for $C_{87}H_{121}ClMoN_4$: C, 77.16; H, 9.01; N, 4.14. Found: C, 77.04; H, 9.04; N 4.11.

[TripHIPT$_2$N$_3$N]MoCl This was synthesized similarly to others of its type. Briefly, 0.35 g (0.25 mmol) of **[TripHIPT$_2$N$_3$N]**H$_3$ was dissolved in 50 mL of THF. Then, 0.112 g (0.29 mmol) of $MoCl_4(THF)_2$ was added and the solution stirred for 2 hours as the solution changed from orange to bright red. To this, 0.138 g (0.83 mmol) of $(Me_3Si)_2NLi$ was slowly added and the solution stirred for an additional hour, at which time the solvent was removed *in vacuo*. The resulting solid was taken up in pentane and filtered through Celite. Recrystallization yields 0.22 g (56%) of a bright orange powder in multiple crops. ^{1}H NMR (C_6D_6, 20°C) δ 18.14 (br s), 9.66 (br s), 7.30 (s), 7.20 (s), 4.09 (br s), 3.53 (br s), 3.20 (br s), 2.99 (m), 1.40 (br s), 1.26 (s), -11.52 (br s), -16.97 (br s), -23.75 (br s), -61.65 (br s), -83.70 (br s), -96.15 (br s). Anal Calc'd for $C_{93}H_{133}ClMoN_4$: C, 77.65; H, 9.32; N, 3.89. Found: C, 77.42; H, 9.38; N, 3.77.

[*p*BrHIPTN$_3$N]MoN[5] The procedure followed was nearly identical to those previously published. Briefly, **[*p*BrHIPTN$_3$N]MoCl** (0.25 g, 0.013 mmol) and Me_3SiN_3 (0.10 g, 0.087 mmol) were added to benzene (40 mL) in a Teflon® sealed flask. This was heated at 90°C for 3 days. All volatiles were then removed *in vacuo* and the solid recrystalized from pentane, yielding 0.167 g (67 %) of bright yellow powder in multiple crops. ^{1}H NMR (C_6D_6, 20°C) δ 7.90 (br s, 6H, 4',6' -*H*), 7.25 (s, 12H, 3,5,3",5" -*H*), 3.53 (br t, J_{HH}=5Hz, 6H, ArNC*H*$_2$CH$_2$), 3.00 (overlapping septets, J_{HH}=6.9Hz, 18H, 4,4" -C*H*Me$_2$ and 2,6,2",6"-C*H*Me$_2$), 1.90 (br t, J_{HH}=5Hz, 6H, NHCH$_2$C*H*$_2$), 1.47 (d, J_{HH}=6.9Hz, 36H, 4,4"-CH(C*H*$_3$)$_2$), 1.34 (d, J_{HH}=6.9Hz 36H, 2,6,2'6'-CH(C*H*$_3$)$_2$), 1.08 (d, J_{HH}=6.6Hz, 36H, 2,6,2'6'-CH(C*H*$_3$)$_2$) Anal Calc'd for $C_{114}H_{156}Br_3MoN_5$: C, 70.87; H 8.14, N, 3.62; Br,

12.41. Found: C, 70.73; H, 8.20; N, 3.69; Br, 12.37. IR (C_6D_6) 1013 cm-1 (ν_{MoN})

[*p*BrHIPTN$_3$N]Mo^{15}N (50%)[5] [*p*BrHIPTN3N]MoCl (0.311 g, 0.017 mmol), ^{15}N labeled NaN_3 (0.0443 g, 0.068 mmol), and TMEDA (0.1g) were placed in 75 mL of benzene and heated at 100-110°C for 6 days. The reaction was then stripped to dryness *in vacuo* and the compound recrystallized from pentane, yielding 0.048 mg (14 %) of a bright yellow powder. IR (C_6D_6) 1013 cm-1 (ν_{MoN}), 985 cm-1 (ν_{Mo15N})

[LutHIPT$_2$N$_3$N]MoN This could not be isolated as a pure compound, as the reaction of **[LutHIPT$_2$N$_3$N]**MoCl and Me_3SiN_3 is low yielding and the final product of recrystallization impure due to an inability to separate the desired product away from **[LutHIPT$_2$N$_3$N]**H$_3$. A sample containing ~10% **[LutHIPT$_2$N$_3$N]**H$_3$ (by ^{1}H NMR) was utilized in test catalytic runs.

[PhLutHIPT$_2$N$_3$N]MoN Me_3SiN_3 (0.044 g, 0.38 mmol) and **[PhLutHIPT$_2$N$_3$N]**MoCl (0.138 g, 0.092 mmol) were added to 25 mL of benzene and heated overnight at 90°C. The resulting yellow solution was stripped to dryness *in vacuo*, taken up in pentane, filtered through Celite, and reduced to 0.5 ml *in vacuo*. After cooling, 50 mg of a bright, canary yellow solid was obtained (37%). ^{1}H NMR (C_6D_6, 20°C) δ 8.35 (d, 4H, J_{HH}=1.3 Hz, PhLut, 2,6,2",6"-*H*), 8.14 (s, 2H, PhLut 3',5'-*H*), 7.79 (d, 4H, J_{HH}=1.1 Hz, HIPT 3',5'-*H*), 7.40 (m, 6H, PhLut 3,4,5,3",4",5"-*H*), 7.17 (m, 8H, HIPT 3,5,3",5"-*H*), 6.73 (br t, 2H, J_{HH}= 1.1 Hz, HIPT 4'-*H*), 3.59 (br t, 4H, J_{HH}= 5.1 Hz, HIPT-NHCH$_2$C*H*$_2$), 3.20 (br t, 2H, J_{HH}= 4.2 Hz, PhLut-NCH$_2$C*H*$_2$), 3.11 (septet, 8H, J_{HH}= 6.9 Hz, 8H, 2,6,2",6"-C*H*Me$_2$), 2.89 (septet, J_{HH}= 6.9 Hz, 4H, 4,4" -C*H*Me$_2$), 2.08 (br t, 2H, JHH= 3.4 Hz, PhLut-NC*H*$_2$CH$_2$), 2.02 (br t, 4H, J_{HH}= 5.1 Hz, HIPT-NC*H*$_2$CH$_2$), 1.33 (dd, 24H, 4,4"-CH(C*H*$_3$)$_2$), 1.22 (d, J_{HH}= 6.9 Hz, 12H, 2,6,2",6" -CH(C*H*$_3$)$_2$), 1.19 (d, J_{HH}= 6.9 Hz, 12H, 2,6,2",6" -CH(C*H*$_3$)$_2$), 1.16 (d, J_{HH}= 6.9 Hz, 12H, 2,6,2",6" -CH(C*H*$_3$)$_2$), 1.11 (d, J_{HH}= 6.9 Hz, 12H, 2,6,2",6" -CH(C*H*$_3$)$_2$). Anal Calc'd for $C_{95}H_{122}MoN_6$: C, 79.02; H, 8.52; N, 5.82. Found: C, 78.88; H, 8.45; N, 5.88.

[3,5-Bis(CF$_3$)HIPT$_2$N$_3$N]MoN This compound was made similarly to other compounds

of its type. Briefly, 0.17 g (117 mmol) of [**3,5-bis(CF_3)HIPT$_2$N$_3$N**]MoCl and 0.07 g (608 mmol) of Me_3SiN_3 was added to 50 mL of benzene in a Teflon® sealed glass bomb. This was heated to 90°C for 12 hours and then brought to dryness *in vacuo*. The resulting yellow solid was taken into pentane and filtered through Celite. Recrystallization from pentane yields 0.12 g (72%) of a bright yellow solid. ^{1}H NMR (C_6D_6, 20°C) δ 7.93 (s, 2H, CF_3 arm 2,6-*H*), 7.70 (d, JHH= 1.4 Hz, 4H, HIPT-2',6'-*H*), 7.39 (s, 1H, CF_3 arm 4-*H*), 7.19 (s, 8H, HIPT 3,5,3",5"-*H*), 6.81 (br t, J_{HH}= 1.1 Hz, 2H, HIPT 4'-*H*), 3.53 (br t, J_{HH}= 4.7 Hz, 4H, HIPT-NCH_2CH$_2$), 3.15 (overlapping septets, J_{HH}= 6.9 Hz, 8H, 2,6,2",6"-C*H*Me$_2$), 2.90 (septet, J_{HH}= 6.9 Hz, 4H, 4,4" -C*H*Me$_2$), 2.83 (br t, J_{HH}= 4.8 Hz, 2H, CF_3 arm-NCH_2CH$_2$), 1.97 (br t, J_{HH}= 5.1 Hz, 4H, HIPT-NHCH$_2$CH_2), 1.92 (br t, J_{HH}= 5.0 Hz, 2H, CF_3 arm-NCH$_2$CH_2), 1.34 (d, J_{HH}= 6.9 Hz, 24H, 4,4"-CH(CH_3)$_2$), 1.26 (d, J_{HH}= 6.9 Hz, 12H, 2,6,2",6" -CH(CH_3)$_2$), 1.22 (d, J_{HH}= 6.9 Hz, 12H, 2,6,2",6" -CH(CH_3)$_2$), 1.20 (d, J_{HH}= 6.9 Hz, 12H, 2,6,2",6" -CH(CH_3)$_2$), 1.11 (d, J_{HH}= 6.9 Hz, 12H, 2,6,2",6" -CH(CH_3)$_2$). ^{19}F NMR (C_6D_6, 20°C), δ -62.4. Anal Calc'd for $C_{86}H_{113}F_6MoN_5$: C, 72.40; H, 7.98; N, 4.91. Found: C, 72.56; H, 7.98; N, 4.81.

[3,5-DimethylHIPT$_2$N$_3$N]MoN This compound was made in a similar manner to other compounds of this type. Briefly, 0.15 g (0.11 mmol)of [**3,5-dimethylHIPT$_2$N$_3$N**]MoCl and 0.064 g (0.56 mmol) of Me_3SiN_3 was added to 40 mL benzene and heated in a Teflon® sealed bomb at 100°C for one day, at which time the volatiles were removed *in vacuo*. The resulting solid was taken up in pentane and filtered through Celite. Recrystallization yields 0.073 g (50%) of a bright yellow powder. ^{1}H NMR (C_6D_6, 20°C) δ 7.86 (d, J_{HH}= 1.1 Hz, 4H, HIPT-2',6'-*H*), 7.21 (dd, J_{HH}=1.4 Hz and 3.3 Hz, 8H, HIPT 3,5,3",5"-*H*), 7.05 (s, 2H, dimethyl-2,6-*H*), 7.76 (br t, J_{HH}= 1.1 Hz, 2H, HIPT 4'-*H*), 6.51 (s, 1H, dimethyl-4-*H*), 3.54 (br t, J_{HH}= 5.2 Hz, 4H, HIPT-NCH_2CH$_2$), 3.64 (br t, J_{HH}= 5.2 Hz, 2H, dimethyl-NCH_2CH$_2$), 3.19 (septet, J_{HH}= 6.9 Hz, 8H, HIPT-2,6,2",6" -C*H*Me$_2$), 2.93 (septet, J_{HH}= 6.9 Hz, 4H, HIPT-4,4" -C*H*Me$_2$), 2.18 (s, 6H, dimethyl-CH_3), 2.03 (m, 8H, contains HIPT-NCH$_2$CH_2 and dimethyl-NCH$_2$CH_2), 1.34 (d, J_{HH}= 6.9 Hz, 24H, 4,4"-

$CH(CH_3)_2$), 1.26 (d, J_{HH}= 6.9 Hz, 24H, 2,2",6,6"-$CH(CH_3)_2$), 1.21 (d, J_{HH}=6.9 Hz, 12H, 2,6,2",6" -$CH(CH_3)_2$), 1.16 (d, J_{HH}=6.9 Hz, 24H, 2,6,2",6" -$CH(CH_3)_2$). Anal Calc'd for $C_{86}H_{119}MoN_5$: C, 78.32; H, 9.09; N, 5.31. Found: C, 78.19; H, 8.96; N, 5.23.

[3,5-DimethoxyHIPT$_2$N$_3$N]MoN This was synthesized similarly to other compounds of its type. Briefly, 0.12 g (0.08 mmol) of **[3,5-dimethoxyHIPT$_2$N$_3$N]**MoCl was added to 0.05 g (0.4 mmol) of Me_3SiN_3 in 25 mL of benzene. This was heated at ~100°C overnight. The solvent was removed *in vacuo* and the resulting solid taken up in pentane and filtered through Celite. The compound was recrystallized from pentane, yielding 0.07 g (55%) of a bright yellow powder in multiple crops. ^{1}H NMR (C_6D_6, 20°C) δ 7.91 (d, J_{HH}= 0.8 Hz, 4H, HIPT-2',6'-*H*), 7.23 (d, J_{HH}= 1.8 Hz, 2H, dimethoxy-2,6-*H*), 7.21 (s, 8H, HIPT 3,5,3",5"-*H*), 6.76 (s, 2H, HIPT 4'-*H*), 6.30 (t, J_{HH}= 1.8 Hz, 1H, dimethoxy-4-*H*), 3.55 (br t, 4H, HIPT-NCH_2CH_2), 3.43 (s, 6H, -OC*H*3), 3.31 (br t, 2H, dimethoxy-NCH_2CH_2), 3.20 (septet, J_{HH}= 6.9 Hz, 8H, 2,6,2",6"-$CHMe_2$), 2.92 (septet, J_{HH}= 6.9 Hz, 4H, 4,4""-$CHMe_2$), 1.94 (br t, 6H, overlapped HIPTNCH_2CH_2 and dimethoxyNCH_2CH_2), 1.32 (d, J_{HH}= 6.9 Hz, 24H, 4,4"-$CH(CH_3)_2$), 1.22 (overlapping doublets, J_{HH}= 6.9 Hz, 24H, 2,6,2",6" -$CH(CH_3)_2$), 1.14 (d, J_{HH}= 6.9 Hz, 12H, 2,6,2",6" -$CH(CH_3)_2$). Anal. Calc'd for $C_{86}H_{119}MoN_5O_2$: C, 76.47; H, 8.88; N, 5.18. Found: C, 76.38; H, 8.85; N, 5.06.

[MesHIPT$_2$N$_3$N]MoN This was synthesized similarly to compounds of this type. Briefly, 0.19 g (0.14 mmol) of **[MesHIPT$_2$N$_3$N]**MoCl was combined with 0.1 g (0.86 mmol) of Me_3SiN_3 in 25 mL of benzene and heated in a Teflon® sealed glass bomb at 90°C for one day. The solvent was removed in vacuo, and the solid taken up in pentane and filtered through Celite. Recrystallization yields 0.11 g (59%) of a bright yellow powder. ^{1}H NMR (C_6D_6, 20°C) δ 7.76 (d, J_{HH}= 1.1 Hz, 4H, HIPT-2',6'-*H*), 7.20 (s, 8H, HIPT 3,5,3",5"-*H*), 6.70 (br t, J_{HH}= 1.1 Hz, 2H, HIPT 4'-*H*), 6.65 (s, 2H, Mes-3,5-*H*), 3.47 (m, 4H, HIPT-NCH_2CH_2), 3.20 (m, 10H, containing 2,6,2",6"-$CHMe_2$ and Mes-NCH_2CH_2), 2.90 (septet, J_{HH}= 6.9 Hz, 4H, 4,4" -$CHMe_2$), 2.25 (s, 9H, Mes-CH_3) 2.1 (m, 6H, containing Mes-NCH_2CH_2, and HIPT-NCH_2CH_2), 1.34 (d, J_{HH}= 6.9 Hz, 24H, 4,4"-

$CH(CH_3)_2$), 1.30 (d, J_{HH}= 6.9 Hz, 24H, 2,6,2",6" -$CH(CH_3)_2$), 1.20 (d, J_{HH}= 6.9 Hz, 12H, 2,6,2",6" -$CH(CH_3)_2$), 1.17 (d, J_{HH}= 6.9 Hz, 12H, 2,6,2",6" -$CH(CH_3)_2$). Anal Calc'd for $C_{87}H_{121}MoN_5$: C, 78.40; H, 9.15; N, 5.25. Found: C, 77.26; H, 9.17; N, 5.19.

[TripHIPT$_2$N$_3$N]MoN This was synthesized in a manner similar to previously characterized compounds of this type. Briefly, 0.05 g (0.035 mmol) of **[TripHIPT$_2$N$_3$N]**MoCl was combined with 0.028 g (0.24 mmol) in 10 mL of benzene and heated 100°C for one day. The solvent was removed *in vacuo* and the resulting solid taken up into pentane and filtered through Celite. Recrystallization from pentane yields 0.04 g (80%) of a bright yellow powder. ^{1}H NMR (C_6D_6, 20°C) δ 7.77 (d, J_{HH}= 1.1 Hz, 4H, HIPT-2',6'-*H*), 7.19 (m, 8H, HIPT 3,5,3",5"-*H*), 7.08 (s, 2H, Trip-3,5-*H*), 6.73 (br t, J_{HH}= 1.1 Hz, 2H, HIPT 4'-*H*), 3.52 (m, 6H, HIPT-NCH_2CH_2), 3.34 (br t, J_{HH}= 5.5 Hz, 2H, Trip-NCH_2CH_2), 3.17 (m, 10H, containing HIPT-2,6,2",6"-$CHMe_2$, and Trip-2,6-$CHMe_2$), 2.95 (septet, J_{HH}= 6.9 Hz, 2H, HIPT-4,4"-$CHMe_2$), 2.81 (septet, J_{HH}= 6.9 Hz, 1H, Trip-4-$CHMe_2$), 2.21 (m, 8H, containing Trip-NCH_2CH_2 and HIPT-NCH_2CH_2), 1.38 (d, J_{HH}= 6.9 Hz, 24H, HIPT 4,4"-$CH(CH_3)_2$), 1.24 (m, 36H, contains Trip-4- $CH(CH_3)_2$ and HIPT- 2,6,2",6" -$CH(CH_3)_2$), 1.13 (m, 24H, contains Trip- 2,6,2",6" - $CH(CH_3)_2$ and HIPT- 2,6,2",6" -$CH(CH_3)_2$). Anal Calc'd for $C_{93}H_{133}MoN_5$: C, 78.83; H, 9.46; N, 4.94. Found: C, 78.91; H, 9.48; N, 4.86.

[[*p*BrHIPTN$_3$N]MoNH][BAr'4][5] The procedure followed was nearly identical to the procedure published by our lab previously. Briefly, **[*p*BrHIPTN$_3$N]**MoN (0.109 g, 0.05 mmol) and $H(OEt_2)_2BAr_4$' (0.069 g, 0.07 mmol) were added to 20 mL THF and stirred for 3 hours. The solution went from bright yellow to deep red. The resulting solution was taken to dryness *in vacuo*. The resulting solid was dissolved in pentane, filtered through Celite, and taken to dryness *in vacuo,* yielding 0.116 g of a deep red/purple solid. Along with the major product, a small amount of the free ligand **[*p*BrHIPTN$_3$N]**H_3 was also observed. ^{1}H NMR (C_6D_6, 20°C) δ 8.35 (br s, BAr4'-*H*), 7.68 (s, BAr4'-*H*), 7.20 (s, 12H, 3,5,3",5" -*H*), 6.90 (s, 6H, 4',6' -*H*), 3.68 (br t, J_{HH}=5Hz, 6H, ArNCH_2CH_2), 2.89 (sept,

J_{HH}=6.9Hz, 12H, 2,6,2",6"-C*H*Me$_2$), 2.58 (sept, J_{HH}=6.9Hz, 6H, 4,4" -C*H*Me$_2$) 2.41 (br t, J_{HH}=5Hz, 6H, NHCH$_2$C*H*$_2$), 1.36 (d, J_{HH}=6.9Hz, 36H, 4,4"-CH(C*H*$_3$)$_2$), 1.31 (d, J_{HH}=6.9Hz 36H, 2,6,2'6'-CH(C*H*$_3$)$_2$), 1.01 (d, J_{HH}=6.6Hz, 36H, 2,6,2'6'-CH(C*H*$_3$)$_2$). Due to impurities, the MoN-*H* proton could not unambiguously be assigned. IR shows two peaks in the ν_{N-H} region:. a sharp peak 3336 cm-1 corresponding to the MoN-H bond and a broad peak at 3409 cm-1 corresponding to the N-H bond in [***p*BrHIPTN$_3$N**]H$_3$.

[*p*BrHIPTN$_3$N]Mo-N$_2$-Mg(THF)$_x$Cl + [*p*BrHIPTN$_3$N]MoN$_2$ [5] The procedure followed was nearly identical to the procedure published by our lab previously. Briefly, **[*p*BrHIPTN$_3$N]**MoCl (0.16 g) and magnesium powder (0.14 g) were added to ~30 mL of THF and stirred with a glass stirbar. The magnesium was then activated with dibromoethane, and the reaction allowed to proceed for two hours, during which time the reaction turned from orange to emerald green. This was stripped to dryness *in vacuo*, and the resulting solid taken up in pentane and filtered through Celite. This deep red/purple solution was then stripped to dryness, yielding a reddish brown solid that contains both the magnesium salt and the neutral dinitrogen species. Attempts to synthesize the neutral species alone have so far proven unsuccessful. Important paramagnetically shifted NMR peaks (that correspond to the neutral dinitrogen species) are located at 22.8, -6.9, and -33.50 ppm. IR shows both species distinctly, with the peak due to **[*p*BrHIPTN$_3$N]**MoN$_2$ at ν_{N-N} = 1992 cm^{-1} and a broad peak due to **[*p*BrHIPTN$_3$N]**MoN$_2$-Mg(THF)$_x$Cl at ν_{N-N} =1788 cm^{-1}.

[3,5-Bis(CF$_3$)HIPT$_2$N$_3$N]Mo-N$_2$-Na(THF)$_2$ 0.56 g of **[3,5-bis(CF$_3$)HIPT$_2$N$_3$N]**MoCl was dissolved in 20 mL THF and 4.8 g of 0.5% Na/Hg amalgam was added. This was stirred with a glass stirbar for two hours until the solution had turned a deep green. The solution was decanted from the mercury and the volatiles removed *in vacuo*. The resulting solids were dissolved in pentane and filtered through Celite yielding a deep purple solution. The compound was recrystallized from pentane yielding 0.45 g (70%) of a purple powder in multiple crops. A similar method was utilized to synthesize the $^{15}N_2$

labeled species. ^{1}H NMR (C_6D_6, 20°C) δ 7.68 (s, 1H, CF_3 arm 4-*H*), 7.59 (s, 2H, HIPT 4'-*H*), 7.45 (d, J_{HH}= 1.2 Hz, 2H, CF_3 arm 2,6-*H*), 7.35 (d, J_{HH}= 1.3 Hz, 4H, HIPT- 2',6'-*H*), 7.18 (s, 4H, HIPT 3,5,3",5"-*H*), 7.13 (s, 4H, HIPT 3,5,3",5"-*H*), 3.76 (m, 6H, containing both HIPT-NC*H*$_2$CH$_2$ and CF_3-NC*H*$_2$CH$_2$), 3.38 (overlapping septets, J_{HH}= 6.9 Hz, 8H, 2,6,2",6"-C*H*Me$_2$), 3.22 (br m, 8H, THF O-C*H*$_2$), 2.84 (overlapping septets, J_{HH}= 6.9 Hz, 4H, 4, 4"-C*H*Me$_2$), 1.94 (br m, containing both HIPT-NCH$_2$C*H*$_2$ and CF_3-NCH$_2$C*H*$_2$), 1.23 (overlapping doublets, 52H containing 2,4,6,2",4",6"-CH(C*H*$_3$)$_2$), 1.1 (d, J_{HH}= 6.9 Hz, 12H, 4, 4"-CH(C*H*$_3$)$_2$). ^{19}F NMR (C_6D_6, 20°C), δ -61.76. IR ($\nu_{N\text{-}N}$ 1801 cm^{-1}, $^{15}N_2$ labeled = 1741 cm^{-1}). Elemental Analysis has not passed, presumably due to a variable amount of THF coordination depending on individual preparation and isolation procedures.

LMoN$_2$Na(THF)$_2$ Procedures for all other LMoN$_2$Na(THF)$_2$ compounds were similar to that for **[3,5-bis(CF$_3$)HIPT$_2$N$_3$N]Mo-N$_2$-Na(THF)$_2$**. It was found that both Na/Hg amalgam or finely divided Na sand would reduce LMoCl similarly, so typically Na sand was used. A crystal structure was performed on **[3,5-dimethylHIPT$_2$N$_3$N]Mo-N$_2$-Na(THF)$_2$**, but samples for elemental analysis could not be isolated (presumably due to variable THF coordination) of any compound of this type.

LMoN$_2$ All neutral dinitrogen complexes were unable to be isolated as pure compounds. However, we were able to observe these complexes *via* IR and NMR spectroscopy. To do so, LMoCl was treated with a 0.5 % Na/Hg amalgam or sodium sand in THF. When the solution had turned from bright orange to either green (L= **[PhLutHIPT$_2$N$_3$N]**, **[MesHIPT$_2$N$_3$N]**, and **[TripHIPT$_2$N$_3$N]**) or purple (L= **[LutHIPT$_2$N$_3$N]**, **[3,5-bis(CF$_3$)HIPT$_2$N$_3$N]**, **[3,5-dimethylHIPT$_2$N$_3$N]**, **[3,5-dimethoxyHIPT$_2$N$_3$N]**) it was filtered through a Celite plug onto a mild oxidant such as $ZnCl_2$. The resulting brown solution was then filtered through Celite and the solvent removed *in vacuo*. The resulting solid was characterized by NMR and IR, with 10-20% free ligand present depending on the compound and the attempt. The paramagnetically shifted protons in the ^{1}H NMR

were similar to those of the symmetric compounds of this type (3 peaks at δ ~ 10 to 20ppm, 2 peaks at ~ -3 to -10 ppm, and 3 peaks at -20 to -40 ppm).

[[*p*BrHIPTN$_3$N]MoNH$_3$][BAr$_4$'][5] The procedure followed was similar to the procedure published by our lab previously. Briefly, [***p*BrHIPTN$_3$N**]MoCl (0.5 g, 0.25 mmol), NaBAr$_4$' (0.4 g, 0.45 mmol), and NH_3 (100mL, 440 torr, transferred from a bronze solution with Na, ~8 equivalents to [***p*BrHIPTN$_3$N**]MoCl) were allowed to stir in 75 mL if degassed dichloromethane for 12 hours in a Teflon® sealed glass bomb. The reaction turned from deep orange to bright red, and the resulting solution was taken to dryness *in vacuo*. The solid was then dissolved in pentane, filtered through celite, and reduced to ~1.5 mL. This concentrated solution was cooled to –30°C for 6 days, at which time crystallization occurred, yielding 0.58 g (81% yield) of a bright red solid. ^{1}H NMR (C_6D_6, 20°C) δ 8.27 (s, BAr$_4$'-*H*), 7.65 (s, BAr$_4$'-*H*), 2.91 (br m), 2.71 (br m), 1.31 (br m), 1.09 (br m), -16.3 (br s), -109.5 (br s). Anal Calc'd for $C_{146}H_{171}BBr_3F_{24}MoN_5$: C, 62.66; H 6.16, N, 2.50. Found: C, 62.54; H, 6.22; N, 2.43.

[(3,5-Bis(CF$_3$)HIPT$_2$N$_3$N)MoNH$_3$][BAr$_4$'] This compound has been identified *via* NMR from the 1:1 reaction of **[3,5-Bis(CF$_3$)HIPT$_2$N$_3$N]**MoCl and NaBAr4' under 6 equivalents of ammonia in dichloromethane. After one day of stirring, the solvent was removed *in vacuo* and the resulting solid filtered through Celite with pentane. Recrystallization from pentane yielded the product as a red solid. ^{1}H NMR (C_6D_6, 20°C) δ 8.23 (s, BAr4'), 7.61 (s, BAr4'), 7.12 (br s), 2.88 (br s), 2.68 (br s), 1.29 (br s), 1.16 (br s), -12.5 (br s), -17.5 (br s), -33 (br s). ^{19}F NMR (C_6D_6, 20°C) δ –61.3 ($MoNH_3^+$), -61.45 (BAr$_4$'). We were unable to completely remove NaBAr$_4$' from the solid (~5% *via* ^{19}F NMR), the impure product was utilized in NH_3 to N_2 exchange reactions as described in chapter 4.

[(3,5-DimethoxyHIPT$_2$N$_3$N)Mo(NH$_3$)][BAr$_4$']. **[3,5-DimethoxyHIPT$_2$N$_3$N]**MoCl (100 mg) and 65 mg of Na[BAr$_4$'] were dissolved in 10 mL of CH_2Cl_2 in a 50 mL Teflon® sealed vessel. 200 torr (~6 equivalents) of dry ammonia was vacuum-transferred onto

this solution. The reaction mixture turned bright red after being stirred for 6 h. The volatiles were removed *in vacuo*, the resulting solid was extracted into pentane, and the pentane extract was filtered through Celite. The product was isolated as a red solid through crystallization from pentane; yield 120 mg (75%). ^{1}H NMR (C_6D_6, 20°C) δ 8.36 (br s, BAr_4'), 7.68 (br s, BAr_4'), 6.67 (br s), 6.36 (br s), 3.5 (br s), 3.2 (s), 2.7 (br m), 1.85 (br m), 1.2 (br m), -4.0 (br s), -8.5 (br s). Anal. Calc'd for $C_{118}H_{134}BF_{24}MoN_5O_2$: C, 63.92; H, 6.09; N, 3.16. Found: C, 64.10; H, 6.13; N, 2.97.

References

1. Yandulov, D.V.; Schrock, R.R. *Science* **2003**, *76*, 301.

2. Yandulov, D.V.; Schrock, R.R. *J. Am Chem. Soc.* **2002**, *124*, 6252.

3. Yandulov, D.V.; Schrock, R.R.; Rheingold, A.L.; Ceccarelli, C.; Davis, W.M. *Inorg. Chem.* **2003**, *42*, 796.

4. Yandulov, D.V.; Schrock, R.R. *Inorg. Chem.* **2005**, *44*, 1103.

5. Ritleng, V.; Yandulov, D. V.; Weare, W. W.; Schrock, R. R.; Hock, A. S.; Davis, W. M. *J. Am. Chem. Soc.* **2004**, *126*, 6150.

6. Mösch-Zanetti, N.C.; Schrock, R.R.; Davis, W.M.; Wanninger, K.; Seidel, S.W.; O'Donoghue, M.B. *J. Am. Chem. Soc.* **1997**, *119*, 11037.

7. O'Donoghue, M.B.; Zanetti, N.C.; Davis, W.M.; Schrock, R.R. *J. Am. Chem. Soc.* **1997**, *119*, 2753.

8. Yandulov, D.V. *personal communication.*

9. MacKay, B.A.; Fryzuk, M.D. *Chem. Rev.* **2004**, *104*, 385.

10. Pangborn, A.B.; Giardello, M.A.; Grubbs, R.H.; Rosen, R.K.; Timmers, F.J. *Organometallics* **1996**, *15*, 1518.

11. Stoffelbach, F.; Saurenz, D.; Poli, R. *Eur. J. Inorg. Chem.* **2001**, 2699.

CHAPTER 4

Evaluating the Factors that Control Success of Dinitrogen Reduction Catalysis with Triamidoamine Molybdenum Complexes.

Portions of the material covered in this chapter have appeared in print:

Ritleng, V.; Yandulov, D. V.; Weare, W. W.; Schrock, R. R.; Hock, A. S.; Davis, W. M. *J. Am. Chem. Soc.* **2003**, *126*, 6150-6163.

Introduction

With compounds in hand that support many of the intermediates in the dinitrogen reduction cycle[1] (both the parent [**HIPTN$_3$N**]MoX compounds as well as those described in chapter 3), a technical solution was needed to overcome the chemical challenges to realizing catalysis. The primary obstacle is that the H^+ and e^- sources utilized for this transformation spontaneously react with one another to form H_2 (Equation 4.1). Preliminary evidence from early catalytic attempts suggested that the rate constant for H_2 formation is faster than that of the individual reactions to ultimately form NH_3. To overcome this difficulty, the design of the catalytic experiment focused on keeping the concentration of the reducing agent and proton source low, therefore making [LMoX] >> [H^+] and [e^-]. This was done by choosing a solvent in which the proton source was only slightly soluble (in our case, pyridinium acids in heptane), and through the addition of the reducing agent (metallocenes) slowly through the use of a mechanical syringe pump. To maintain the heptane solubility of cationic intermediates, the [BAr_4'] anion was utilized. Under such conditions, we succeeded in our goal of catalyzing dinitrogen reduction under ambient conditions.[2,3]

$$H^+ + e^- \xrightarrow{k_1} 1/2\ H_2$$

$$H^+ + e^- + \text{LMoX} \xrightarrow{k_2} NH_3 \qquad \textbf{(4.1)}$$

This chapter describes my work studying dinitrogen reduction catalysis and the reactions that ultimately limit activity in the systems under scrutiny. Most of the compounds described in chapter 3 do not support catalysis, but their study has allowed us to evaluate several elementary steps of the postulated cycled in greater detail than that possible if only one compound is studied. The compounds utilized in this chapter are diagrammed in Figure 4.1.

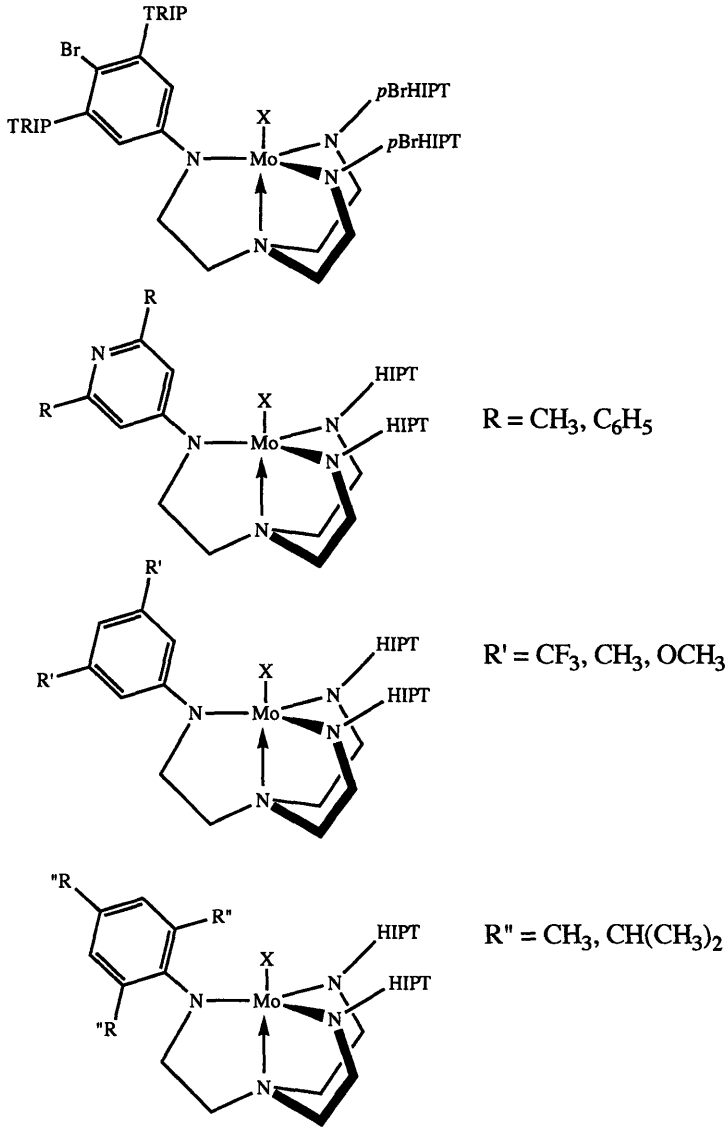

Figure 4.1) Compounds utilized for catalytic dinitrogen study. X = N^{3-}, N_2^-, or NH_3.

Results and Discussion

Catalytic Results

Standard catalytic reactions were performed on many of the compounds described in chapter 3. "Standard" catalytic runs involve the addition of reducing agent (decamethylchromocene) in 10 mL heptane over 6 hours into LMoN and a slurried

suspension of [2,6-lutidinium][BAr_4'] in 2 mL of heptane. Results of these reactions are summarized in Table 4.1.

The only compounds of this group that successfully catalyze dinitrogen reduction under these conditions are the parent [**HIPTN$_3$N**]MoN,[4] the symmetric [***p*BrHIPTN$_3$N**][1] and the "hybrid" [**TripHIPT$_2$N$_3$N**]MoN. These three compounds are the most sterically bulky of the compounds listed (with the exception of [**PhLutHIPT$_2$N$_3$N**]MoN, which presumably fails due to the pyridine arm allowing [H^+] to approach [**L**MoX], enhancing H_2 formation relative to NH_3). Our conclusion based upon this data is that steric bulk is important, which was already suspected from earlier work with sterically varied (hexa-*t*-butyl terphenyl (HTBT) and hexamethylterphenyl (HMT)) symmetric ligands. In the hybrid cases, catalytic failure appears to be related to instability of the diazenido compound **L**MoN$_2$H toward H_2 loss, and is discussed later in this chapter. (Note: the results for all catalytic runs performed during my graduate career are included in Appendix 4)

Table 4.1) Results for Standard Catalytic Runs ([2,6-lutidinium][BAr_4'] and Cp^*_2Cr)

Pre-Catalyst	**NH_3(actual)/ NH_3(calculated)**	**% Yield**	**# NH_3 from N_2**
[**HIPTN$_3$N**]MoN	7.5/12	62.5	6.5
[***p*BrHIPTN$_3$N**]MoN	6.9/12	59	5.9
[**LutHIPT$_2$N$_3$N**]MoN	1.3/11.3	11	0.3
[**PhLutHIPT$_2$N$_3$N**]MoN	1.4/10.6	13	0.4
[**MesHIPT$_2$N$_3$N**]MoN	1.2/6.4	19	0.2
[**TripHIPT$_2$N$_3$N**]MoN	2.5/11	23	1.5
[**3,5-Bis(CF$_3$)HIPT$_2$N$_3$N**]MoN	0.97/11.4	8	0
[**3,5-DimethylHIPT$_2$N$_3$N**]MoN	0.9/6.4	14	0
[**3,5-DimethoxyHIPT$_2$N$_3$N**]MoN	0.87/7.2	12	0

Symmetric electron withdrawing ligands were initially synthesized in order to lower the reduction potentials necessary to traverse the dinitrogen catalytic cycle. Electrochemistry of [***p*BrHIPTN$_3$N**]MoN$_2^{0/-}$ revealed that the reduction potential for one of the intermediates was shifted by 100 mV (from -1.81 V for [**HIPTN$_3$N**]MoN$_2^{0/-}$ to -1.71 V for [***p*BrHIPTN$_3$N**]MoN$_2^{0/-}$).[1] To test whether this shift allowed for weaker reducing agents to be utilized for catalysis, cobaltocene (-1.33 V in C_6H_5F) was used as the electron source instead of decamethylchromocene (-1.63 V in C_6H_5F).[1] As seen in Table 4.2, catalytic turnover does occur with cobaltocene as the electron source. However, [**HIPTN$_3$N**]MoN remains the most efficient, even with the less powerful reductant. Apparently, the observed shift in reduction potential is not enough to allow a productive change to a weaker reducing agent.

Even though this result did not demonstrate improvement in our ligand design, it did show that the reducing agent is most likely acting only as a simple electron donor to the catalytic system. It seems unlikely that both Cr(II) and Co(II) would result in the same products if catalysis involved metallocene coordinated intermediates.

Table 4.2) Results of Catalytic Runs Utilizing [2,6-Lutidinium][BAr$_4$'] and Cp$_2$Co.

Pre-Catalyst	**NH$_3$(actual)/ NH$_3$(calculated)**	**% Yield**	**# NH$_3$ from N$_2$**
[**HIPTN$_3$N**]MoN	3.6/9.8	37	2.6
[***p*BrHIPTN$_3$N**]MoN	2.2/12.2	18	1.2

Alternative acids were also employed in an attempt to understand how protonation of catalytic intermediates takes place. Results of these experiments are shown in Table 4.3. They show that 2,6-dimethyl substituted pyridinium salts are far and away the most efficient at catalyzing dinitrogen reduction (2,6-lutidinium and 2,4,6-collidinium). If we add steric bulk, as in the case of 2,6-diethylpyridinium or 2,6-diphenylpyridinium, catalytic efficiency is lowered or turned off, respectively. If steric

bulk is removed, as in the case of 2,4-lutidinium or 3,5-lutidinium, we also see efficiency hindered or the reaction halted at one equivalent of NH_3. For the bulkier acids, we believe that the reason for catalytic failure is that the proton cannot be readily delivered to the catalyst. This is either through steric hindrance, or through changes in solubility that make the resulting acid more soluble (diethylpyridinium) or less soluble (diphenylpyridinium) in heptane. These effects in tandem lower catalyst efficiency to the levels observed. For the less bulky acids, we feel that the conjugate base of the acid can interact directly with the metal, as in the crystallographically characterized compound [[**HIPTN$_3$N**]Mo-2,6-lutidine][BPh_4].[5] Sequestering the catalyst as a lutidine adduct, particularly in the case of 3,5-lutidine, seems the most likely cause of the relatively poor turnover when using these acids. [Et_3NH][BAr_4'] was also proved ineffective as a proton source, but we have not yet probed in detail the reasons for its failure. It seems likely that its relatively high pK_a (~11 vs. ~5 for 2,6-lutidine) may not allow this acid to efficient protonate catalytic intermediates.

Table 4.3) Results of Catalytic Runs Utilizing [HIPTN$_3$N]MoN and Cp^*_2Cr.

Proton Source	**NH_3(actual)/ NH_3(calculated)**	**% Yield**	**# NH_3 from N_2**
[2,4-Lutidinium][BAr_4']	5.1/12	43	4.1
[3,5-Lutidinium][BAr_4']	1.02/11.2	9	0.02
[2,6-Diethylpyridinium][BAr_4']	3.7/12	31	2.7
[2,6-Diphenylpyridinium][BAr_4']	0.35/6.5	4	0
[2,4,6-Collidinium][BAr_4']	6.7/11	61	5.7
[Triethylammonium][BAr_4']	0.63/12.2	5	0

The use of additives such as THF or 2,6-lutidine have been explored. It was thought that such compounds, present in excess, might speed the displacement of ammonia from the metal center. However, addition of ~150 equivalents of THF or 2,6-

lutidine dramatically lowers catalytic efficiency under otherwise standard conditions. In the case of THF, I posit that this is most likely due to its presence increasing [H^+], speeding H_2 formation. 2,6-lutidine likely inhibits turnover by deprotonating cationic dinitrogen reduction intermediates. This result must be taken into account when considering the scalability of our catalytic reactor, as it shows that as [2,6-lutidine] rises, catalytic efficiency will eventually suffer. Since previous workers have shown that the 36 equivalents of 2,6-lutidine formed during a standard catalytic run have negligible effects on catalyst efficiency more studies are needed to find the point at which 2,6-lutidine dramatically inhibits N_2 reduction.

These catalytic studies serve as a starting point for our focused studies of individual steps in the catalytic cycle. These systems, at the minimum, appear to form ammonia from the initially bound nitrides. Therefore, we now turn attention to the first possible place for catalytic failure, the dinitrogen to ammonia exchange reaction for Mo(III).

Studying the rate of Dinitrogen for Ammonia Exchange

Reduction of [$LMoNH_3$][BAr_4'] by Cp^*_2Cr in heptane is complete within seconds. Therefore $LMoNH_3$ can be prepared and studied *in situ*. We are particularly interested in the rate of the forward reaction in Equation 4.2. When we follow this conversion by taking aliquots from a capped, quickly stirred vial for IR spectra and plot $\ln(1-A/A_\infty)$ versus time (where A is the absorbance for the $LMoN_2$ that is formed), we obtain a nearly straight line through two half-lives from which an observed first order rate constant of approximately $1x10^{-4}$ s^{-1} can be obtained (see the experimental section for an example of such an experiment).

$$[HIPTN_3N]MoNH_3 + N_2 \leftrightarrows [HIPTN_3N]MoN_2 + NH_3 \qquad (4.2)$$

The conversion of $LMoNH_3$ to $LMoN_2$ actually is not a simple reaction. A typical starting concentration of $LMoNH_3$ might be 0.02 M so at $t_{1/2}$ the ammonia concentration (0.01 M if none leaves the solution) is much greater than what it would be

at equilibrium. The rapid back reaction of NH_3 with $\mathbf{L}MoN_2$ makes study of this reaction complicated. For instance, ammonia must back react with $\mathbf{L}MoN_2$ to yield $\mathbf{L}MoNH_3$ many times before it diffuses out of benzene on a time scale of 1-2 h (we know that equilibrium is not established for 1-2 h from equilibrium studies discussed later). Therefore the apparent rate constant found in the bulk experiments is much less than what it would be if the ammonia were somehow completely removed as it formed and somewhat dependent on the reaction conditions (volume of solvent, headspace, rate of stirring, etc.). We also can calculate that if conversion of $\mathbf{L}Mo(NH_3)$ to $\mathbf{L}MoN_2$ is observed in a *closed* vial or other small vessel the equilibrium amount of $\mathbf{L}Mo(NH_3)$ remaining is *not* negligible, the exact amount of course depending upon the headspace in the closed vessel. How much ammonia is lost entirely will then depend upon how often the vessel is opened, and for how long, etc. In most runs in fact the plot or $\ln(1-A/A_\infty)$ versus time is curved toward the "end" of the run, (Figure 4.5) consistent with an approach to an equilibrium and/or an incorrect value for A_∞. We also find that results vary with conditions, e.g., solvent volume, as one might expect.

With these caveats in mind, results for experiments of this type are displayed in Table 4.4. These clearly show that, with the exception of **[HTBTN$_3$N]**$MoNH_3$, dinitrogen can displace ammonia on a catalytically reasonable time scale in all the compounds studied. The differences in rate are not significant, except in the case of **[3,5-dimethoxyHIPT$_2$N$_3$N]**$MoNH_3$. This shows that we may wish to synthesize donating groups into future ligand designs to speed this transformation, perhaps increasing the overall catalyst turnover rate significantly.

Table 4.4) $LMoNH_3$ to $LMoN_2$ exchange rates.

Compound	$t_{1/2}$ (min)
[HIPTN_3N]$MoNH_3$	110
[*p*BrHIPTN_3N]$MoNH_3$	120
[HTBTN_3N]$MoNH_3$	> 6000
[3,5-bis(CF_3)HIPT$_2N_3$N]$MoNH_3$	170
[3,5-dimethoxyHIPT$_2N_3$N]$MoNH_3$	< 45

A Study of the Dinitrogen for Ammonia Exchange Equilibrium

In order to accurately determine the equilibrium constant of the dinitrogen for ammonia exchange reaction (Equation 4.2) the solubility of both NH_3 and N_2 needed to be established. As described in more detail in Appendix 1, NMR was utilized to quantify the concentration of NH_3 and N_2 in solution at several different pressures. For NH_3, triphenylmethane was the internal standard and $[NH_3]$ in C_6D_6 at 22 °C quantified *via* ^1H NMR, resulting in $[NH_3] = 103 \pm 5$ mM/atm(NH_3). For N_2, ^{15}N-nitromethane was the internal standard and $[N_2]$ in C_6D_6 at 22 °C was quantified via ^{15}N NMR, resulting in $[N_2] = 44 \pm 1$ mM/atm(N_2).

With these data in hand it is now possible to determine equilibrium constants at room temperature. [**[HIPTN_3N]**$MoNH_3$][BAr_4'] was dissolved in benzene in a glass bomb containing a side-arm with a glass stopcock and sealed with a septum. A known amount of ammonia was transferred into the vessel and dinitrogen introduced to bring the total pressure in the flask to one atmosphere. One equivalent of decamethylchromocene dissolved in benzene was then added via syringe in order to generate **[HIPTN_3N]**$MoNH_3$ *in situ*. After equilibrium is reached (~2 h), an aliquot was removed for IR analysis and the area of the peak due to **[HIPTN_3N]**MoN_2 at equilibrium was quantified (**L**MoN_2(at equilibrium)). The flask was then flushed with a stream of nitrogen for 30 seconds, at which time the mixture sat for another 12 hours. A second aliquot was analyzed by IR

and the area of the peak due to **[HIPTN$_3$N]**MoN$_2$ was again quantified (**L**MoN$_2$(total)). (Repeating the flushing procedure does not result in an increase for the area of the peak due to **L**MoN$_2$.) Using the standard equilibrium expression (Equation 4.3), and the values for [N$_2$] and [NH$_3$] from appendix 1, we were able to show that K = 0.108 ± 0.016 in benzene at 22 °C.

$$K = \frac{[NH_3][\mathbf{L}MoN_2]}{[N_2][\mathbf{L}MoNH_3]} \qquad [\mathbf{L}MoNH_3] = [\mathbf{L}MoN_2(\text{total})] - [\mathbf{L}MoN_2(\text{at equilibrium})] \tag{4.3}$$

This number should be contrasted with that previously obtained by Dr. Dmitry Yandulov utilizing ^{1}H NMR. It was necessary to heat the system to obtain sufficient peak separation, but at 50 °C, K = 1.[5] This temperature dependence, which favors N$_2$ association at higher temperatures, has yet to be fully explored. It would be particularly interesting to perform catalytic runs at slightly elevated temperatures, although technical issues surrounding such a system would need to be addressed as well as chemical ones (particularly leaking of the apparatus and increased solubility of the proton sources)

Study of a "Hybrid" Diazenido Compound

The half-life for conversion of **[3,5-bis(CF$_3$)HIPT$_2$N$_3$N]**Mo(NH$_3$) into **[3,5-bis(CF$_3$)HIPT$_2$N$_3$N]**MoN$_2$ was shown to be ~170 min, which we do not feel is significantly longer than the half-life for conversion of **[HIPTN$_3$N]**Mo(NH$_3$) into **[HIPTN$_3$N]**MoN$_2$ (~120 min) to result in failure of the catalytic reaction in the **[3,5-bis(CF$_3$)HIPT$_2$N$_3$N]**$^{3-}$ system. Therefore reduction must fail in the **[3,5-bis(CF$_3$)HIPT$_2$N$_3$N]**$^{3-}$ system for some reason other than a slow conversion of the ammonia complex into the nitrogen complex.

As briefly described in chapter 3, **[3,5-bis(CF$_3$)HIPT$_2$N$_3$N]**Mo-N$_2$H can be prepared by treating [**[3,5-bis(CF$_3$)HIPT$_2$N$_3$N]**MoN$_2$-Na(THF)$_2$ with H(OEt$_2$)$_2$BAr$_4$' (0.95

equiv, Figure 4.1). It has not been possible to isolate **[3,5-bis(CF$_3$)HIPT$_2$N$_3$N]**Mo-N$_2$H, as a consequence of its extreme solubility and its instability. Proton NMR spectra reveal a Mo-N$_2$*H* resonance at 8.6 ppm; in the ^{15}N labeled compound $J_{N\text{-}\beta H}$ = 54.5 Hz and $J_{N\text{-}\alpha H}$ = 8 Hz, close to those for the previously characterized **[HIPTN$_3$N]**Mo-N$_2$H species. When prepared in benzene-d$_6$, **[3,5-bis(CF$_3$)HIPT$_2$N$_3$N]**Mo-N$_2$H has been observed to decompose to **[3,5-bis(CF$_3$)HIPT$_2$N$_3$N]**MoN$_2$ at a rate that is first order in Mo with a rate constant of 6.6 ± 0.7 x 10^{-4} min^{-1} ($t_{1/2}$ = 17 ± 2 h). If we compare this to the decomposition of **[HIPTN$_3$N]**Mo-N$_2$H, two differences are readily apparent. First, **[HIPTN$_3$N]**Mo-N$_2$H decomposes to **[HIPT$_2$N$_3$N]**MoH[6] while **[3,5-bis(CF$_3$)HIPT$_2$N$_3$N]**Mo-N$_2$H decomposes to **[3,5-bis(CF$_3$)HIPT$_2$N$_3$N]**MoN$_2$ with the release of H$_2$ (observable by ^{1}H NMR). Second, the rate of decomposition of **[3,5-bis(CF$_3$)HIPT$_2$N$_3$N]**Mo-N$_2$H is significantly faster than that of **[HIPTN$_3$N]**Mo-N$_2$H which decomposes at a rate where k = 1.3 x 10^{-4} min^{-1} ($t_{1/2}$ = 92 h) at 61 °C.[5] It may be important to recognize that **[3,5-bis(CF$_3$)HIPT$_2$N$_3$N]**Mo-N$_2$H is prepared *in situ*, so the product or products of any side reaction (e.g., free ligand) are present. On the basis of the results explained below, the decomposition that we observe may be catalyzed by some side product.

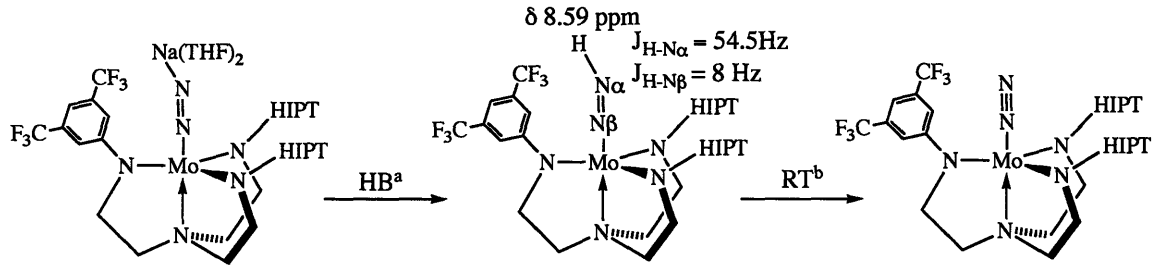

Figure 4.2) Synthesis and reactivity of **[3,5-bis(CF$_3$)HIPT$_2$N$_3$N]**MoN$_2$H. a) Conjugate bases utilized include $(OEt_2)_2$, Et$_3$N, 2,6-lutidine, and 2,4,6-collidine. b) This process is base catalyzed: OEt_2 << 2,6-lutidine ~ 2,4,6-collidine < Et$_3$N.

Labeling studies are informative. **[3,5-bis(CF$_3$)HIPT$_2$N$_3$N]**Mo-N$_2$D was found to

decompose to **[3,5-bis(CF_3)HIPT$_2$N$_3$N]**MoN_2 with k_H/k_D = 3.9; therefore an N-H(D) bond must be cleaved during the rate limiting step. As noted in chapter 3, **[3,5-bis(CF_3)HIPT$_2$N$_3$N]**MoN_2H]Mo-$^{15}N_2$H under $^{14}N_2$ forms **[3,5-bis(CF_3)HIPT$_2$N$_3$N]**Mo$^{14}N_2$H. This conversion is first order in Mo with k = 2.6 x 10^{-2} min^{-1} ($t_{1/2}$= 4.5 h). We re-examined **[HIPTN$_3$N]**Mo-$^{15}N_2$H under similar conditions and found that it also undergoes this exchange reaction, but at a rate at least 100 times slower than that of **[3,5-bis(CF_3)HIPT$_2$N$_3$N]**Mo-N_2H. Whether this difference in ^{15}N exchange rate is important for understanding why catalytic reduction of dinitrogen fails in the [CF_3Hybrid]$^{3-}$ system is not yet known.

In an attempt to utilize catalytically relevant proton sources, [2,6-lutidinium][BAr_4'] was used to form **[3,5-bis(CF_3)HIPT$_2$N$_3$N]**Mo-N_2H *in situ*. The rate of decomposition of **[3,5-bis(CF_3)HIPT$_2$N$_3$N]**Mo-N_2H was accelerated by an order to magnitude to 1.05 x 10^{-2} min^{-1} ($t_{1/2}$ = 1.1 h). Use of [2,4,6-collidinium][BAr_4'] results in a decomposition rate that is qualitatively of the same magnitude (a peak due to [BAr_4'] partially overlaps **[3,5-bis(CF_3)HIPT$_2$N$_3$N]**Mo-N_2*H*, making quantification of the rate impossible). Use of [Et_3NH]BAr_4' as the proton source results in a $t_{1/2}$ of less than 5 minutes; only trace amounts of **[3,5-bis(CF_3)HIPT$_2$N$_3$N]**Mo-N_2*H* were observed 10 minutes after addition. In order to confirm that the conjugate base accelerates the decomposition of **[3,5-bis(CF_3)HIPT$_2$N$_3$N]**Mo-N_2H, 4 equivalents of 2,6-lutidine, 2,4,6-collidine, or Et_3N were added to samples of **[3,5-bis(CF_3)HIPT$_2$N$_3$N]**Mo-N_2H prepared *in situ* using H(OEt_2)$_2$$BAr_4$'. In all three cases, the observed **[3,5-bis(CF_3)HIPT$_2$N$_3$N]**Mo-N_2H decomposed to **[3,5-bis(CF_3)HIPT$_2$N$_3$N]**MoN_2 within 5 minutes.

On the basis of these experiments, we conclude that the less sterically encumbered hybrid systems fail to reduce dinitrogen catalytically as a consequence of a base-catalyzed hydrogenase shunt at the **L**Mo-N_2H point in the catalytic cycle (Figure 4.3). Since we typically utilize the nitride as the pre-catalyst for our catalytic runs, at

least 4 equivalents of base have formed when LMo-N_2H is present in catalytic reactions, which is sufficient to reduce the half-life for **[3,5-bis(CF_3)HIPT$_2$N$_3$N]**Mo-N_2H decomposition to <5 min. Interestingly, when **[3,5-bis(CF_3)HIPT$_2$N$_3$N]**MoN_2 is employed as the precatalyst, 0.7 equivalents of NH_3 are produced, indicating that **[3,5-bis(CF_3)HIPT$_2$N$_3$N]**Mo-N_2H can be (partially) traversed under catalytic conditions when only approximately one equivalent of base is present.

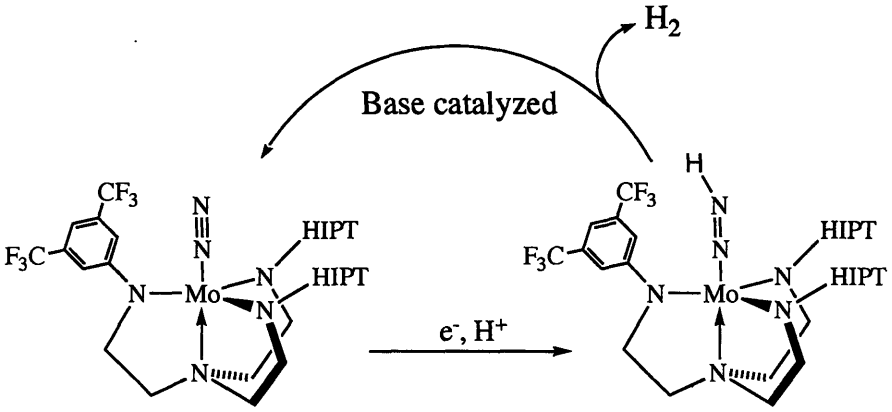

Figure 4.3) Hydrogenase shunt proposed to be present in the hybrid triamidoamine molybdenum systems.

Total Quantification of Reduction Products (NH_3 + H_2)

In order to quantify the products of reduction, we first needed to confirm that NH_3 is the only nitrogen-containing product of catalysis. While previous workers had not observed hydrazine by ^1H and ^{15}N NMR, we desired spectrophotometric confirmation of this result. Therefore, hydrazine quantification was performed on the collected fractions of a standard catalytic run (**[HIPTN$_3$N]**MoN, [2,6-lutidinium][BAr_4'], Cp^*_2Cr). This clearly showed no hydrazine present, down to a detection limit of under 1% per **[HIPTN$_3$N]**MoN. Therefore, over the approximately 3 turnovers of these reactions no hydrazine remains. Whether this is due to it not being formed (most likely) or is due to its disproportionation by the products of the reaction cannot be determined at this time.

In order to further confirm that NH_3 and H_2 are the primary products of the catalytic reaction, we have been developing a simple means by which H_2 can be

quantified. It has been found that gas chromatography allows us, through the use of argon carrier gas and a thermal conductivity detector, to detect and quantify hydrogen in concentrations as low as half a percent (Figure 4.4).

With an accurate method to measure hydrogen, the first step was to run controls of our reagents with no nitrogen molybdenum compounds present. To our surprise, reacting [2,6-Lutidinium][BAr_4'] with Cp^*_2Cr resulted in a yield of 62.5% ± 3.4%. Upon an inspection of the literature, we found that this result is due to a 4,4' coupling of 2,6-lutidine, similar to that observed by Hünig and Wehner to synthesize of 2,6,2',6'-tetramethyl-4,4'-bipyridine.[7] This was synthesized independently and compared to the solids of the above reaction after they were allowed to oxidize in air, confirming the presence of this compound in the final mixture. To prevent this coupling reaction, we moved to pyridinium acids that have the 2, 6 and 4 positions blocked. Reacting [2,4,6-Collidinium][BAr_4'] and Cp^*_2Cr results in H_2 yields > 95%. Similar yields of H_2 were also obtained when [Et_3NH][BAr_4'] or $H(OEt_2)_2BAr_4$' were used as proton sources.

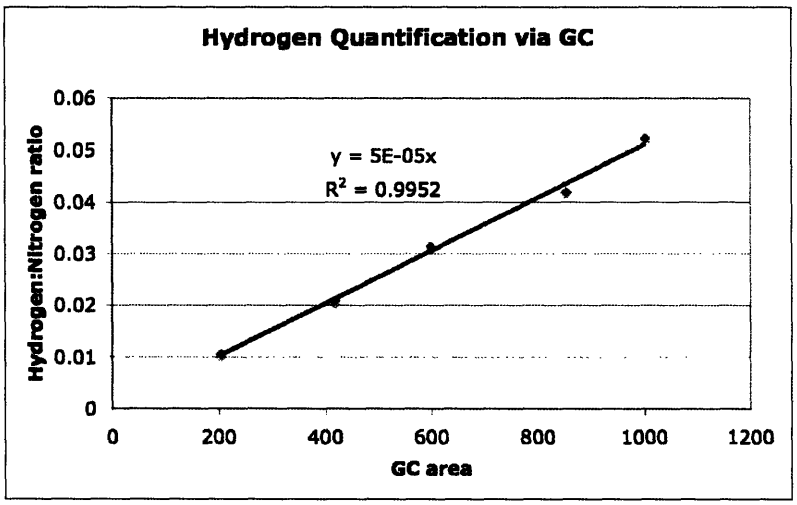

Figure 4.4) Calibration curve for H_2 quantification

We then turned our attention to quantifying all of the products of catalytic reactions. This research is still in its early stages, but the initial results are promising. In short, we are now able to account for > 95% of the reducing equivalents added into the

catalytic runs; either as NH_3, *via* indophenol quantification, or as H_2, by GC measurements. Under standard conditions utilizing [2,6-Lutidinium][BAr_4'] the yield of NH_3 is 58% and the yield of H_2 is 37%, resulting in a 95% overall yield with respect to Cp^*_2Cr. It therefore appears that the catalyst prevents the formation of the 4,4' dimer of 2,6-lutidine, or utilizes it as an H• source (it is possible that H• can directly reduce certain intermediates in the catalytic cycle). In a catalytic run utilizing [2,4,6-collidinium][BAr_4'], the yield of NH_3 is 63%, with H_2 accounting for 33%. The 96% overall yield, as well as the 63% NH_3 yield, is slightly higher than that for 2,6-lutidinium. Determining if this efficiency enhancement is real requires more experimentation, but if true it is most likely due to the preferential reaction of the 4,4' dimer of 2,6-lutidinium to form H_2 over NH_3, lowering ammonia yields.

It is clear that H_2 quantification will serve as a useful tool for future researchers, particularly due to the relative speed at which one can receive the results vs. indophenol quantification of ammonia (minutes vs. days).

Conclusions

The evaluation of the various elementary steps of catalytic dinitrogen reduction in bulky triamidoamine molybdenum compounds remains an area of opportunity for future study. While the majority of new compounds synthesized did not yield new dinitrogen reduction catalysts, their study allowed for further understanding of the catalytic cycle. For example, we have discovered that less bulky "hybrid" systems fail to catalyze the reaction due to a base-catalyzed hydrogenase shunt, the precise mechanism of which remains to be elucidated. Our exploration of alternative proton and electron sources is also still in the beginning phases, and the quantification of H_2 will now allow us to rationally direct us toward new areas of study in this area.

Experimental Section

Procedure for L$MoNH_3$ to LMoN_2 Kinetics [[**HIPTN_3N**]$MoNH_3$][BAr_4'] (50 mg, 0.02 mmol) was dissolved into 2 mL of heptane in a vial with a glass stirbar. To this

was then added Cp^*_2Cr (7 mg, 0.02 mmol) also dissolved in 2 mL of heptane. Aliquots of this sample were periodically removed and IR spectrum taken. Between aliquots, the vial was kept tightly capped. The MoN_2 peak was identified at 1990 cm^{-1} and its growth was followed during the experiment by quantification of the peak area. Fitting this data to $\ln(1\text{-Area/Area}_{infinity})$ vs. time results in a linear fit with $t_{1/2} = 100 \pm 5$ min. An example for the data obtained from this type of experiment is shown in Figure 4.5, which clearly shows the "bending" of points taken later in the reaction, presumably due to incomplete evacuation of NH_3 from the system.

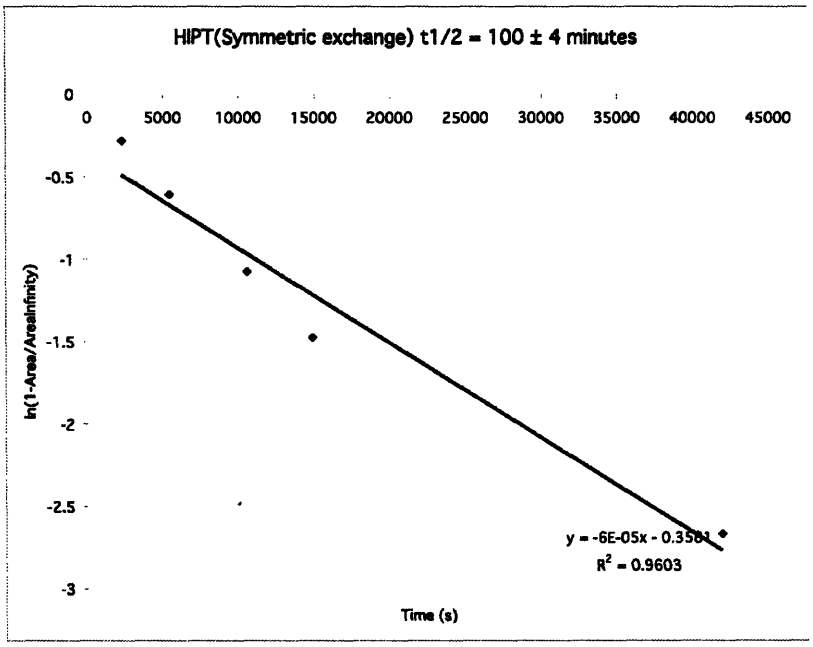

Figure 4.5) Exchange of **[HIPTN$_3$N]**MoNH$_3$ to form **[HIPTN$_3$N]**MoN$_2$. Note the "bending" of the curve at long times.

Dinitrogen Catalysis Procedure The experimental for the catalytic process has been reported in print[2] and in an in lab document prepared by Dr. Dmitry Yandulov (a PDF of this document is included the "Data" folder of this chapter on our server). A brief version containing the salient points is presented below.

Our lab has developed an apparatus that allows for slow addition of reducing agent while maintaining the sealed environment necessary for catalyst stability and

ammonia quantification (Figure 4.6). To section A of this apparatus [**HIPTN$_3$N**]MoN (9.8 mg, 5.7 μmol) and [2,6-lutidinium][BAr$_4$'] (282 mg, 290 μmol) are added to 2 mL of heptane (freshly vacuum transferred from Na/benzophenone ketyl). Decamethylchromocene (72.5 mg, 22.4 μmol) is then dissolved in 10 mL of heptane and carefully pulled into section B of the apparatus utilizing the magnetically driven Teflon® plunger. The apparatus is then assembled, placed onto a syringe pump, and the magnet scaffold connected to the drive arm of the pump.

The addition rate of the syringe pump is set to 1.7 mL per hour and the reaction is stirred during the addition (~ 6 h), then allowed to stir an additional hour after addition is complete. The resulting mixture in solution A is now bright yellow due to the presence of solid [Cp*$_2$Cr][BAr$_4$']. The volatiles are then vacuum transferred onto 2 mL of a 1 M HCl in ether collection flask. The resulting solids in the apparatus are then treated with a solution of 1 mL THF, 2 mL methanol, and NaO^{t}Bu (220 mg, 2.8 mmol) and allowed to stir for 5 minutes, at which time the resulting volatiles are vacuum transferred onto the same acidified collection flask. All volatiles are then removed *in vacuo* from the collection flasks, taking care to not heat the vessel to avoid sublimation of NH_4Cl.

The amount of ammonium chloride in the flasks is then quantified utilizing the indophenol method.[8] Again, a PDF version of the procedure by Dr. Dmitry Yandulov is available in the "Data" folder of this thesis on the server. Briefly, an aqueous solution containing phenol and $Na_3Fe(NO)(CN)_5 \cdot 2H_2O$ is mixed with the NH_4Cl solution of interest. To this is added an aqueous solution containing NaOH and NaOCl. This initiates the reaction to form the bright blue indophenol product, which is quantified using UV/Vis spectroscopy at 625 nm. With proper dilution, ammonia can be detected from the catalytic runs in amounts as low as 0.2 μmol.

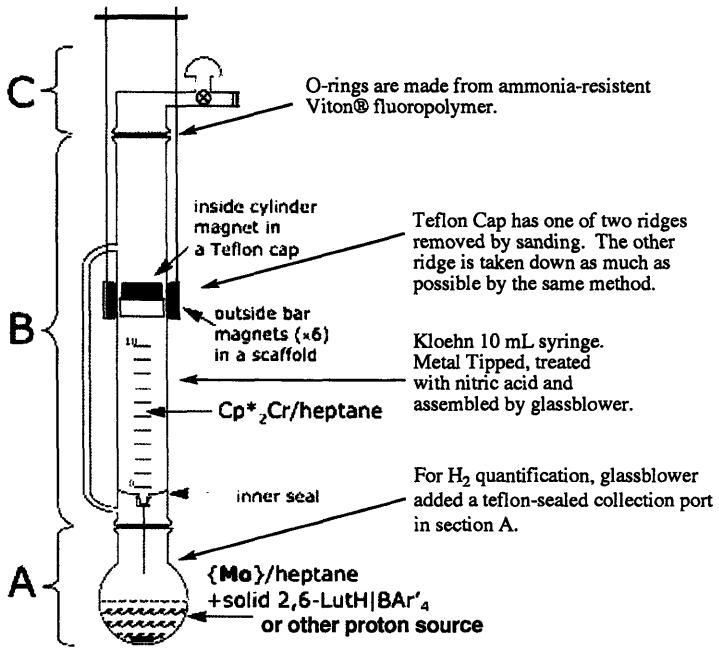

Figure 4.6) Apparatus used for catalytic reduction of dinitrogen. Notes are included for future assembly and modification

Procedure for Hydrogen Quantification

As seen in Figure 4.7, the apparatus used for ammonia quantification utilizes a fully Teflon® sealed system in which the reagents are contained. The components can be added separately into the two bulbs, and mixed together quickly by simply rotating the apparatus. For example, Cp^*_2Cr (14.5 mg, 44 mmol) in 4 mL of heptane is added to the upper bulb, while [2,4,6-collidinium][BAr_4'] (102 mg, 104 mmol) is added to 2 mL of heptane in the lower bulb. When mixed the solution slowly turns the bright yellow color of [Cp^*_2Cr][BAr_4'] over 5 h, with the final liquid being completely colorless as the yellow [Cp^*_2Cr][BAr_4'] crashes out of solution. Hydrogen quantification, utilizing a gas chromatograph fitted with a TCD detector and a 30 m, 0.5 mm, 25 μm, MolSeive

column, showed that 0.65% of the volatiles were H_2. This is 95% of that expected for the described reaction in an 86 mL reaction vessel.

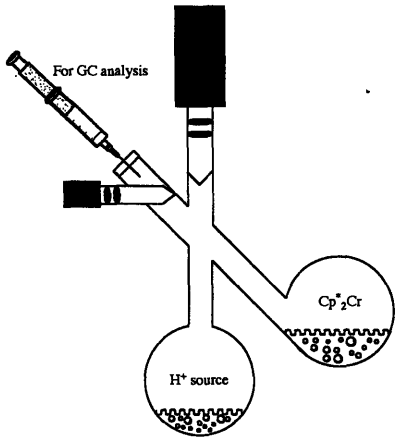

Figure 4.7) Apparatus for quantification of H_2 from a two component reaction.

References

1. Ritleng, V.; Yandulov, D. V.; Weare, W. W.; Schrock, R. R.; Hock, A. S.; Davis, W. M. *J. Am. Chem. Soc.* **2004**, *126*, 6150.

2. Yandulov, D.V.; Schrock, R.R. *Science* **2003**, *76*, 301.

3. Schrock, R.R. *Acc. Chem. Res.* **2005**, *38*, 955.

4. Yandulov, D.V.; Schrock, R.R. *J. Am Chem. Soc.* **2002**, *124*, 6252.

5. Yandulov, D.V.; Schrock, R.R. *Inorg. Chem.* **2005**, *44*, 1103.

6. Yandulov, D.V.; Schrock, R.R.; Rheingold, A.L.; Ceccarelli, C.; Davis, W.M. *Inorg. Chem.* **2003**, *42*, 796.

7. Hünig, S.; Wehner, L. *Synthesis* **1989**, 552.

8. A) Chaney, A.L.; Marbach, E.P. *Clinical Chem.* **1962**, *8*, 130. **B)** Weatherburn, M.W. *Anal. Chem.* **1967**, *39*, 971.

APPENDIX 1

Dinitrogen and Ammonia Solubility in Benzene

Dinitrogen solubility via ^{15}N NMR.

Utilizing ^{15}N labeled nitrobenzene as an internal standard, the amount of dissolved $^{15}N_2$ was measured via ^{15}N NMR. Nitrobenzene was at a concentration of 0.176 M, and differing pressures of $^{15}N_2$ were introduced into a J-Young tube containing the internal standard in 0.7 mL C_6D_6 that had been freeze/pump/thawed 3 times. The concentration of $^{15}N_2$ was found to be linearly dependent with respect to pressure, (Figure A1.1) with a measured solubility of 44.0 ± 1 mmol/atm($^{15}N_2$). The partial pressure of benzene was included in these calculations.

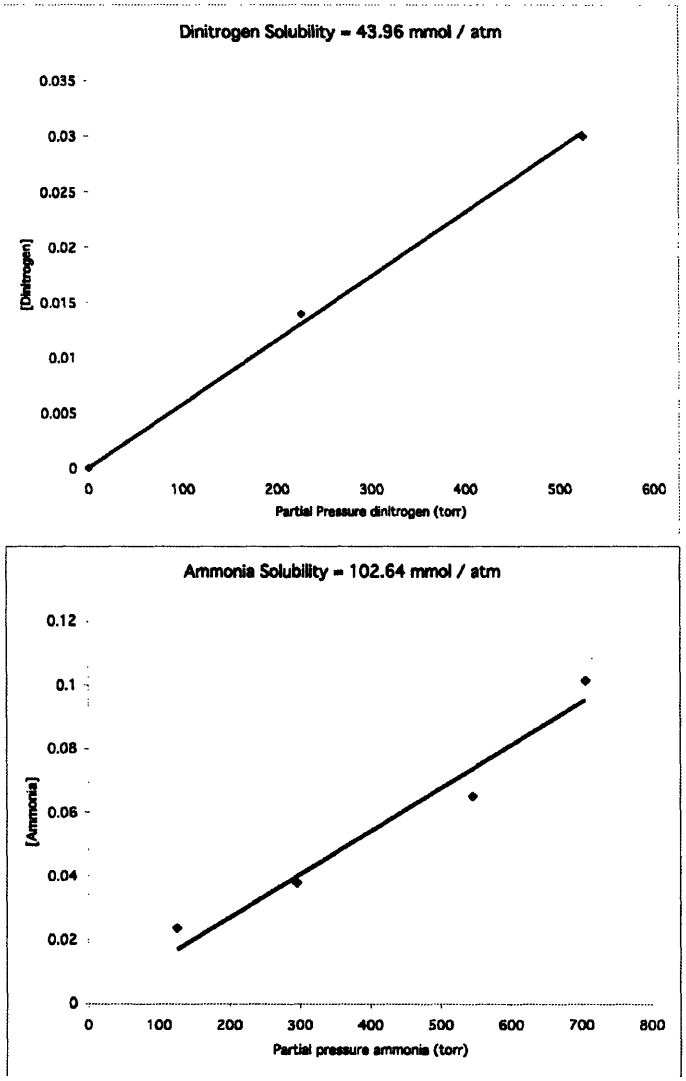

Figure A1.1) $[N_2]$ and $[NH_3]$ in benzene under varied pressures of $N_2$and NH_3 respectively.

NH_3 solubility via ^1H NMR.

Utilizing triphenylmethane as an internal standard, the amount of dissolved NH_3 was measured *via* ^1H NMR. A known pressure of NH_3 was introduced into a freeze/pump/thawed (3x) sample of the internal standard in 0.7 mL C_6D_6 (~ 0.12 M Ph_3CH). The concentration was found to be linearly dependent with respect to pressure, (Figure A1.1) with a measured solubility of 103 ± 6 mmol/atm(NH_3). Values were corrected for the partial pressure of benzene.

APPENDIX 2

"Reduction" of [HIPTN_3N]MoN Using H_2 – The Importance of Control Experiments

We have been attempting to observe reduction of **[HIPTN$_3$N]**Mo complexes using H_2 under relatively mild conditions (see Chirik et. al.[1] for an example this in a non-catalytic process). To test our nitrogen reduction catalysts under such conditions, "hydrogenation" reactions were carried out with only **[HIPTN$_3$N]**Mo compounds present. We also attempted reactions in the presence of known hydrogenation catalysts.

When **[HIPTN$_3$N]**MoN or **[HIPTN$_3$N]**MoH are treated with 1 atm of N_2 and 4 atm of H_2 in benzene at 100 °C for several days, only trace amounts of free ammonia were observed in the volatile collection. ^{1}H NMR characterization of the solids remaining from reaction of **[HIPTN$_3$N]**MoH with H_2, primarily the starting material was observed. However, a minority product was observed that had two sharp singlets (or a doublet) at ~ 5 ppm. These resonances decayed over time, and were quantitatively replaced by **HIPTN$_3$N]**MoN_2. The identity of this compound remains unknown due to it being an unstable minority product, although future workers may wish to examine this reaction directly and in more detail (for instance, by treating **L**MoN_2 with high pressures of H_2).

For hydrogen reduction utilizing external catalysis, we received two hydrogenation catalysts from Prof. Robert H. Morris at University of Toronto. These are are $RuH(PPh_3)_2(H_2N(1,1,2,2\text{-tetramethyl})ethylNH)$[2] and $RuHCl\{en\text{-}P_2(NH)_2\}$[3] (Figure A2.1). The catalysts hydrogenate ketones *via* a two-step process, with an initial protonation step followed by hydride transfer to the resulting carbocation.[3] In essence, the H_2 is split into H^- and H^+ by the Ru complexes, which are used to reduce the ketone. We set out to test whether these compounds were capable having similar reactivity with dinitrogen reduction intermediates, forming ammonia directly from N_2 and H_2.

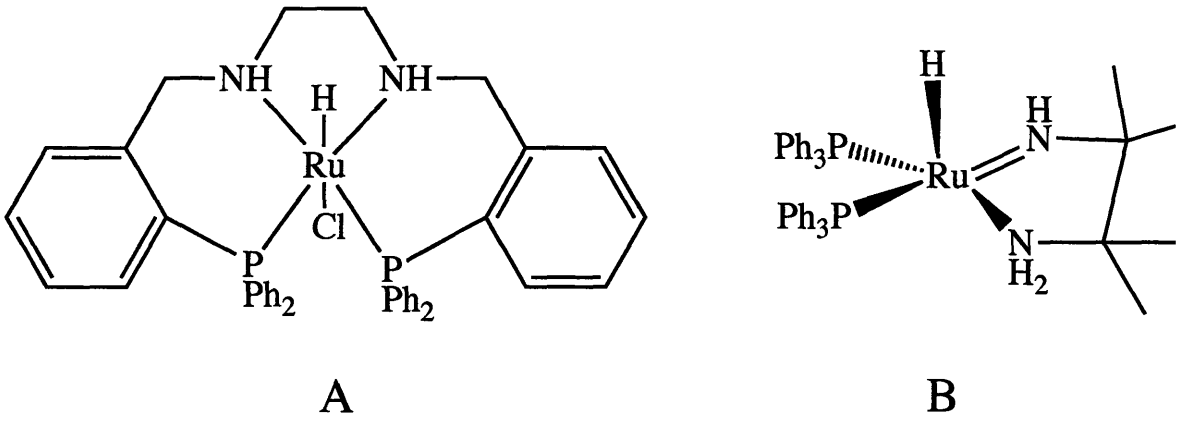

A B

Figure A2.1) A) RuHCl{en-$P_2(NH)_2$} and B) RuH$(PPh_3)_2$(H_2N(1,1,2,2-tetramethyl)ethylNH).

The procedures used for hydrogenation are similar for all reactions. In one case, 5 mg (6.7×10^{-3} mmol) of RuHCl{en$P_2(NH)_2$} and 15.6 mg (9.2×10^{-3} mmol) of HIPTMoN were added to 5 mL of benzene in a glass jacketed 50 mL parr bomb in the box under an N_2 atmosphere. This was then pressurized with ~4 atmospheres of H_2 and allowed to sit at 90°C for 2 days. The volatiles were then removed and vacuum transferred onto a 1 M HCl in ether solution, allowed to warm to room temperature, and all the volatiles removed. Indophenol quantification of the residue resulted in 0.03 equivalents of ammonia being observed relative to HIPTMoN, and 0.04 equivalents relative to RuHCl{en$P_2(NH)_2$}.

For the other hydrogenation catalyst, 5.1 mg (6.9×10^{-3} mmol) of RuH$(PPh_3)_2$(H_2N(1,1,2,2tetramethyl)ethylNH) and 16.2 mg (9.5×10^{-3} mmol) of HIPTMoN were added to 5 mL of benzene in a glass jacketed 50 mL parr bomb in the box under an N_2 atmosphere. This was then pressurized with ~4 atm of H_2 and allowed to sit at 90°C for 2 days. The volatiles were then removed and vacuum transferred onto a 1 M HCl in ether solution, allowed to warm to room temperature. The solids were brought back into the box, and transferred (via dissolution in pentane) to a 50 mL glass bomb. A mixture of THF/Methanol/NaO^{t}Bu was then added, and the volatiles again vacuum transferred onto the same HCl/ether solution. This was allowed to warm to room temperature, and the volatiles were entirely removed. Indophenol analysis of the residue resulted in 0.73 equivalents of ammonia

being observed relative to HIPTMoN, and 1.01 equivalents relative to $RuH(PPh_3)_2(H_2N(1,1,2,2tetramethyl)ethylNH)$.

Control reactions in only the presence of Ru catalysts were shown to not be enough to produce NH_3 under these conditions. It was also found in control reactions with only **[HIPTN$_3$N]**MoN present, a work-up of the solid residue produced 1 equivalent of free ammonia. To check if this result was due to hydrogenation conditions or the following workup, a solution of **[HIPTN$_3$N]**MoN in THF was treated with the standard THF/methanol/NaO^{t}Bu solution and the volatiles vacuum transferred onto 1M HCl/ether. We found that this resulted in ~1 equivalent of NH_3 to be released from the nitride. Our controls thus showed that the Ru-based hydrogenation catalysts do not improve NH_3 yield, but instead lower ammonia yields by decomposing **[HIPTN$_3$N]**MoN. Finally, H_2 itself does not produce ammonia from the nitride, but instead it is the workup conditions that "reduce" the nitride to free ammonia.

This set of experiments caused us to consider more experiments in order to interpret catalytic reactions where only 1 equivalent of NH_3 is observed. To ensure that our results depict actual NH_3 formation from catalytic conditions, we now perform a second standard catalytic run if only 1 equivalent of NH_3 is observed. In this run, separate collection flasks for the initial volatiles and final solids workup are individually collected and analyzed for NH_3 content. For the unsymmetric ligands described in this thesis we observe free NH_3 in the initial volatiles, consistent with our hypothesis that a hydrogenase shunt is active at the **L**MoNNH step.

Future workers need to consider that the standard workup conditions can yield ammonia directly from the nitride, and accommodate for this in experimental design and interpretation.

References

1. Pool, J.A.; Lobkovsky, E.; Chirik, P.J. *Nature* **2004**, *427*, 527.

2. Li, T.; Churlaud, R.; Lough, A. J.; Abdur-Rashid K.; Morris R. H. *Organometallics* **2004**, *23*, 6239.

3. Clapham, S.; Hadzovic, A.; Morris; R.H. *Coord. Chem. Rev.* **2004**, *248*, 2201.

APPENDIX 3

Synthesis and Crystal Structure of a Symmetric Triamidoamine Iron(III) Compound

Synthesis of [*p*BrHIPTN$_3$N]FeCl-Li(THF)$_3$

The synthesis of triamidoamine iron complexes was previously examined by our group in the silylated TREN ligands. The major discovery in that work was the observation of an Fe^V imido compound.[1] However, the study of dinitrogen reduction intermediates using iron has yet to be undertaken with this ligand type. This appendix describes the synthesis and characterization of one possibly entry into such studies – [*p*BrHIPTN$_3$N]FeCl-Li(THF)$_3$.

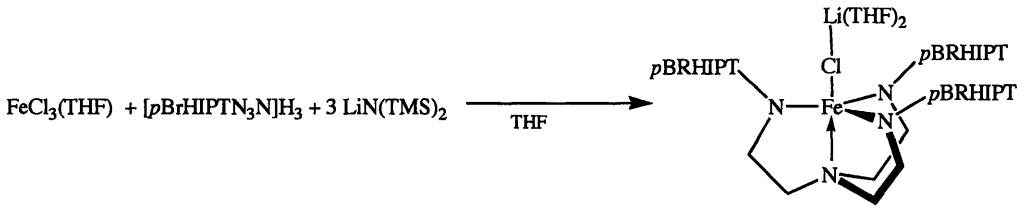

Figure A3.1) Synthesis of [*p*BrHIPTN$_3$N]FeCl-Li(THF)$_3$

The *para*-bromo ligand [*p*BrHIPTN$_3$N]H$_3$ was utilized in this study for several reasons. First, I had several grams of the ligand on hand that was receiving no further attention with molybdenum. Second, the heavy bromine atoms ease crystallographic characterization, which due to the paramagnetic nature of the high spin iron complexes formed will have to be a major source of data for these compounds.

Since the lithium salts of the HIPT ligands are problematic to synthesize cleanly, I utilized a similar procedure to the molybdenum compounds in the synthesis of this iron compound. It was initially assumed that this compound would be similar in nature to the "naked" Fe(III) species originally synthesized our group.[2] However crystallography revealed that a Fe(III) "ate" compound with a Cl-Li(THF)$_2$ group coordinated within the binding pocket was the characterized product of this reaction. (Figures 1, 2, and 3, Table 1) Close examination of the crystal structure revealed that the amide nitrogen atoms of the compound are highly pyramidalized (the sum of angles around an amide nitrogen is 348.3°, a planar nitrogen would have a value of 360°), suggesting, at best, a weak pseudo-double bond between the amides and the metal center as is present in the

molybdenum compounds. (Figures A3.2, and A3.3, Table A3.1) We posit that this is due to the partial filling (by the metal) of the orbitals necessary to interact with the pseudo triple bond formed by the amides, weakening this interaction in Fe(III) relative to Mo(III-VI) of the parent molybdenum system. The bond lengths and angles are otherwise unremarkable for compounds of this type. ^{1}H NMR studies show several broad peaks, with a particularly broad peak centered at 4.6 ppm which appears to be diagnostic for the species (other observed peaks appear to be coordinated THF and the phenyl protons). UV/Vis spectroscopy of this compound shows a unique absorbance at 595 nm. A magnetic susceptibility measurement was performed by Dr. Xuliang Dai, which resulted in μ_{eff}= 5.30 μ_B. Thus, the metal in this system is high-spin F(III) d_5.

Initial studies were undertaken attempting to understand the reactivity of this compound. Reduction with Na/Hg amalgam resulted in a yellow solution that had no discernable N_2 infrared resonance. Xuliang Dai has shown (by synthesis of the parent HIPT compound *via* another route) that this compound is most likely [***p*BrHIPTN$_3$N**]Fe^{II}-(THF).

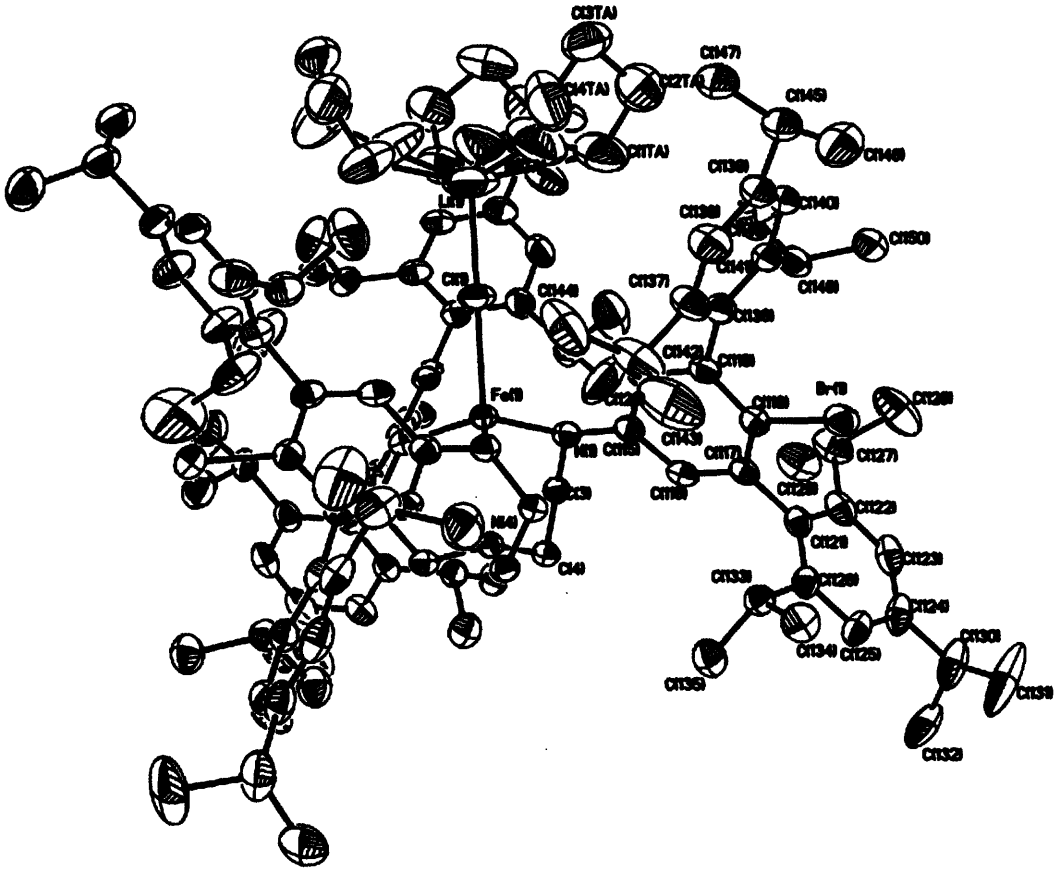

Figure A3.2) X-ray determined crystal structure for [***p*BrHIPTN$_3$N**]FeCl-Li(THF)$_3$. Hydrogen atoms are omitted for clarity.

Table A3.1) Selected bond distances and angles for [*p*BrHIPTN$_3$N]FeCl-Li(THF)$_3$

Bond	**Metric Parameter**
Fe-N(1) (amide)	1.972(4) Å
Fe-N(4) (amine)	2.545(6) Å
Fe-Cl	2.368(2) Å
Cl-Li	2.26(2) Å
N(1)-Fe-Cl	104.43(11)°
N(1)-Fe-N(4)	75.57(11)°
C(3)-N(1)-Fe	109.9(3)°
C(115)-N(1)-Fe	121.9(3)°
C(115)-N(1)-C(3)	116.5(4)°
Sum of angles around N(1)	348.3°

[***p*BrHIPTN$_3$N**]FeCl-Li(THF)$_3$ was reacted with dry ammonia in CH_2Cl_2 and heated for several days at 60° C. The resulting compound was also a purple solid, but has a few subtle spectroscopic differences to the parent compound. ^{1}H NMR studies show several broad peaks, with a unique peak centered at 5 ppm, a shift of ~0.4 ppm from the starting material. Also, UV/Vis of this compound shows an absorbance at 550 nm, a shift of ~40 nm from ***p*BrHIPT**FeCl-Li(THF)$_3$. This could be ***p*BrHIPT**FeCl-Li(NH$_3$)$_3$, where ammonia has displaced the THF molecules at the lithium atom. I find it unlikely that the observed a small shifts in ^{1}H NMR and UV/Vis spectra would be observed if NH_3 was bound in the pocket, although at this point that cannot be ruled out. In the absence of other data in this system, the identity of this compound remains ambiguous.

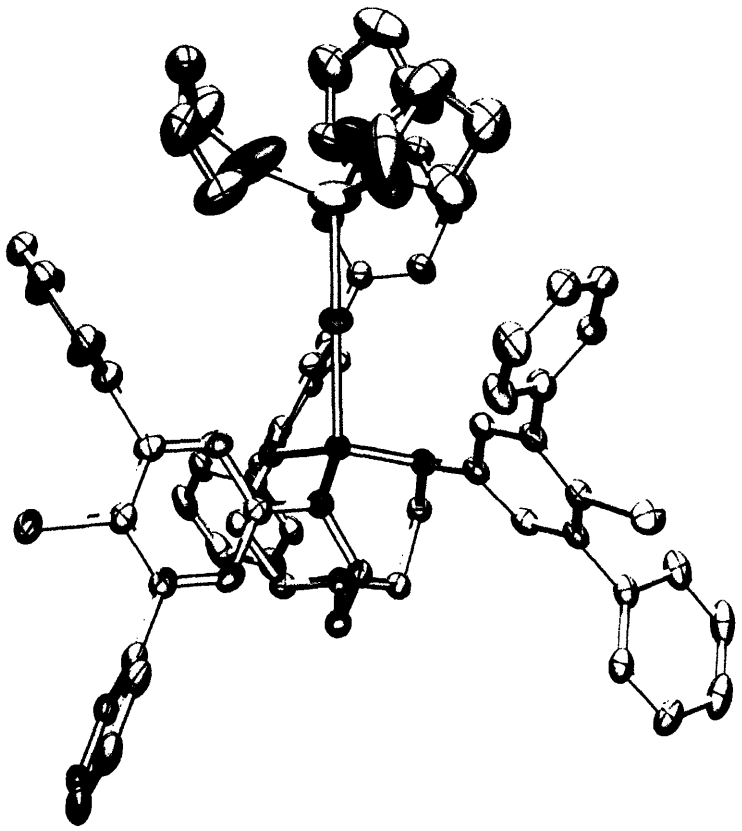

Figure A3.3) POVRAY x-ray structure for [***p*BrHIPTN$_3$N**]FeCl-Li(THF)$_3$.

Experimental Section

[*p*BrHIPTN$_3$N]FeCl-Li(THF)$_2$ Briefly, 0.17 g (0.7 mmol) of $FeCl_3$(THF) (yellow) was added to 1.05 g (0.6 mmol) [*p*BrHIPTN$_3$N]H$_3$ (colorless)in THF, resulting in a dark green solution. This was then heated @ 40° C for 3 hours, upon which time the solution had lightened to a deep yellow color. To this was added 0.33 g (2.0 mmol) LiN(TMS)$_2$ with the solution turning a deep purple immediately. This solution was then heated for 40° C overnight. The solvent was then removed and brought into pentane, filtered through celite, and recrystallized. The first crop was a bright purple crystalline solid yielding 0.168 g (13%). Subsequent crops are yellow in color, but turn purple with

addition of THF. The resulting purple compound has yet to be quantified, but would significantly increase the yield. ^{1}H NMR (C_6D_6, 20°C) δ 4.6 (br s), 2.69 (br m), 1.82 (br m), 1.25 (br m), 0.88 (br s) UV/Vis (C_6H_6, 22°C) 314 nm, 375 nm, and 590 nm. μ_{eff}= 5.30 μ_B in benzene-d_6 with C_6Me_6 serving as an internal standard.

References

1. Cummins, C.C.; Schrock, R.R. *Inorg. Chem.* **1994**, *33*, 395.

2. Cummins, C.C.; Lee, J.; Schrock, R.R.; Davis, W.D. *Angew. Chem. Int. Ed.* **1992**, *31*, 1501.

APPENDIX 4

Table of Catalytic Reactions

Table A4.1 Catalytic Runs Performed During the Completion of this Thesis

Compound	Acid	e^-	NH_3/NH_3(calc)	% of e^-	from N_2	Comments	Exp #
pBrMoN	Lut	Cr	6.35/10.45	61	5.35		135
pBrMoN	Lut	Cr	6.58/11.11	58.5	5.58		136
pBrMoN	Lut	Cr	4.7/11.2	42	3.7	Too fast add[a]	144
pBrMoN	Lut	Cr	6.9/12.14	58.5	5.9		146
pBrMoN	Lut	Co	2.9/12.1	24	1.9		147
LutMoN	Lut	Cr	1.3/11.3	11.4	0.3		148
pBrMoN	Lut	Co	2.5/13.5	18.5	1.5	10h	164
pBrMoN	Lut	Co	2.5/12.4	20	1.5	20h	166
pBrMoN	Lut	Co	1.8/12.6	12.5	0.8	6h	167
PhLutMoN	Lut	Cr	1.4/10.6	13	0.4		180
HIPTMoN	Lut	Co	3.6/9.8	37	2.6		183
PhLutMoN	Lut	Co	1.6/13.7	12	0.6		185
CF_3MoN	Lut	Cr	0.96/10.8	9	0		198
N_2NVN_2	Lut	Cr	0.04/11.4	0.3	0	Nathan (crude)[b]	200
HIPTMoEthyl	Lut	Cr	2.65/11.5	23	1.65	Matt's[c]	202
MesMoN	Lut	Cr	1.2/6.4	19	0.2		217
HIPTMo-PH-Ph	Lut	Cr	0/6.6	0	0	Matt's[c]	218
HIPTMoethene	Lut	Cr	1.7/6.3	27.5	0.7	Matt's[c]	219
HIPTMoN	Lut	Cr	4.4/5.7	77	3.4		230
HIPTMoN	Lut	Cr	1.5/6.1	25	0.5	+ 145 eq Lut[d]	233
DimethylMoN	Lut	Cr	0.9/6.4	14	0		234
TripMoN	Lut	Cr	2.9/6.2	47	1.9		239
HIPTMoN	H_2	H_2	0	0	0	3atm H_2 + 1 N_2[e]	246
DimethoxyMoN	Lut	Cr	0.87/7.2	12	0		252
HIPTMoH	H_2	H_2	0	0	0	3atm H_2 + 1 N_2[e]	254
HIPTMoN	PhLut	Cr	0.35/6.5	4	0		261
HIPTMoN	Lut	Cr	4.3/6	72	3.3		262
HIPTMoN	2,4-Lut	Cr	4.7/6.5	72	3.7		267
HIPTMoN	Lut	Cr	2.9/6.7	43	1.9	+ 145 THF[d]	269
HIPTMoN	Lut	Cr	4.3/6.0	71	3.3		270
HIPTMoN	2,4-Lut	Cr	5.0/11	45	4		275
HIPTMoN	3,5-Lut	Cr	1.02/11.2	9	0.02		278
HIPTMoN	2,6eth Pyr	Cr	3.7/12	31	2.7		280
HIPTMoN	2,4-Lut	Cr	5.1/12	43	4.1		286
HMTMoN	Lut	Cr	0.7/11.1	6	0		287
HIPTMoN	Lut	Cr	5.4/11.2	48	4.4	3 h add time[f]	290
TripMoN	Lut	Cr	2.5/11	23	1.5		294

HIPTMoN	Bu3SnH	←	0.9/15	6	0		297
CF_3MoN	Lut	Cr	0.3/11.4	2.5	0	volatiles	298A
CF_3MoN	Lut	Cr	0.67/11.4	5.7	0	solids	298B
HIPTMoN	Lut	Cr	6.6/11.3	58	5.6	35 psi total[g]	301
HIPTMoN	Lut	Cr	2.05/11.6	18	1.05	35 psi, 30sec[h]	302
HIPTMoN	Bu3SnH	←	0.25/?		0	C_6H_6 110° bomb	313
HIPTMoN	H_2	H_2	0.03/?		0	RuHCl{enP$_2$}[e]	314
HIPTMoN	H_2	H_2	0.72/?		0	RuH(PPh$_3$)$_2$(N.)[e]	317
CF_3MoN_2	Lut	Cr	0.58/10.8	5.4	0	~30% ligand	325
None	H_2	H_2	0/?	0	0	RuH(PPh$_3$)$_2$(N.)[e]	334
HIPTMoN	H_2	H_2	0.54/?	?	0	RuHCl{enP$_2$}[e]	335
HIPTMoN	H_2	H_2	0/?	0	0	No H_2 cat.[e]	338
None	H_2	H_2	0/?	0	0	RuHCl{enP$_2$}[e]	339
HIPTMoN	H_2	H_2	0.63/?	?	0	RuH(PPh$_3$)$_2$(N.)[e]	340
HIPTCrN?	Lut	Cr	0.30/11.9	2.5	0	Nathan's[b]	348
HIPTMoN	Lut	Cr	7.1/12	59	6.1	500mL sidearm[i]	363
HIPTMoN	None	←	0.95/1	95	0	Cat + workup[j]	365
HIPTMoN	Lut	Cr	7.9/13.9	57	6.9	w/GC[k]	388
HIPTMoN	Coll	Cr	4.1/12.5	33	3.1		392
HIPTMoN	Coll	Cr	6.7/11.0	61	5.7	w/GC[k]	394
HIPTMoN	Lut	Cr	5.2/12.1	44	4.2	w/GC[k]	395
HIPTMoN	Coll	Cr	6.9/12.2	56	5.9		404
HIPTMoN	Lut	Cr	6.05/11.8	51	5.05	No solids[l]	407v
HIPTCrN	Lut	Cr	0.32/11.1	2.8	0	Volatiles	409v
HIPTCrN	Lut	Cr	0.47/11.1	4.3	0	Solids	409s
HIPTCrN	None	←	0.1/1	10	0	Cat + workup[j]	410
HIPTMoN	Lut	Cr	6.5/10.9	60	0		412
HIPTMoN	Coll	Cr	4.3/12	36	3.3	Batch run[m]	415A
HIPTMoN	Coll	Cr	1.3/12	11	0.3	415A as precat[m]	415B
propMoNH$_3$	Coll	Cr	0.95/12.1	8	0	Jia Min's[n]	417
HIPTMoN	Coll	Cr	6.7/10.7	63	5.7	w/ GC (33% H_2)[k]	419
HIPTMoN	Lut	Cr	6.6/11.5	60	5.6	37% H_2[k]	425
HIPTMoN	Coll	Cr	1.05/12.2	9	0.05	3 hr (60% H_2)[k]	427
HIPTMoN	Et_3N	Cr	0.02/11.6	.1	0	Volatiles	441v
HIPTMoN	Et_3N	Cr	0.72/11.6	6	0	Solids	441s
HIPTMoN	Et_3N	Cr	0.63/12.2	5	0		442

---

[a] Addition of this was not optimal due to the apparatus "sticking," resulting in uneven addition.

[b] Sample provided by Nathan Smythe.

[c] Sample provided by Dr. Matthew Byrnes

[d] Additive was included in the initial dissolution of the catalyst + acid solution. Upon addition of lutidine, the color instantaneously shifted from red ($\mathbf{L}MoNH^+$) back to the yellow of **L**MoN. No obvious color shift was seen in the THF additive reaction.

[e] In a Parr bomb 3 atm of H_2 was added to the bomb that had been loaded in the box under 1 atm N_2. The solution was then heated at 100 °C for several days.

[f] The rate of addition was 3.4 mL per hour.

[g] The apparatus was pressurized to 35 psi of N_2 for the catalytic run.

[h] The apparatus was pressurized to 35 psi of N_2 for the catalytic run. All the reducing agent was added over a time period of ~ 30 seconds.

[i] The apparatus was fitted with an additional piece which contained a 500 mL sidearm.

[j] The compound was only treated with the standard workup conditions.

[k] H_2 quantification by GC was performed on this sample.

[l] The solid collection broke during collection, therefore this sample only contains the volatiles.

[m] This experiment tested whether collidine would limit the decomposition of the catalyst between batch experiments. For 415B, the solids that remained from 415A were utilized at the pre-catalyst, with only [2,4,6-collidinium][BAr_4'] and Cp^*_2Cr being added (as usual) to do a second run in the same flask.

[n] Sample provided by Jia Min Chin

APPENDIX 5

X-ray Crystallography Tables for [***p*BrHIPTN$_3$N**]MoN, [**HIPTpropylN$_3$N**]MoCl, [**3,5-bis(CF$_3$)HIPT$_2$N$_3$N**]MoCl, [**3,5-dimethylHIPT$_2$N$_3$N**]MoN$_2$-Na(THF)$_2$, and [***p*BrHIPTN$_3$N**]FeCl-Li(THF)$_3$

Portions of the material covered in this chapter have appeared in print:

Ritleng, V.; Yandulov, D. V.; Weare, W. W.; Schrock, R. R.; Hock, A. S.; Davis, W. M. *J. Am. Chem. Soc.* **2003**, *126*, 6150-6163.

X-ray Structural Studies

Low temperature diffraction data were collected on a Siemens Platform three-circle diffractometer coupled to a Bruker-AXS Smart Apex CCD detector with graphite-monochromated MoKα radiation (λ = 0.71073 Å), performing ϕ- and ω-scans. The structures were solved by direct methods using SHELXS[1] and refined against F^2 on all data by full-matrix least squares with SHELXL-97.[2] All non-hydrogen atoms were refined anisotropically. All hydrogen atoms were included into the model at geometrically calculated positions and refined using a riding model. The isotropic displacement parameters of all hydrogen atoms were fixed to 1.2 times the *U* value of the atoms they are linked to (1.5 times for methyl groups). Crystal and structural refinement data for all structures are listed in Tables below.

The structure of **[3,5-bis(CF_3HIPT$_2$N$_3$N]**MoCl is strongly affected by disorder: both CF_3 groups and about half of all carbon atoms are found distributed over two positions. These disorders were refined with the help of similarity restraints on 1-2 and 1-3 distances and displacement parameters as well as rigid bond restraints for anisotropic displacement parameters. The relative occupancies of the disordered components were refined freely, while constraining the total occupancy of both components to unity. Probably owing to the massive disorder the crystal diffracted only to about 1.0 Å resolution and gave rise to data of only mediocre quality. To counteract the effects of the resulting low data-to-parameter ratio, rigid bond and similarity restraints were used for the displacement parameters of all atoms.

[3,5-dimethylHIPT$_2$N$_3$N]MoN$_2$-Na(THF)$_2$ crystallizes with one molecule of $C_{86}H_{119}MoN_6$, one sodium ion and the following solvent molecules in the asymmetric unit: Two thf molecules (one of which disordered) coordinated to the sodium ion, one sixth of a non-coordinated thf molecule (sixfold disordered about the crystallographic -3 axis), two half occupied heptane molecules, and one sixth of a pentane molecule (sixfold disordered about the crystallographic -3 axis). The pentane molecule is probably a

heptane molecule where the two methyl groups are disordered in addition to the disorder described, however refinement as heptane was not stable. These disorders were refined as described above.

References

1. Sheldrick, G. M. *Acta Cryst.* **1990**, *A46*, 467.

2. Sheldrick, G. M (**1997**). SHELXL 97, University of Göttingen, Germany.

Table A5.1) Crystal data and structure refinement for [*p*BrHIPTN$_3$N]MoN

Identification code	03289	
Empirical formula	C114 H156 Br3 Mo N5	
Formula weight	1932.11	
Temperature	193(2) K	
Wavelength	0.71073 ≈	
Crystal system	Orthorhombic	
Space group	Pna2(1)	
Unit cell dimensions	a = 24.5742(13) Å	α= 90°.
	b = 43.729(2) Å	β= 90°.
	c = 25.7954(14) Å	γ = 90°.
Volume	27720(3) Å^3	
Z	8	
Density (calculated)	0.926 Mg/m^3	
Absorption coefficient	0.996 mm^{-1}	
F(000)	8176	
Crystal size	? x ? x ? mm^3	
Theta range for data collection	1.24 to 20.00°.	
Index ranges	-23<=h<=23, -42<=k<=42, -24<=l<=24	
Reflections collected	125318	
Independent reflections	25869 [R(int) = 0.1276]	
Completeness to theta = 20.00∞	100.0 %	
Refinement method	Full-matrix least-squares on F^2	
Data / restraints / parameters	25869 / 2 / 1733	
Goodness-of-fit on F^2	1.028	
Final R indices [I>2sigma(I)]	R1 = 0.0574, wR2 = 0.1058	
R indices (all data)	R1 = 0.0983, wR2 = 0.1115	
Absolute structure parameter	0.024(7)	
Extinction coefficient	0.000391(13)	
Largest diff. peak and hole	0.592 and -0.503 e. Å $^{-3}$	

Table A5.2) Selected Bond lengths [Å] and angles [°] for [*p*BrHIPTN$_3$N]MoN

Mo(1)-N(5A)	1.679(9)	N(3A)-Mo(1)-N(2A)	119.3(4)
Mo(1)-N(3A)	1.980(10)	N(5A)-Mo(1)-N(1A)	103.2(4)
Mo(1)-N(2A)	2.018(10)	N(3A)-Mo(1)-N(1A)	113.5(4)
Mo(1)-N(1A)	2.047(8)	N(2A)-Mo(1)-N(1A)	114.2(4)
Mo(1)-N(4A)	2.324(9)	N(5A)-Mo(1)-N(4A)	178.1(4)
C(1A)-N(4A)	1.537(13)	N(3A)-Mo(1)-N(4A)	75.8(4)
C(1A)-C(2A)	1.555(14)	N(2A)-Mo(1)-N(4A)	79.3(5)
C(2A)-N(1A)	1.474(12)	N(1A)-Mo(1)-N(4A)	78.3(4)
C(3A)-N(4A)	1.465(13)	N(4A)-C(1A)-C(2A)	108.0(11)
C(3A)-C(4A)	1.518(13)	N(1A)-C(2A)-C(1A)	108.3(10)
C(4A)-N(2A)	1.516(13)	N(4A)-C(3A)-C(4A)	110.4(11)
C(5A)-N(4A)	1.445(12)	N(2A)-C(4A)-C(3A)	110.4(11)
C(5A)-C(6A)	1.583(13)	N(4A)-C(5A)-C(6A)	108.7(10)
C(6A)-N(3A)	1.456(13)	N(3A)-C(6A)-C(5A)	105.0(11)
C(1B)-N(4B)	1.528(13)	N(4B)-C(1B)-C(2B)	110.9(11)
C(1B)-C(2B)	1.534(14)	N(1B)-C(2B)-C(1B)	111.0(11)
C(2B)-N(1B)	1.483(13)	N(4B)-C(3B)-C(4B)	106.5(11)
C(3B)-N(4B)	1.510(13)	N(2B)-C(4B)-C(3B)	107.8(10)
C(3B)-C(4B)	1.593(14)	C(6B)-C(5B)-N(4B)	104.0(11)
C(4B)-N(2B)	1.482(13)	C(5B)-C(6B)-N(3B)	117.4(12)
C(5B)-C(6B)	1.461(15)	N(2A)-C(10B)-C(15B)	124.3(15)
C(5B)-N(4B)	1.493(13)	N(2A)-C(10B)-C(11B)	122.0(16)
C(6B)-N(3B)	1.465(14)	N(3A)-C(10C)-C(15C)	118.9(15)
C(10B)-N(2A)	1.367(15)	C(10A)-N(1A)-C(2A)	112.5(9)
Mo(2)-N(5B)	1.689(9)	C(10A)-N(1A)-Mo(1)	128.0(9)
Mo(2)-N(2B)	2.016(9)	C(2A)-N(1A)-Mo(1)	119.0(8)
Mo(2)-N(1B)	2.025(9)	C(10B)-N(2A)-C(4A)	112.8(11)
Mo(2)-N(3B)	2.032(10)	C(10B)-N(2A)-Mo(1)	130.5(10)
Mo(2)-N(4B)	2.389(9)	C(4A)-N(2A)-Mo(1)	116.2(9)
C(10D)-N(1B)	1.373(13)	C(10C)-N(3A)-C(6A)	106.4(10)
C(10E)-N(2B)	1.468(15)	C(10C)-N(3A)-Mo(1)	128.5(9)
C(10F)-N(3B)	1.456(15)	C(6A)-N(3A)-Mo(1)	124.0(8)
N(5A)-Mo(1)-N(3A)	102.4(5)	C(5A)-N(4A)-C(3A)	109.7(10)
N(5A)-Mo(1)-N(2A)	101.1(5)	C(5A)-N(4A)-C(1A)	112.7(11)

C(3A)-N(4A)-C(1A)	114.5(10)	C(10D)-N(1B)-C(2B)	110.7(10)
C(5A)-N(4A)-Mo(1)	107.0(7)	C(10D)-N(1B)-Mo(2)	131.3(9)
C(3A)-N(4A)-Mo(1)	107.0(8)	C(2B)-N(1B)-Mo(2)	118.0(8)
C(1A)-N(4A)-Mo(1)	105.4(7)	C(10E)-N(2B)-C(4B)	111.3(11)
N(5B)-Mo(2)-N(2B)	105.4(5)	C(10E)-N(2B)-Mo(2)	126.9(11)
N(5B)-Mo(2)-N(1B)	98.4(4)	C(4B)-N(2B)-Mo(2)	120.3(8)
N(2B)-Mo(2)-N(1B)	119.2(4)	C(10F)-N(3B)-C(6B)	117.1(13)
N(5B)-Mo(2)-N(3B)	102.8(5)	C(10F)-N(3B)-Mo(2)	127.5(11)
N(2B)-Mo(2)-N(3B)	110.8(4)	C(6B)-N(3B)-Mo(2)	115.1(9)
N(1B)-Mo(2)-N(3B)	117.0(4)	C(5B)-N(4B)-C(3B)	108.6(10)
N(5B)-Mo(2)-N(4B)	177.4(4)	C(5B)-N(4B)-C(1B)	114.8(10)
N(2B)-Mo(2)-N(4B)	77.2(4)	C(3B)-N(4B)-C(1B)	116.1(11)
N(1B)-Mo(2)-N(4B)	79.7(4)	C(5B)-N(4B)-Mo(2)	107.6(8)
N(3B)-Mo(2)-N(4B)	76.5(5)	C(3B)-N(4B)-Mo(2)	106.3(7)
N(1B)-C(10D)-C(15D)	120.7(14)	C(1B)-N(4B)-Mo(2)	102.5(6)
N(1B)-C(10D)-C(11D)	124.2(13)		

Table A5.3) Crystal data and structure refinement for 05228 [HIPTpropylN$_3$N]MoCl

Identification code	05228	
Empirical formula	C135 H183 Cl Mo N4	
Formula weight	1993.24	
Temperature	100(2) K	
Wavelength	0.71073 ≈	
Crystal system	Orthorhombic	
Space group	P2(1)2(1)2(1)	
Unit cell dimensions	a = 14.1152(6) Å	α= 90°.
	b = 27.4121(12) Å	β= 90°.
	c = 31.7436(15) Å	γ = 90°.
Volume	12282.5(9) Å ^{3}	
Z	4	
Density (calculated)	1.078 Mg/m^3	
Absorption coefficient	0.177 mm^{-1}	
F(000)	4320	
Crystal size	0.25 x 0.20 x 0.10 mm^3	
Theta range for data collection	1.93 to 28.70°.	
Index ranges	-19<=h<=19, -35<=k<=37, -42<=l<=42	
Reflections collected	243653	
Independent reflections	31712 [R(int) = 0.1059]	
Completeness to theta = 28.70∞	100.0 %	
Absorption correction	Semi-empirical from equivalents	
Max. and min. transmission	0.9826 and 0.9572	
Refinement method	Full-matrix least-squares on F^2	
Data / restraints / parameters	31712 / 384 / 1327	
Goodness-of-fit on F^2	1.033	
Final R indices [I>2sigma(I)]	R1 = 0.0459, wR2 = 0.0920	
R indices (all data)	R1 = 0.0639, wR2 = 0.0996	
Absolute structure parameter	-0.028(14)	
Largest diff. peak and hole	0.644 and -0.338 e. Å $^{-3}$	

Table A5.4) Selected Bond lengths [Å] and angles [°] for 05228

Cl(1)-Mo(1)	2.3843(5)	C(115)-N(1)-Mo(1)	122.32(14)
Mo(1)-N(1)	1.9688(17)	C(1)-N(1)-Mo(1)	127.91(14)
Mo(1)-N(2)	1.9709(18)	C(215)-N(2)-C(4)	109.62(18)
Mo(1)-N(3)	1.9743(18)	C(215)-N(2)-Mo(1)	122.37(14)
Mo(1)-N(4)	2.3230(18)	C(4)-N(2)-Mo(1)	127.54(15)
N(1)-C(115)	1.435(3)	C(315)-N(3)-C(7)	110.78(17)
N(1)-C(1)	1.472(3)	C(315)-N(3)-Mo(1)	121.57(14)
N(2)-C(215)	1.437(3)		
N(2)-C(4)	1.471(3)		
N(3)-C(315)	1.438(3)	C(7)-N(3)-Mo(1)	127.29(14)
N(3)-C(7)	1.465(3)	C(9)-N(4)-C(3)	106.93(17)
N(4)-C(9)	1.489(3)	C(9)-N(4)-C(6)	106.43(17)
N(4)-C(3)	1.499(3)	C(3)-N(4)-C(6)	106.81(17)
N(4)-C(6)	1.503(3)	C(9)-N(4)-Mo(1)	111.50(12)
		C(3)-N(4)-Mo(1)	112.12(13)
N(1)-Mo(1)-N(2)	120.85(8)	C(6)-N(4)-Mo(1)	112.67(13)
N(1)-Mo(1)-N(3)	119.36(8)	N(1)-C(1)-C(2)	112.59(18)
N(2)-Mo(1)-N(3)	119.63(7)	C(1)-C(2)-C(3)	111.56(19)
N(1)-Mo(1)-N(4)	89.03(7)	N(4)-C(3)-C(2)	113.13(18)
N(2)-Mo(1)-N(4)	89.26(7)	N(2)-C(4)-C(5)	113.47(19)
N(3)-Mo(1)-N(4)	87.76(7)	C(6)-C(5)-C(4)	111.93(19)
N(1)-Mo(1)-Cl(1)	91.15(5)	N(4)-C(6)-C(5)	113.25(18)
N(2)-Mo(1)-Cl(1)	91.50(5)	N(3)-C(7)-C(8)	111.88(18)
N(3)-Mo(1)-Cl(1)	91.28(5)	C(7)-C(8)-C(9)	110.3(2)
N(4)-Mo(1)-Cl(1)	178.99(5)	N(4)-C(9)-C(8)	112.37(18)
C(115)-N(1)-C(1)	109.71(16)		

Table A5.5) Crystal data and structure refinement for 04072 [3,5-Bis(CF_3)HIPT$_2$$N_3$N]MoCl

Identification code	pm	
Empirical formula	C86 H113 Cl F6 Mo N4	
Formula weight	1448.19	
Temperature	193(2) K	
Wavelength	0.71073 ≈	
Crystal system	Orthorhombic	
Space group	Pbcn	
Unit cell dimensions	a = 33.780(7) Å	α= 90°.
	b = 23.053(5) Å	β= 90°.
	c = 21.560(4) Å	γ = 90°.
Volume	16790(6) Å ^{3}	
Z	8	
Density (calculated)	1.146 Mg/m^3	
Absorption coefficient	0.244 mm^{-1}	
F(000)	6160	
Crystal size	0.28 x 0.15 x 0.08 mm^3	
Theta range for data collection	1.77 to 21.01°.	
Index ranges	0<=h<=34, 0<=k<=23, 0<=l<=21	
Reflections collected	62854	
Independent reflections	8986 [R(int) = 0.1130]	
Completeness to theta = 21.01∞	99.5 %	
Absorption correction	Semi-empirical from equivalents	
Max. and min. transmission	0.9807 and 0.9348	
Refinement method	Full-matrix least-squares on F^2	
Data / restraints / parameters	8986 / 2559 / 1311	
Goodness-of-fit on F^2	1.121	
Final R indices [I>2sigma(I)]	R1 = 0.0743, wR2 = 0.1900	
R indices (all data)	R1 = 0.1187, wR2 = 0.2208	
Largest diff. peak and hole	0.823 and -0.786 e. Å $^{-3}$	

Table A5.6) Selected bond lengths [Å] and angles [°] for 04072

Cl(1)-Mo(1)	2.331(2)
Mo(1)-N(3)	1.931(7)
Mo(1)-N(2)	1.959(6)
Mo(1)-N(1)	1.978(7)
Mo(1)-N(4)	2.199(6)
N(1)-C(11)	1.382(10)
N(1)-C(1)	1.465(9)
N(3)-Mo(1)-N(2)	120.2(3)
N(3)-Mo(1)-N(1)	117.1(3)
N(2)-Mo(1)-N(1)	114.5(3)
N(3)-Mo(1)-N(4)	79.9(2)
N(2)-Mo(1)-N(4)	80.9(2)
N(1)-Mo(1)-N(4)	80.3(2)
N(3)-Mo(1)-Cl(1)	96.47(19)
N(2)-Mo(1)-Cl(1)	102.32(17)
N(1)-Mo(1)-Cl(1)	100.20(18)
N(4)-Mo(1)-Cl(1)	176.10(17)
C(11)-N(1)-C(1)	114.3(6)
C(11)-N(1)-Mo(1)	130.1(5)
C(1)-N(1)-Mo(1)	115.0(5)
N(1)-C(11)-C(16)	124.1(7)
N(1)-C(11)-C(12)	121.0(7)

Table A5.7) Crystal data and structure refinement for 04169

[3,5-dimethylHIPT$_2$N$_3$N]MoN$_2$Na(THF)$_2$

Identification code	04169	
Empirical formula	C155 H234.50 Mo1.50 N9 Na1.50 O3.25	
Formula weight	2454.41	
Temperature	100(2) K	
Wavelength	0.71073 ≈	
Crystal system	Rhombohedral	
Space group	R-3	
Unit cell dimensions	a = 32.204(5) Å	α= 90°.
	b = 32.204(5) Å	β= 90°.
	c = 51.045(10) Å	γ = 120°.
Volume	45845(13) Å ^{3}	
Z	12	
Density (calculated)	1.067 Mg/m^3	
Absorption coefficient	0.180 mm^{-1}	
F(000)	15996	
Crystal size	0.24 x 0.18 x 0.04 mm^3	
Theta range for data collection	0.83 to 25.02°.	
Index ranges	-38<=h<=19, 0<=k<=38, 0<=l<=60	
Reflections collected	229429	
Independent reflections	17866 [R(int) = 0.1206]	
Completeness to theta = 25.02∞	99.3 %	
Absorption correction	Semi-empirical from equivalents	
Max. and min. transmission	0.9928 and 0.9580	
Refinement method	Full-matrix least-squares on F^2	
Data / restraints / parameters	17866 / 1707 / 1197	
Goodness-of-fit on F^2	1.043	
Final R indices [I>2sigma(I)]	R1 = 0.0742, wR2 = 0.1953	
R indices (all data)	R1 = 0.1066, wR2 = 0.2130	
Largest diff. peak and hole	1.135 and -0.466 e. Å $^{-3}$	

Table A5.8) Bond lengths [Å] and angles [°] for 04169

Mo(1)-N(5)	1.882(4)	N(1)-Mo(1)-N(4)	81.21(16)
Mo(1)-N(2)	2.012(4)	C(215)-N(1)-C(1)	113.1(4)
Mo(1)-N(3)	2.022(4)	C(215)-N(1)-Mo(1)	132.1(3)
Mo(1)-N(1)	2.053(4)	C(1)-N(1)-Mo(1)	114.0(3)
Mo(1)-N(4)	2.209(4)	C(315)-N(2)-C(3)	114.9(4)
N(1)-C(215)	1.404(6)	C(315)-N(2)-Mo(1)	128.1(3)
N(1)-C(1)	1.488(6)	C(3)-N(2)-Mo(1)	116.5(3)
N(2)-C(315)	1.418(7)	C(115)-N(3)-C(5)	114.9(4)
N(2)-C(3)	1.481(7)	C(115)-N(3)-Mo(1)	130.7(3)
N(3)-C(115)	1.413(6)	C(5)-N(3)-Mo(1)	114.2(3)
N(3)-C(5)	1.482(6)	C(6)-N(4)-C(2)	111.4(4)
N(4)-C(6)	1.477(7)	C(6)-N(4)-C(4)	113.0(4)
N(4)-C(2)	1.483(7)	C(2)-N(4)-C(4)	112.1(4)
N(4)-C(4)	1.490(7)	C(6)-N(4)-Mo(1)	106.6(3)
N(5)-N(6)	1.171(6)	C(2)-N(4)-Mo(1)	106.6(3)
N(5)-Na(1)	2.976(5)	C(4)-N(4)-Mo(1)	106.6(3)
N(6)-Na(1)	2.353(6)	N(6)-N(5)-Mo(1)	174.2(4)
N(5)-Mo(1)-N(2)	94.50(17)	N(6)-N(5)-Na(1)	47.7(3)
N(5)-Mo(1)-N(3)	103.59(16)	Mo(1)-N(5)-Na(1)	126.69(19)
N(2)-Mo(1)-N(3)	113.78(17)	N(5)-N(6)-Na(1)	110.7(4)
N(5)-Mo(1)-N(1)	99.39(17)	N(1)-C(1)-C(2)	108.6(4)
N(2)-Mo(1)-N(1)	122.50(17)	N(4)-C(2)-C(1)	111.4(4)
N(3)-Mo(1)-N(1)	116.36(16)	N(2)-C(3)-C(4)	110.5(4)
N(5)-Mo(1)-N(4)	174.09(17)	N(4)-C(4)-C(3)	110.8(4)
N(2)-Mo(1)-N(4)	80.32(17)	N(3)-C(5)-C(6)	108.9(4)
N(3)-Mo(1)-N(4)	81.25(16)	N(4)-C(6)-C(5)	110.3(4)

Table A5.9) Crystal data and structure refinement for 05065 [*p*BrHIPTN$_3$N]FeClLi(THF)$_3$

Identification code	05065	
Empirical formula	C126 H180 Br3 Cl Fe Li N4 O3	
Formula weight	2136.71	
Temperature	100(2) K	
Wavelength	0.71073 ≈	
Crystal system	Cubic	
Space group	Pa-3	
Unit cell dimensions	a = 29.7122(8) Å	α= 90°.
	b = 29.7122(8) Å	β= 90°.
	c = 29.7122(8) Å	γ = 90°.
Volume	26230.4(12) Å ^{3}	
Z	8	
Density (calculated)	1.082 Mg/m^3	
Absorption coefficient	1.095 mm^{-1}	
F(000)	9112	
Crystal size	0.15 x 0.15 x 0.15 mm^3	
Theta range for data collection	2.06 to 25.03°.	
Index ranges	-35<=h<=35, -35<=k<=35, -35<=l<=35	
Reflections collected	360589	
Independent reflections	7737 [R(int) = 0.1018]	
Completeness to theta = 25.03∞	99.9 %	
Absorption correction	Semi-empirical from equivalents	
Max. and min. transmission	0.8530 and 0.8530	
Refinement method	Full-matrix least-squares on F^2	
Data / restraints / parameters	7737 / 74 / 440	
Goodness-of-fit on F^2	1.145	
Final R indices [I>2sigma(I)]	R1 = 0.0677, wR2 = 0.2045	
R indices (all data)	R1 = 0.0966, wR2 = 0.2372	
Largest diff. peak and hole	1.386 and -0.637 e. Å $^{-3}$	

Table A5.10) Selected bond lengths [Å] and angles [°] for 05065

Fe(1)-N(1)#1	1.972(4)	N(1)#1-Fe(1)-N(4)	75.57(11)
Fe(1)-N(1)#2	1.972(4)	N(1)#2-Fe(1)-N(4)	75.57(11)
Fe(1)-N(1)	1.972(4)	N(1)-Fe(1)-N(4)	75.57(11)
Fe(1)-Cl(1)	2.368(2)	Cl(1)-Fe(1)-N(4)	180.00(10)
Fe(1)-N(4)	2.545(6)	Li(1)-Cl(1)-Fe(1)	180.0(3)
Cl(1)-Li(1)	2.26(2)	C(115)-N(1)-C(3)	116.5(4)
Br(1)-C(118)	1.906(5)	C(115)-N(1)-Fe(1)	121.9(3)
N(1)-C(115)	1.382(6)	C(3)-N(1)-Fe(1)	109.9(3)
N(1)-C(3)	1.466(6)	C(4)#1-N(4)-C(4)	115.0(2)
N(4)-C(4)#1	1.475(5)	C(4)#1-N(4)-C(4)#2	115.0(2)
N(4)-C(4)	1.475(5)	C(4)-N(4)-C(4)#2	115.0(2)
N(4)-C(4)#2	1.475(5)	C(4)#1-N(4)-Fe(1)	103.1(3)
		C(4)-N(4)-Fe(1)	103.1(3)
N(1)#1-Fe(1)-N(1)#2	114.01(9)	C(4)#2-N(4)-Fe(1)	103.1(3)
N(1)#1-Fe(1)-N(1)	114.00(9)	N(1)-C(3)-C(4)	109.8(4)
N(1)#2-Fe(1)-N(1)	114.01(9)	N(4)-C(4)-C(3)	109.3(4)
N(1)#1-Fe(1)-Cl(1)	104.43(11)	N(1)-C(115)-C(116)	124.1(4)
N(1)#2-Fe(1)-Cl(1)	104.43(11)	N(1)-C(115)-C(120)	118.9(4)
N(1)-Fe(1)-Cl(1)	104.43(11)		

Acknowledgements

I'm usually not much for stuff like this, so I'll keep it short. First of all, I'd like to thank Adam, Zach, and Saskia for reading early versions of this thesis. All errors that remain are entirely my own. As for my graduate career, I have been fortunate to have had a great lab space for the past few years. Dai, Roje, Zach, and myself have created a productive, yet fun, place to work. Also, the rest of the Schrock group, particularly Adam, have allowed me to grow as a person and a scientist. As for Dick, I truly appreciate the opportunity to have worked for/with you on this project. I did not always get everything finished that I thought would get done, but we managed to learn quite a bit. To everybody else who has touched my life in graduate school one way or the other, I am glad to have experienced it all.

Personally, I'd like to thank my family for their support over the years. My Mom and Dad have been there when I need them, even though they live over the ocean. I am lucky enough to have a good friend in my brother, Neil. I'm glad I'm finishing up before he gets his lawyer degree though, would be kind of embarrassing to have a little brother all done while I'm in school. Last, but not least, I'd like to thank my partner in crime – Sasky. As we've gone through the years, it's been a blessing to know that I have that special someone to come home to. It's time for the next phase in our lives together, but this time back on the other coast.

Massachusetts Institute of Technology
Room 6-421
77 Massachusetts Ave.
Cambridge, MA 02139
(617) 253 – 5047

189 Tremont St. #2R
Somerville, MA 02143
(617) 312–2911
wwweare@mit.edu

EDUCATION

Graduate: **Massachusetts Institute of Technology** *2001-Present*
Cambridge, MA
Inorganic synthesis, small molecule activation, homogenous inorganic catalysis
(Prof. Richard R. Schrock)

B. Sc. *Magna Cum Laude* **University of Oregon** *1996-2000*
Eugene, OR
Synthetic materials chemistry **(Prof. James E. Hutchison)**

AWARDS

2006 Massachusetts Institute of Technology Morse Travel Grant
2006 Division of Inorganic Chemistry of the American Chemical Society Travel Grant
2005 Cambridge Science Foundation Travel Grant
2000 Outstanding Graduate in Chemistry, American Institute of Chemists, University of Oregon
2000 Phi Beta Kappa, University of Oregon
1999 NSF/REU Summer Fellowship, University of Oregon
1999 HHMI Summer Fellowship, University of Oregon
1996 CRC Press Freshman Chemistry Achievement Award, University of Oregon

PUBLICATIONS

Weare, W.W.; Byrnes, M.J.; Chin, J.M.; Dai, X.; Schrock, R.R.; Müller, P. "Nitrogen fixation at a single molybdenum atom: recent advances in understanding this catalytic cycle." *Proceedings of the National Academy of Sciences* **2006**, *submitted.*

Ritleng V.; Yandulov D.V.; Weare W.W.; Schrock R.R.; Hock A.S.; and Davis W.M. "Molybdenum triamidoamine complexes that contain hexa-*tert*-butylterphenyl, hexamethylterphenyl, or *p*-bromohexaisopropylterphenyl substituents. An examination of some catalyst variations for the catalytic reduction of dinitrogen", *J. Am. Chem. Soc.* **2004**, *119,* 6150-6163.

Hutchison, J.E.; Foster, E.W.; Warner, M.G.; Reed, S.M.; and Weare, W.W. "1.5 nm triphenylphosphine-stabilized gold nanoparticles." Inorg. Synth. **2004,** *34*, 228-232.

Weare W.W.; Reed S.M.; Warner M.G.; and Hutchison J.E. "Improved synthesis of small ($d_{CORE} \approx 1.5$ nm) phosphine-stabilized gold nanoparticles." *J. Am. Chem. Soc.* **2000**, *122*, 12890-12891.